

THE CRYSTAL STRUCTURES OF SOME TERNARY  
OXIDES AND FLUORIDES

THE CRYSTAL STRUCTURES OF SOME  
TERNARY OXIDES AND FLUORIDES

by

ELISABETH ANN MARSEGLIA, M.A.

A Thesis

Submitted to the School of Graduate Studies  
in Partial Fulfilment of the Requirements

for the Degree

Doctor of Philosophy

McMaster University

May 1971

DOCTOR OF PHILOSOPHY (1971)  
(Chemistry)

McMASTER UNIVERSITY  
Hamilton, Ontario

TITLE: The Crystal Structures of Some Ternary  
Oxides and Fluorides

AUTHOR: Elisabeth Ann Marseglia, B.A. (University of  
Delaware)  
M.A. (The John Hopkins  
University)

SUPERVISOR: Dr. I. D. Brown

NUMBER OF PAGES: vii , 130

SCOPE AND CONTENTS:

The crystal structures of five ternary oxides and fluorides have been determined. It is shown that the gross features of these structures and the coordination of the atoms can be described in terms of the theory of close-packing of spheres. However, in each of the structures there appear cations whose coordination cannot be uniquely predicted, as the cation-anion radius ratios are close to the critical value for transition from one coordination to another.

### Acknowledgements

I would like to thank my supervisor, Dr. I. D. Brown, for his advice and guidance throughout the course of this research. In addition, I am very much indebted to Doctors C. Calvo and J. Rutherford for their help and encouragement and to the other members of the crystallography group for many stimulating discussions on this and related topics. Scholarships from the National Research Council and McMaster University have also made this research possible, and are gratefully acknowledged. Most of all, I would like to thank my husband, Eugene, without whose constant support and encouragement this work would never have been completed.

## TABLE OF CONTENTS

	<u>Page</u>
INTRODUCTION	1
CHAPTER I CRYSTALLOGRAPHIC THEORY AND PROCEDURE	7
i. X-ray Structure Determination	7
ii. General Experimental Procedure	14
CHAPTER II FLUORIDES	18
i. Crystal Structure of $\text{Li}_2\text{TiF}_6 \cdot 2\text{H}_2\text{O}$ and $\text{Li}_2\text{SnF}_6 \cdot 2\text{H}_2\text{O}$	18
ii. Crystal Structure of $\text{Na}_2\text{TiF}_6$	53
CHAPTER III OXIDES	77
i. Crystal Structure of $\text{LiAl}_5\text{O}_8$	77
ii. Crystal Structure of $\text{LiAlO}_2$	88
CHAPTER IV CONCLUSION	115
APPENDIX Radius Ratio and the Simple Ionic Theory	123
BIBLIOGRAPHY	125

## LIST OF ILLUSTRATIONS

	<u>Page</u>
1. Diversity of compounds described by model of closest packing of spheres	2
2. Close-packing of spheres	3
3. $\text{Li}_2\text{TiF}_6 \cdot 2\text{H}_2\text{O}$ - h0l Patterson projection	22
4. Linkage of titanium and lithium octahedra	37
5. Linkage of titanium and sodium octahedra	66
6. Projection on a cubeface of the atoms in the lower half of a unit cell of $\text{LiAl}_5\text{O}_8$	87
7. a. Lithium atom sites	98
b. Possible occupation of lithium sites	99
8. Aluminum and oxygen bonding in $\beta\text{-LiAlO}_2$	102
9. $\beta$ -cristobalite (cubic)	113

LIST OF TABLES

		<u>Page</u>
I.	Crystal Data for $\text{Li}_2\text{TiF}_6 \cdot 2\text{H}_2\text{O}$	19
IIa.	Final Positional Parameters in $\text{Li}_2\text{TiF}_6 \cdot 2\text{H}_2\text{O}$ and $\text{Li}_2\text{SnF}_6 \cdot 2\text{H}_2\text{O}$	24
IIb.	Final Thermal Parameters in $\text{Li}_2\text{TiF}_6 \cdot 2\text{H}_2\text{O}$ and $\text{Li}_2\text{SnF}_6 \cdot 2\text{H}_2\text{O}$	25
III.	Observed and Calculated Structure Factors for $\text{Li}_2\text{SnF}_6 \cdot 2\text{H}_2\text{O}$	26
IV.	Crystal Data for $\text{Li}_2\text{SnF}_6 \cdot 2\text{H}_2\text{O}$	29
V.	Observed and Calculated Structure Factors for $\text{Li}_2\text{TiF}_6 \cdot 2\text{H}_2\text{O}$	32
VIa.	Bond Distances and Angles for $\text{TiF}_6$ and $\text{SnF}_6$ Octahedra	38
VIb.	Bond Distances and Angles for $\text{LiF}_6$ Octahedra	39
VIIa.	Fluorine-fluorine Bond Lengths in $\text{Li}_2\text{TiF}_6 \cdot 2\text{H}_2\text{O}$	41
VIIb.	Fluorine-fluorine Bond Lengths in $\text{Li}_2\text{SnF}_6 \cdot 2\text{H}_2\text{O}$	41
VIII.	Principal Axes Analysis for Anisotropic Temperature Factors	43
IX.	Thermal Corrections for Bond Lengths	46
X.	$\text{K}_2\text{TiF}_6$ -type Crystals Belonging to $\text{P}\bar{3}\text{m1}$	48
XI.	Crystal Data for $\text{K}_2\text{TiF}_6$	50
XII.	Comparison of Oxygen-Fluorine Distances in $\text{Li}_2\text{TiF}_6 \cdot 2\text{H}_2\text{O}$ and $\text{Li}_2\text{SnF}_6 \cdot 2\text{H}_2\text{O}$ with Potas- sium-Fluorine Distances in $\text{K}_2\text{TiF}_6$ in Å Units	51
XIII.	Crystal Data for $\text{Na}_2\text{TiF}_6$	56

	<u>Page</u>
XIVa.	Final Positional Parameters in $\text{Na}_2\text{TiF}_6$ and $\text{Na}_2\text{SiF}_6$ 59
XIVb.	Final Thermal Parameters in $\text{Na}_2\text{TiF}_6$ and $\text{Na}_2\text{SiF}_6$ 60
XV.	Observed and Calculated Structure Factors for $\text{Na}_2\text{TiF}_6$ 61
XVIa.	Bond Distances and Angles for $\text{TiF}_6$ and $\text{SiF}_6$ Octahedra 68
XVib.	Bond Distances and Angles for $\text{NaF}_6$ Octahedra 70
XVII.	Principal Axis Analysis for Anisotropic Temperature Factors 73
XVIII.	Thermal Corrections for Bond Lengths - $\text{Na}_2\text{TiF}_6$ 74
XIX.	Crystal Data for $\text{LiAl}_5\text{O}_8$ 79
XX.	$\text{LiAl}_5\text{O}_8$ - $\text{R}_2$ for various values of w 82
XXI.	Final Parameters in $\text{LiAl}_5\text{O}_8$ 83
XXII.	Observed and Calculated Structure Factors for $\text{LiAl}_5\text{O}_8$ 84
XXIII.	Crystal Data for $\beta\text{-LiAlO}_2$ 91
XXIV.	Atomic Parameters for $\beta\text{-LiAlO}_2$ 95
XXV.	Observed and Calculated Structure Factors for $\text{LiAlO}_2$ 96
XXVI.	Interatomic distances and angles in $\beta\text{-LiAlO}_2$ , $\text{LiAlSi}_2\text{O}_6$ -III, $\text{Li}_2\text{Al}_2\text{Si}_3\text{O}_{10}$ and $\beta\text{-quartz}$ (Å) 104
XXVII.	$\beta\text{-quartz}$ Structures in the $\text{Li}_2\text{O}\cdot\text{Al}_2\text{O}_3\cdot x\text{SiO}_2$ System 109

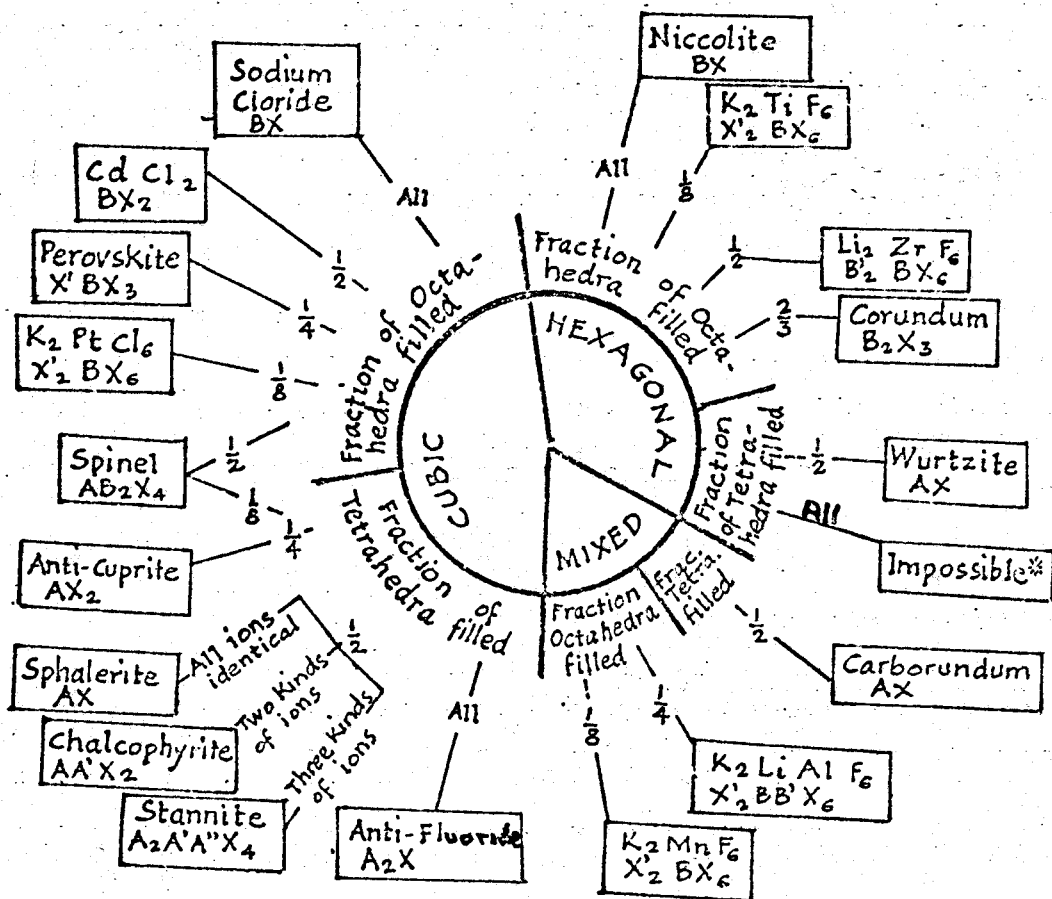


## INTRODUCTION

A great number of structures of inorganic ionic crystals may be understood by using the model of closely packed spheres. Close-packing is a term applied to the geometrically most compact arrangement of spheres in space. The model is a simple one and when applied to ions requires the underlying assumption that ions are incompressible, non-polarizable spheres. The fact that many structures contain complex ions of fixed geometry is often a secondary consideration, especially if the coordinating element is small enough to fit into interstitial spaces and is tetrahedrally or octahedrally coordinated. There are as many octahedral spaces and twice as many tetrahedral spaces as there are close-packed ions. Figure 1. illustrates the diversity of compounds that can be included in this model. <sup>(1)</sup>

If spheres of equal size are placed together as closely as possible on a plane surface each sphere is in contact with six others, and such layers may be stacked to give a three dimensional array, (Figure 2.) If one layer is labelled A, then the next layer B is placed as closely as possible on the first so that each sphere is in contact with three spheres of the bottom layer (position b in Figure 2.). There are two alternatives for the third layer. Either it lies directly above A, or directly above the position c in

FIG. 1  
SOME INORGANIC STRUCTURES  
BASED ON  
CLOSE-PACKING



X = close-packed atoms  
A = atoms in tetrahedral interstices  
B = atoms in octahedral interstices  
\* too close proximity of interstitials

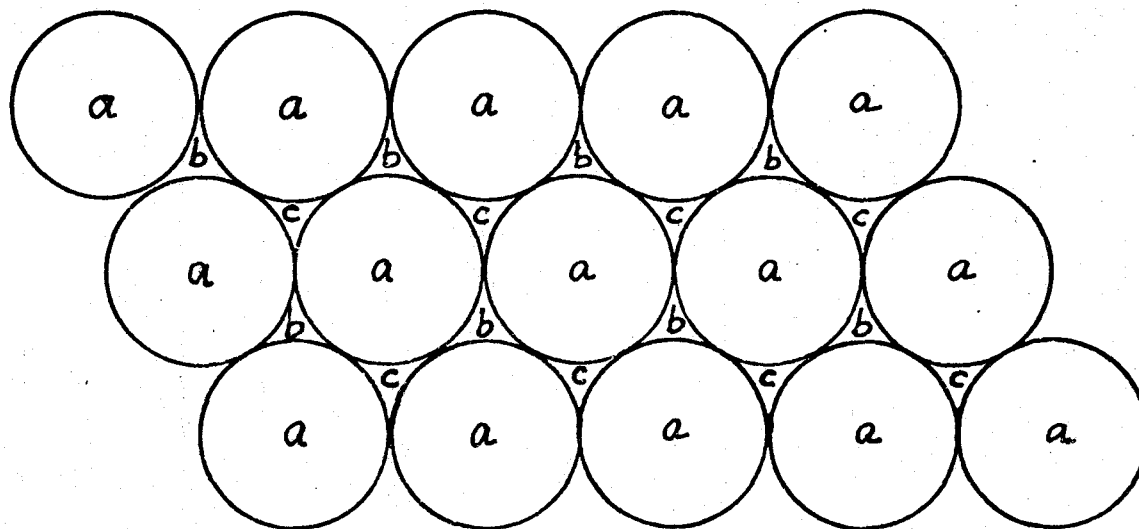


FIG. 2 CLOSE-PACKING OF IDENTICAL SPHERES

Figure 2. The two simplest sequences of layers are then ABAB... known as hexagonal closest packing, and ABCABC... known as cubic closest packing. Each sphere is in contact with twelve others or has a coordination number of twelve.

To concentrate our attention on ternary fluorides and oxides, we can recognize three major divisions. The system may consist of close-packed anions with cations that fit into interstitial positions, as in  $\text{Li}_2\text{TiF}_6 \cdot 2\text{H}_2\text{O}$ ,  $\text{Li}_2\text{SnF}_6 \cdot 2\text{H}_2\text{O}$  and  $\text{LiAl}_5\text{O}_8$ . Alternatively, if anions and cations are approximately the same size, as for example  $\text{K}^+$  and  $\text{F}^-$ , then close-packing of both can occur. It is not possible to form a close-packed layer in which each ion is surrounded entirely by ions of the other kind, for as soon as six X ions are placed around an A ion each X ion already has two X ions as nearest neighbours, giving a stoichiometry of  $\text{AX}_2$ , thus a 12-coordinated structure is not found in potassium fluoride. However, many structures are built up from close-packed layers of composition  $\text{AX}_2$  or  $\text{AX}_3$ .  $\text{K}_2\text{TiF}_6$  is an example of the latter. If the cations are too large to fit into an interstitial position and too small to close-pack uniformly with the anions then a distorted close-packed structure occurs as in  $\text{Na}_2\text{TiF}_6$  and  $\text{Na}_3\text{AlF}_6$  (cryolite). Also, there are some compounds which in one phase have a close packed arrangement and in another a more open arrangement of atoms. This interesting case occurs in  $\text{LiAlO}_2$  and  $\text{GeO}_2$ .

It was said earlier that the presence of complex ions is a secondary consideration and this is borne out by the fact that a large number of close-packed ternary fluorides and oxides crystallize in a few structure types, these types being more dependent on the relative sizes of the ions than on their individual composition. Covalent contributions to the bonding do cause small deviations among the structures although they cannot always be distinguished from polarization effects, especially in oxides, as oxygen is more polarizable than fluorine. <sup>(2)</sup> The electron density distribution between the central ion and its ligands derived from x-ray work is not yet sufficiently accurate to give direct evidence of bonding types because of interference from thermal vibration effects, but a certain amount can be inferred from bond distances. In some ternary fluorides containing  $\text{MeF}_6$  ions for example, the influence of partial covalency may be implied in the contraction of the  $\text{MeF}_6$  octahedra which diminishes the distances below the ionic radii sums. However, supporting evidence from other methods is usually required. Octahedral or tetrahedral coordination in a crystal does not imply covalency as these are the arrangements which place the anions as far apart as possible in accordance with the simple ionic theory (see Appendix I).

This thesis undertakes to describe the crystal structure determination of five crystals representative of the

types mentioned above and to discuss them in terms of the model of close-packing. Two of them are hydrated and belong to a class of hydrated crystals in which the oxygen in the water forms part of the close packed network.

CHAPTER I  
CRYSTALLOGRAPHIC THEORY AND PROCEDURE

i. X-ray Structure Determination

The following discussion attempts only to outline the methods used for a single crystal structure determination by X-ray diffraction, since the technique is well established and excellent accounts are available in standard references and texts. (3 -9)

A. Reciprocal Lattice

An ideal crystal consists of a unit of volume, of the order of  $10^3 \text{ \AA}^3$  units on edge, that together with other identical units, forms a larger unit with translational periodicity. The unit of volume, called the unit cell, is a parallelepiped, and can be described by the vectors  $\vec{a}_1$ ,  $\vec{a}_2$  and  $\vec{a}_3$ . Thus, for any physical property P,

$$P(\vec{r}) = P(n_1\vec{a}_1 + n_2\vec{a}_2 + n_3\vec{a}_3 + \vec{r})$$

where  $n_i$  are integers. The vector product of any two unit cell vectors defines another vector viz:

$$\vec{a}_1 \times \vec{a}_2 = (\text{volume of cell}) (\vec{b}_3)$$

similarly

$$\vec{a}_2 \times \vec{a}_3 = (\text{volume of cell}) (\vec{b}_1)$$

$$\vec{a}_3 \times \vec{a}_1 = (\text{volume of cell}) (\vec{b}_2)$$

The vectors  $\vec{b}_1$ ,  $\vec{b}_2$ ,  $\vec{b}_3$ , so defined are called reciprocal lattice vectors and arise naturally in describing the scattering of x-rays by a crystal.\* For example, any plane in the crystal will contain two real vectors

$$\vec{r}_p = q_p \vec{a}_1 + m_p \vec{a}_2 + n_p \vec{a}_3$$

$$\vec{r}_s = q_s \vec{a}_1 + m_s \vec{a}_2 + n_s \vec{a}_3$$

and the normal  $\vec{H}$  to this face, a vector proportional to  $\vec{r}_p \times \vec{r}_s$ , can be described as

$$\vec{H} = h\vec{b}_1 + k\vec{b}_2 + \ell\vec{b}_3 \text{ where}$$

$$h = m_p n_s - m_s n_p$$

with  $k$  and  $\ell$  derived by simple permutation. Since  $q, m$  and  $n$  are integers,  $h, k$ , and  $\ell$  must also be integers. Thus, all the possible planes in the crystal can be described as lattice points in a vector space with basis vectors given by the reciprocal lattice vectors  $\vec{b}_1$ ,  $\vec{b}_2$ , and  $\vec{b}_3$ .

#### B. Scattering of X-rays from a Crystal.

X-rays are scattered by electrons. In considering the amplitude of scattering from a crystal one regards any electron as associated with one atom and the atoms associated

---

\*It is more common to refer to the real cell parameters as  $a$ ,  $b$  and  $c$  with corresponding angles  $\alpha$ ,  $\beta$  and  $\gamma$ , and the reciprocal cell parameters as  $a^*$ ,  $b^*$ , and  $c^*$  with angles  $\alpha^*$ ,  $\beta^*$  and  $\gamma^*$ . The above notation is used to be consistent with later derivations.



with some unit cell. This approach makes it possible to take the periodicity of the structure into account.

Making the approximation that an atom has a continuous distribution of electrons, the amplitude of scattering by an atom in the direction  $\vec{k}$  can be described as

$$f_j(\vec{s}) = \int \rho(\vec{r}) e^{i(\vec{s} \cdot \vec{r})} d\vec{r}$$

where  $\rho(\vec{r})$  = the electron density at the point  $\vec{r}$ , and  $\vec{s} = 2\pi(\vec{k}_0 - \vec{k})$  where  $\vec{k}_0$  is the wave vector for the incident wave and  $\vec{k}$  is the wave vector for the scattered wave.  $f_j(\vec{s})$  is called the atomic scattering factor and is calculated from Hartree-Fock self-consistent field equations<sup>(10)</sup>. Values for all elements are tabulated in International Tables, Volume III<sup>(6)</sup>.

For all the atoms in one unit cell, the amplitude of scattering is

$$F_u(\vec{s}) = \sum_{\substack{j=\text{all} \\ \text{atoms in cell}}} e^{i(\vec{s} \cdot \vec{r}_j)} f_j$$

where  $\vec{r}_j$  is the distance from the origin of the cell to the  $j^{\text{th}}$  atom.  $F_u$  is called the structure factor for the unit cell. The scattering from a small crystal is given simply by adding the amplitude of scattering from all the unit cells in the crystal.

$$F_{cr}(\vec{s}) = \sum_{\substack{n_1 \\ n_2 \\ n_3 \\ -\infty}}^{\infty} \sum_j f_j e^{i(\vec{s} \cdot (\vec{r}_j + n_1 \vec{a}_1 + n_2 \vec{a}_2 + n_3 \vec{a}_3))}$$

The intensity of scattering for the crystal,  $I_{cr}$ , is proportional to  $F_{cr} F_{cr}^*$  and it can be shown that <sup>(4)</sup>

$$I_{cr} \sim F_u F_u^* \prod_{j=1,2,3} \frac{\sin^2(\frac{1}{2} N \mathbf{s} \cdot \vec{a}_j)}{\sin^2 \frac{1}{2} (\mathbf{s} \cdot \vec{a}_j)} .$$

The  $\vec{a}_j$  correspond to the real cell vectors  $\vec{a}_1, \vec{a}_2, \vec{a}_3$  defined earlier. Unless  $\mathbf{s} \cdot \vec{a}_1$ ,  $\mathbf{s} \cdot \vec{a}_2$ , and  $\mathbf{s} \cdot \vec{a}_3$  are  $2\pi$  times an integer, the function is zero, therefore

$$\vec{s} \cdot \vec{a}_1 = 2\pi h; \quad \vec{s} \cdot \vec{a}_2 = 2\pi k; \quad \vec{s} \cdot \vec{a}_3 = 2\pi l$$

$$\text{or } \vec{s} = 2\pi (h\vec{b}_1 + k\vec{b}_2 + l\vec{b}_3) = 2\pi \vec{H} .$$

The structure factor can now be rewritten

$$F(\vec{H}) = F(hkl) = \sum_j^N f_j e^{2\pi i (\vec{H} \cdot \vec{r}_j)}$$

The x-rays will be scattered in discrete directions only and the diffraction pattern of a single crystal appears as discrete spots. For these directions

$$I = F_u(hkl) F_u^*(hkl) .$$

The symmetry of the diffraction pattern thus obtained contains the symmetry within the unit cell. Once the symmetry operations are deduced the number of possible unknowns whose value must be specified in order to calculate the electron density in the crystal has been reduced. Thus, the crystal structure problem becomes one of finding the positions of the center of electron density for a certain fraction of the

total number of atoms in the unit cell.

Only the intensities of the diffracted spots can be observed however, and it is not possible to measure the phases of the structure factors directly. The usual procedure is to calculate the magnitudes and phases using a set of trial atomic coordinates for the atoms in the crystal. These trial coordinates can be derived either from pair correlation functions (known as Patterson functions) which can be derived without knowledge of the phases<sup>(11)</sup>, or from comparison with a known structure. Sometimes a model can be constructed from a knowledge of the molecular structure of the compound, and a consideration of how these molecules would pack together in a three dimensional array within the constraints of the dimensions of the unit cell and the known symmetry of the cell.

If the calculated structure amplitudes,  $F_c(hkl)$ , for the model are similar to the experimental set,  $F_o(hkl)$ , then the model is considered a reasonable approximation to the true structure. The comparison is made by calculating an agreement index  $R_2$ , henceforth referred to as the  $R_2$  factor.

$$R_2 = \left[ \frac{\sum_{i=1}^N w_i (|F_o(hkl)| - |F_c(hkl)|)_i^2}{\sum_{i=1}^N w_i |F_o(hkl)|_i^2} \right]^{1/2}$$

The summations are over  $N$  reflections and  $w_i$  is a weighting factor which is discussed in section E. The phases of the

calculated  $F_c(hkl)$  are used with the observed magnitudes  $F_o(hkl)$  to calculate an electron density<sup>(12)</sup> or a difference electron density<sup>(13)</sup>. A plot of one of these usually suggests changes which will improve the model, and the whole procedure can be repeated. A decreasing  $R_2$  factor indicates an improved fit between observed and calculated structure amplitudes. A final  $R_2$  factor at 0.05 to 0.10 can be expected for intensities measured photographically.

### C. Temperature Factor

The calculated structure factors can be brought closer to those observed by the inclusion of a temperature factor

$$\exp(-\vec{H} \cdot \beta \cdot \vec{H})$$

which takes account of the thermal motion of atoms about their mean positions. Thus  $F_c(hkl)$  becomes

$$F_c(hkl) = F_c(\vec{H}) = \sum f_j \exp(-\vec{H} \cdot \beta \cdot \vec{H}) \exp(2\pi i \vec{H} \cdot \vec{r}_j).$$

$\beta$  is a variable tensor for each atom and can be related<sup>(8)</sup> to the root mean square displacement of the atom by

$$\beta_{ii} = 2\pi^2 b_i b_i u_{ii} \text{ and } \beta_{ij} = 4\pi^2 b_i b_j u_{ij}$$

where  $b_i b_j$  are the reciprocal lattice parameters. The eigenvectors of the matrix  $\underline{u}$  are the direction cosines of the principal axes of the thermal ellipsoid and the eigenvalues are the root mean square displacements along the principal axes. All thermal parameters given in the thesis are in terms of the  $u_{ij}$ .

#### D. Least Squares Procedure

Once a reasonable model has been found the parameters can be further refined by the method of least squares. This method allows a quantitative determination of the estimated standard deviations (esd's) of the atomic parameters, although no account is taken of systematic errors.

As mentioned in Section B, a small  $R_2$  factor indicates a good fit between the observed and calculated structure amplitudes. The least squares process varies the atomic parameters  $x_1, x_2, x_3 \dots x_M$  to minimize  $R_2$ . If there are  $M$  parameters to be varied simultaneously, then the solution of  $M$  simultaneous equations is required.

$$\frac{\partial R_2}{\partial x_k} = 0 \quad k = 1, 2, 3 \dots M$$

If  $F_c(x_1, x_2, \dots, x_M)$  is the structure factor calculated using a set of trial parameters  $x_1, x_2, \dots, x_M$ , then the true value of the structure factor can be written

$$F_c(x_1 + \Delta x_1, \dots, x_M + \Delta x_M) = F_c(x_1, \dots, x_M) + \sum_{k=1}^M \frac{\partial F_c(x_1, \dots, x_M)}{\partial x_k} \cdot \Delta x_k + \dots$$

where  $x_1 + \Delta x_1$  etc. are the true parameters.

If the Taylor expansion is expanded only to first order the normal equations,  $\partial R_2 / \partial x_k = 0$ , are linear in the parameter corrections,  $\Delta x_k$ , and can be solved. This method (called non-linear least squares) is used when a number of parameters are to be determined from a larger number of observations.

### E. Weighting Scheme

The full power of the least squares method is realized when a correct choice of the weights  $w_i$  is made. In the preliminary stages of the refinement it is convenient to use unit weights. Later, the weights can be approximated by a simple function of some systematic parameter, usually  $|F_o|$ . The absolute values of the uncertainties are frequently more strongly dependent on  $|F_o|$  than on any other factor<sup>(14)</sup>. The functional form taken is

$$w_i^{-1} = A + B|F_o|_i + C|F_o|_i^2$$

where A, B, and C are constants determined by satisfying the criterion that the average weighted discrepancy

$$\langle w_i \Delta^2 \rangle = \langle w_i ||F_o| - |F_c||_i^2 \rangle$$

be a constant function of  $|F_o|$ . The weights were calculated using this method for all structures refined in these studies.

### ii. General Experimental Procedures

#### A. Measurement of Unit Cell Constants

All unit cell constants have been accurately determined from photographs which were calibrated with the diffraction pattern of a single crystal of rutile, the tetragonal modification of  $TiO_2$ . The cell constants of rutile are given by Cromer and Herrington as  $a = 4.5929(5)\text{\AA}$ , and  $c = 2.9591(3)\text{\AA}$ <sup>(15)</sup>. All measurements were made using Buerger precession photographs. For this method the measured distance of the dif-

fraction spot from the centre ( $\Delta$ ) is related to the reciprocal cell spacings by the expression

$$d^* = \frac{\Delta}{D \times \lambda}$$

where  $D$  is the distance from the crystal to the film holder, and  $\lambda$  is the wavelength of the x-rays. The known values of  $d^*$  for  $\text{TiO}_2$  were used to calculate values of  $D$ , thus correcting for film shrinkage. These corrected values were then used to calculate the unknown reciprocal cell spacings. The wave lengths used for all accurate cell constant determinations in this study are

$$\begin{aligned} \text{Mo K } \alpha_1 &= 0.70926 \text{ \AA} \\ \alpha_2 &= 0.71354 \text{ \AA} \\ \bar{\alpha} &= 0.71069 \text{ \AA} \end{aligned}$$

The  $d^*$  spacings thus obtained were refined by a least squares procedure using the FORTRAN program DESLS written by Dr. B. Robertson.

#### B. Measurement and Correction of Intensities

All intensities have been measured by photographic techniques using either Weissenberg or precession integrating single crystal cameras, the range of intensities being increased by the use of multiple films. The intensities of the reflections were measured on a Joyce Loebel recording photomicrodensitometer. Intensities that were too small to measure were given the lowest value measured on the particular photograph.

The intensities measured are related to the structure factors by the relationship

$$I(\vec{H}) = k |F(\vec{H})|^2 \cdot A \cdot L \cdot p$$

where  $k$  is a constant which depends on the volume, intensity and wavelength of the incident x-ray beam but is independent of  $\vec{H}$ ,  $A$  is the absorption factor,  $L$  is the Lorentz factor and  $p$  is the polarization factor. The Lorentz factor arises because the time required for crystal planes to move through their reflecting positions is not constant but varies with the positions of the planes and the directions in which they approach the reflecting position. This factor also depends on the geometry of the camera <sup>(6)</sup>. The polarization factor arises from the variation in the degrees of polarization at different diffracting angles. Lorentz and polarization ( $Lp$ ) corrections were applied to the observed intensities using the FORTRAN programs WEILPC (Weissenberg) and PRELPC (precession) written in this laboratory.

The absorption factor  $A$  is due to the absorption of the incident and diffracted x-rays as they pass through the crystal.

$$A = \frac{1}{V} \int_V \exp(-\mu x) dv$$

$x$  is the total path length of x-rays diffracted by a volume element  $dv$  in the crystal, and  $\mu$  is the linear absorption coefficient of the crystal for the particular x-ray wave length. Ideally if  $\mu R$  is less than 1.0, i.e. if  $\mu$  and the crystal



radius (R) are sufficiently small, then this effect can be ignored. Absorption corrections were only considered necessary for one of the crystals in this investigation ( $\text{Li}_2\text{TiF}_6 \cdot 2\text{H}_2\text{O}$ ).

Refinements were carried out using a full matrix nonlinear least squares program (CUDLS) written by Dr. J. S. Stephens. All Patterson maps, electron density maps and difference electron density maps were calculated using the FORTRAN program SYMFOU written by Dr. J. S. Rutherford.

For the calculation of structure factors, the scattering factors ( $f_j(\vec{H})$  page 9) were those for the ionic species  $\text{Ti}^{+4}$ ,  $\text{Li}^{+1}$ ,  $\text{Na}^{+1}$ ,  $\text{F}^{-1}$ ,  $\text{O}^{-2}$ ,  $\text{Sn}^{+4}$ , and  $\text{Al}^{+3}$ , obtained by linear interpolation from the values given in the International Tables for X-ray Crystallography<sup>(6)</sup>.

### C. Bond Distances and Angles

All interatomic bond distances and bond angles and their estimated standard deviations were calculated using the Fortran program (CUDLS) written by Dr. J. S. Stephens. The thermal corrections to bond lengths, and the rms displacements and direction cosines for the thermal ellipsoids were calculated using the Fortran program (MOLG) written by Dr. I. D. Brown and Dr. J. Brandon.

## CHAPTER II

### FLUORIDES

#### i. Crystal Structure Determination of $\text{Li}_2\text{TiF}_6 \cdot 2\text{H}_2\text{O}$

##### A. Preliminary Investigations

$\text{Li}_2\text{TiF}_6 \cdot 2\text{H}_2\text{O}$  was prepared by dissolving commercial grade  $\text{Li}_2\text{TiF}_6$  in 40% aqueous HF and slowly crystallizing from solution. The colourless crystals were slightly unstable in air.

A single crystal that measured 0.75 mm  $\times$  0.65 mm  $\times$  0.70 mm was cut and immediately placed in a completely dry capillary tube 3 mm. in diameter. This crystal was used for all further x-ray studies. Preliminary x-ray photographs showed that the crystal had monoclinic symmetry, with space group  $C2$ ,  $Cm$ , or  $C2/m$ . The systematic absences,  $hk\ell$ ,  $h+k = 2n$ , did not allow an unambiguous determination of space group. An  $hk0$  photograph showed 'quasi'-hexagonal symmetry.\*

The unit cell constants were accurately determined following the procedure outlined in Chapter I, using an  $h0\ell$  precession photograph for  $a^*$ ,  $c^*$ , and  $\beta^*$ , and  $0k\ell$  precession photograph for  $b^*$ . The final values are given in Table I.

---

\*The term pseudo-hexagonal would normally be applied if the angles between the hexagonal axes were exactly 60 degrees but the intensities did not have the correct symmetry. In this case the angles are also slightly different so the term quasi-hexagonal has been coined.

Table I - Crystal Data for  $\text{Li}_2\text{TiF}_6 \cdot 2\text{H}_2\text{O}$

System	Monoclinic
Systematic Absences	$h, k, l \quad h+k = 2n+1$
Space Group	$C2, C_m, C2/m$
Cell Constants	
a	10.294(1) Å <sup>°*</sup>
b	5.934(2) Å <sup>°</sup>
c	4.8032(5) Å <sup>°</sup>
$\beta$	90.13(8)°
Unit Cell Volume	293.45 Å <sup>3</sup>
Reciprocal Cell Constants	
$a^*$	0.09714(1) Å <sup>-1</sup>
$b^*$	0.16849(6) Å <sup>-1</sup>
$c^*$	0.20819(3) Å <sup>-1</sup>
$\beta^*$	89.87(8)°
Density	
measured	2.46(9) g/cm <sup>3</sup>
calculated	2.40(3) g/cm <sup>3</sup>
Number of Formula Units per Unit Cell (Z)	2
x-ray absorption coefficients	
Cu $K_\alpha$	58.4 cm <sup>-1</sup>
Mo $K_\alpha$	6.6 cm <sup>-1</sup>

\*The error (or standard deviation where least squares is involved) in the final digit will be designated by placing ° in parentheses e.g. 10.294(1)Å is equivalent to 10.294±0.001 Å.

Multiple film x-ray photographs were taken with an equi-inclination integrating Weissenberg camera for layers  $h0l$ ,  $h1l$ ,  $h2l$ ,  $h3h0$ ,  $hh0$ ,  $hh2$ ,  $hh4$ ,  $hh6$ ,  $hh8$ , and  $hh10$ , using filtered  $\text{CuK}_\alpha$  radiation. The  $hk0$  photographs were taken with an integrating Buerger precession camera using filtered  $\text{Mo K}_\alpha$  radiation. A total of 698 reflections were recorded.

The linear absorption coefficient ( $\mu$ ) for  $\text{Li}_2\text{TiF}_6 \cdot 2\text{H}_2\text{O}$  is  $58.4 \text{ cm}^{-1}$  for  $\text{Cu K}_\alpha$  radiation, and  $6.6 \text{ cm}^{-1}$  for  $\text{Mo K}_\alpha$  radiation. As the average radius,  $R$ , of the crystal was  $0.36 \text{ mm}$ , the absorption parameter  $\mu R$  was  $2.1$  for  $\text{Cu K}_\alpha$  radiation and absorption corrections corresponding to this value of  $R$  for a spherical crystal were applied to all the reflections measured with  $\text{Cu K}_\alpha$  radiation. Corrections were not considered necessary for reflections measured with  $\text{Mo K}_\alpha$  radiation.

The density of the crystals, measured by flotation in a solution of bromoform and methyl iodide, was found to be  $2.46(9) \text{ g/cm}^3$ . The molecular weight is  $211.7$  and the unit cell volume is  $293.45 \text{ \AA}^3$ . Therefore assuming two formula units per unit cell ( $Z$ ) the calculated density

$$\rho_c = \frac{(1.66)(Z)(\text{Molecular weight})}{\text{Volume of Unit Cell } (\text{\AA}^3)}$$

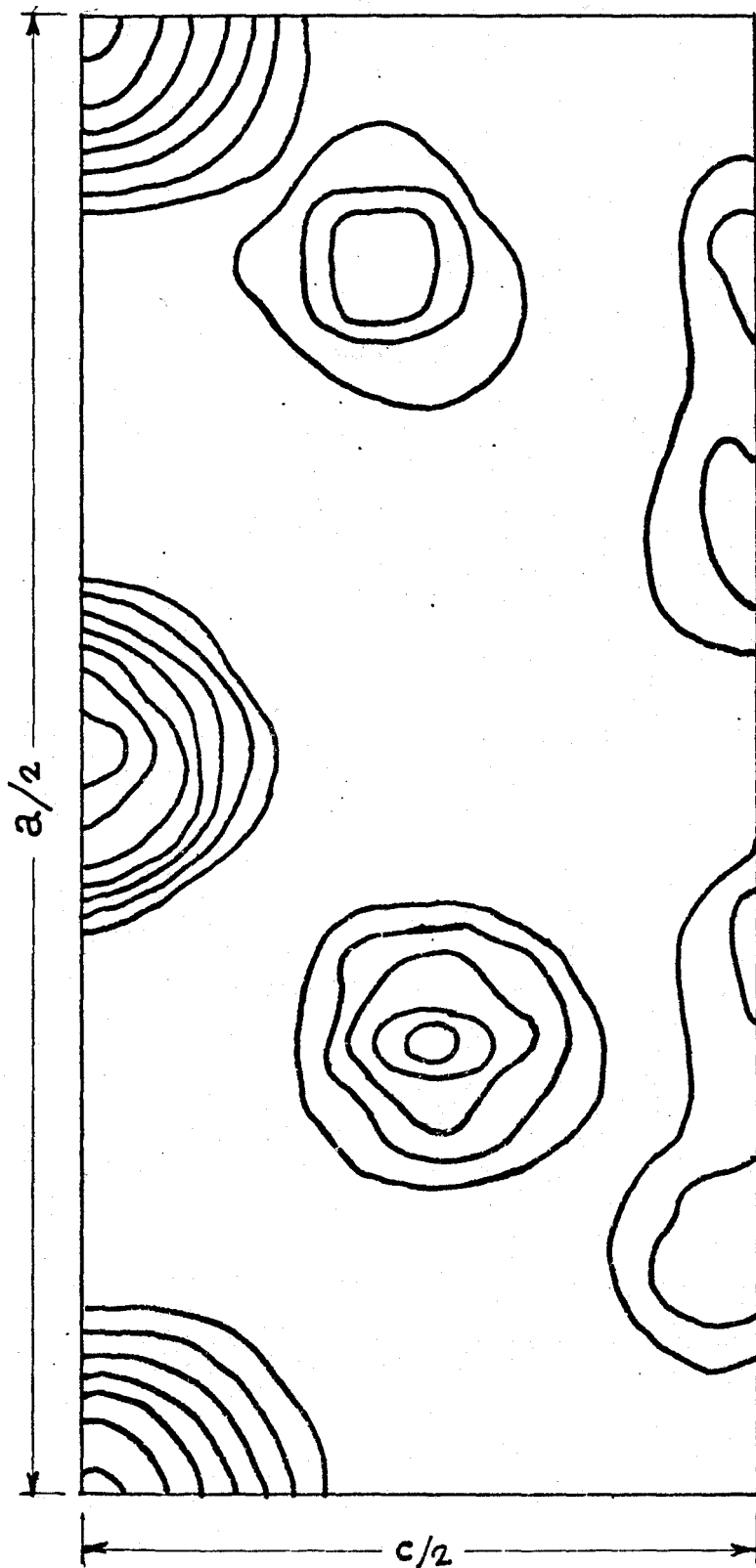
was found to be  $2.40(3) \text{ g/cm}^3$ , in good agreement with the measured value.

## B. Determination and Refinement of Structure

The position of the titanium atom and approximate positions for the fluorine and oxygen atoms were obtained from the h0l Patterson projection, Figure 3. From this it could be seen that in projection the fluorine and oxygen atoms were arranged in approximate rows perpendicular to the c axis with the titanium at the origin. The y coordinates were estimated from the projected lengths of the Ti-F bonds since the Ti-F bond is known to be about  $1.9 \text{ \AA}^{\circ(2)}$ . A preliminary least squares refinement using this model gave  $R_2 = 0.13$ . At first the space group C2 was assumed but the positions of the atoms refined towards those values necessary for a centre of symmetry so that the space group C2/m was chosen for further refinement.

There were several interstitial sites with octahedral symmetry which could accommodate a lithium atom. The total number of octahedral 'holes' was eight, the same as the number of close-packed atoms, but one was occupied by the titanium ion leaving seven possibilities. The positions above and below the titanium atom down the c axis did not seem probable as the Ti-Li distance would be only  $2.35 \text{ \AA}$ , and the faces of the octahedra would be shared as well as corners. This was not a desirable nor a necessary alternative. Similar considerations made the most likely position that of  $1/4, 1/4, 1/2$ . This would allow the lithium atom to be surrounded by both oxygen and fluorine atoms. The lithium atom was placed in this position and the  $R_2$  factor dropped to 0.11.

Figure 3  $\text{Li}_2\text{TiF}_6 \cdot 2\text{H}_2\text{O}$   
H01 Patterson Projection



Final refinement with anisotropic temperature factors and a Cruickshank weighting scheme (see Chapter I, i-E), brought the  $R_2$  factor to 0.10.

The final values of the atomic positional and thermal parameters, together with their esd's, are listed in Table II, and the observed and calculated structure factors are tabulated in Table III.

ib. Crystal Structure Determination of  $\text{Li}_2\text{SnF}_6 \cdot 2\text{H}_2\text{O}$

A. Preliminary Investigations

$\text{Li}_2\text{SnF}_6 \cdot 2\text{H}_2\text{O}$  was prepared by dissolving commercial grade  $\text{Li}_2\text{SnF}_6$  in 40% aqueous HF and slowly crystallizing from solution. Very few crystals were formed, but they were not unstable as in the case of  $\text{Li}_2\text{TiF}_6 \cdot 2\text{H}_2\text{O}$ .

A single crystal that measured 0.04 mm  $\times$  0.04 mm  $\times$  0.09 mm was mounted for x-ray studies. A rotation photograph about the c axis, and hk0 and hkl Weissenberg photographs showed that the crystal was monoclinic, with space group  $C_2$ , Cm or  $C2/m$ . An hk0 photograph showed quasi-hexagonal symmetry.

The unit cell constants were accurately determined following the procedure outlined in Chapter I, ii-A. An h0l precession photograph was used for  $a^*$ ,  $c^*$ , and  $\beta^*$ , and an Okl precession photograph for  $b^*$ . The final values are given in Table IV.

Multiple film x-ray photographs were taken with an equi-inclination integrating Weissenberg camera for layers

Table IIa. Final Positional Parameters in  $\text{Li}_2\text{TiF}_6 \cdot 2\text{H}_2\text{O}$   
 and  $\text{Li}_2\text{SnF}_6 \cdot 2\text{H}_2\text{O}$

Atom	Site Symmetry	x	y	z
$\text{Li}_2\text{TiF}_6 \cdot 2\text{H}_2\text{O}$				
2Ti	2/m	0	0	0
8F <sub>1</sub>	1	0.0852 (3)	0.2203 (6)	0.2232 (7)
4F <sub>3</sub>	m	-0.1576 (4)	0	0.2313 (10)
4O	m	0.3434 (6)	0	0.2861 (12)
4Li	$\bar{1}$	1/4	1/4	1/2
$\text{Li}_2\text{SnF}_6 \cdot 2\text{H}_2\text{O}$				
2Sn	2/m	0	0	0
8F <sub>1</sub>	1	0.0875 (5)	0.2297 (9)	0.2297 (9)
4F <sub>3</sub>	m	-0.1624 (6)	0	0.2440 (15)
4O	m	0.3414 (8)	0	0.2794 (17)
4Li	$\bar{1}$	1/4	1/4	1/2



Table IIb. Final Thermal Parameters in  $\text{Li}_2\text{TiF}_6 \cdot 2\text{H}_2\text{O}$  and  $\text{Li}_2\text{SnF}_6 \cdot 2\text{H}_2\text{O}$

Atom	$U_{11}^*$	$U_{22}$	$U_{33}$	$U_{12}$	$U_{13}$	$U_{23}$
<u><math>\text{Li}_2\text{TiF}_6 \cdot 2\text{H}_2\text{O}</math></u>						
Ti	0.0191 (11)	0.0173 (11)	0.0196 (11)	0	0.0023 (7)	0
F <sub>1</sub>	0.0333 (19)	0.0303 (19)	0.0324 (19)	-0.0017 (13)	0.0012 (14)	-0.0012 (13)
F <sub>3</sub>	0.0280 (24)	0.0274 (24)	0.0320 (25)	0	0.0080 (19)	0
O	0.0219 (29)	0.0211 (26)	0.0293 (29)	0	0.0060 (23)	0
Li	0.0707 (120)	0.0467 (95)	0.0475 (94)	0.0176 (96)	-0.0093 (89)	-0.0280 (84)
<u><math>\text{Li}_2\text{SnF}_6 \cdot 2\text{H}_2\text{O}</math></u>						
Sn	0.0087 (5)	0.0065 (5)	0.0100 (5)	0	0.0014 (3)	0
F <sub>1</sub>	0.0213 (27)	0.0254 (26)	0.0155 (21)	-0.0019 (19)	-0.0039 (19)	-0.0071 (17)
F <sub>3</sub>	0.0198 (34)	0.0274 (38)	0.0191 (30)	0	0.0053 (26)	0
O	0.0166 (39)	0.0224 (40)	0.0141 (32)	0	0.0043 (28)	0
Li	0.0308 (111)	0.0409 (134)	0.0153 (80)	-0.0031 (99)	-0.0016 (81)	-0.0077 (81)

\*The  $U_{ij}$  are from the root mean square displacements defined on page 11.

Table III. Observed and Calculated Structure Factors for  $\text{Li}_2\text{SnF}_6 \cdot 2\text{H}_2\text{O}$ . Reflections for which  $x = 1$  are unobserved, those for which  $x = 2$  are unreliable and were not included in the refinement.

h	k	l	x	F_obs	F_calc	h	k	l	x	F_obs	F_calc
2	4	6	0	45.06	35.47	6	2	1	0	12.51	10.36
2	4	6	0	26.22	-25.68	6	2	-1	0	33.70	30.70
2	4	6	0	15.70	14.81	6	2	-1	0	18.89	19.45
2	4	6	0	9.52	9.97	6	2	-1	0	16.81	16.23
1	0	0	0	6.25	8.38	10	0	-2	0	4.24	-2.90
1	0	0	0	24.20	25.27	10	0	-2	0	22.73	22.94
1	1	1	1	51.10	49.00	10	1	3	0	41.70	37.99
1	1	1	1	30.74	24.54	10	1	3	-1	13.51	12.16
1	1	1	1	19.81	20.63	10	1	3	-1	35.36	35.00
1	1	1	1	17.87	18.25	10	1	3	-1	4.01	-1.10
1	1	1	1	13.07	13.76	10	1	3	-1	25.64	25.02
1	1	1	1	12.21	13.18	10	1	3	-1	25.64	25.02
1	0	0	0	31.71	23.30	10	0	-3	0	18.82	20.38
2	2	2	2	7.02	-6.73	10	0	-3	-1	14.51	14.40
2	2	2	2	14.14	15.54	10	0	-3	-1	25.24	22.71
2	2	2	2	60.76	75.34	10	0	-3	-1	3.02	4.90
2	2	2	2	19.84	20.84	10	0	-3	-1	17.20	16.57
1	0	0	0	3.45	-3.67	10	0	-3	-1	10.70	10.90
1	0	0	0	3.77	-3.67	10	0	-3	-1	20.18	19.15
1	0	0	0	6.65	7.87	10	0	-3	-1	19.17	19.15
1	1	1	1	8.44	9.30	10	0	-3	-1	30.19	29.47
1	1	1	1	24.16	21.42	10	0	-3	-1	21.78	19.09
1	1	1	1	24.62	22.26	10	0	-3	-1	15.16	-13.11
1	1	1	1	24.56	26.38	10	0	-3	-1	43.35	41.38
1	1	1	1	10.54	10.07	10	0	-3	-1	10.58	9.30
1	1	1	1	6.68	6.12	10	0	-3	-1	22.50	19.30
1	0	0	0	67.81	72.89	10	0	-3	-1	26.22	28.20
1	0	0	0	17.56	16.56	10	0	-3	-1	10.41	-8.65
1	0	0	0	3.56	-2.22	10	0	-3	-1	14.61	10.33
1	0	0	0	16.87	16.13	10	0	-3	-1	14.25	13.86
1	0	0	0	9.21	9.14	10	0	-3	-1	26.72	24.87
1	0	0	0	5.70	4.93	10	0	-3	-1	2.60	-1.42
1	1	1	1	32.28	30.74	10	0	-3	-1	26.50	25.62
1	1	1	1	12.31	12.92	10	0	-3	-1	6.12	6.22
1	1	1	1	5.17	4.47	10	0	-3	-1	18.54	17.27
1	1	1	1	5.27	4.80	10	0	-3	-1	19.37	16.99
1	0	0	0	10.22	10.00	10	0	-3	-1	6.20	6.20
1	0	0	0	16.06	18.52	10	0	-3	-1	12.17	2.46
1	0	0	0	6.82	6.55	10	0	-3	-1	12.76	12.55
1	0	0	0	5.00	5.20	10	0	-3	-1	11.92	12.55
1	0	0	0	21.98	23.52	10	0	-3	-1	22.62	25.42
1	0	0	0	25.72	23.52	10	0	-3	-1	4.81	-4.53
1	0	0	0	9.24	9.18	10	0	-3	-1	10.16	9.79
1	0	0	0	2.68	3.19	10	0	-3	-1	14.14	17.11
1	0	0	0	8.51	9.90	10	0	-3	-1	7.40	6.48
1	0	0	0	15.10	12.93	10	0	-3	-1	14.04	12.53
1	0	0	0	37.20	35.88	10	0	-3	-1	8.57	5.71
1	0	0	0	42.69	41.41	10	0	-3	-1	14.13	14.82
1	0	0	0	38.56	46.95	10	0	-3	-1	49.75	-54.22
1	0	0	0	50.48	-50.28	10	0	-3	-1	5.13	5.02
1	0	0	0	76.94	90.04	10	0	-3	-1	32.85	32.81
1	0	0	0	12.99	12.07	10	0	-3	-1	59.14	57.95
1	0	0	0	25.87	28.28	10	0	-3	-1	68.15	77.22
1	0	0	0	42.84	49.99	10	0	-3	-1	20.72	22.06
1	0	0	0	20.01	-24.34	10	0	-3	-1	16.81	17.77
1	0	0	0	18.22	20.66	10	0	-3	-1	26.74	28.70
1	0	0	0	10.40	11.53	10	0	-3	-1	19.14	20.80
1	0	0	0	20.44	17.19	10	0	-3	-1	16.42	15.36
1	1	1	1	30.50	38.54	10	1	0	0	11.87	12.39
1	1	1	1	22.48	39.13	10	1	0	0	3.88	-2.25
1	1	1	1	15.31	12.81	10	1	0	0	9.66	9.00
1	1	1	1	24.28	20.67	10	1	0	0	24.52	29.71
1	1	1	1	20.12	17.28	10	1	0	0	21.24	20.72
1	1	1	1	26.00	31.84	10	1	0	0	17.42	15.60
1	1	1	1	25.01	25.15	10	1	0	0	21.56	24.68
1	1	1	1	15.16	17.25	10	1	0	0	21.42	21.38
1	1	1	1	14.28	15.97	10	1	0	0	12.47	12.88
1	1	1	1	7.25	8.84	10	1	0	0	15.60	16.62
1	1	1	1	10.87	10.37	10	1	0	0	11.07	12.46
1	1	1	1	11.83	12.27	10	1	0	0	5.80	5.82
1	1	1	1	26.55	25.61	10	1	0	0	12.03	11.80
1	1	1	1	32.72	25.61	10	1	0	0	19.92	21.19
1	1	1	1	71.77	95.90	10	1	0	0	24.26	21.19
1	1	1	1	50.22	-58.15	10	1	0	0	61.25	63.55
1	1	1	1	25.45	38.02	10	1	0	0		
1	1	1	1	28.26	20.09	10	1	0	0		

h k l x F\_obs F\_calc h k l x F\_obs F\_calc

2	2	-2	0	45.47	48.48	8	-2	3	0	10.84	10.61
4	2	-2	0	30.57	28.62	10	-2	-3	0	12.89	13.97
4	2	-2	0	15.07	12.60	10	-2	-3	0	18.77	17.16
6	2	-2	0	15.24	-15.46	10	-2	-3	0	4.30	2.20
6	-2	-2	0	16.10	-17.10	11	-2	-3	0	8.75	8.24
8	-2	-2	0	33.33	1.95	11	3	-3	0	22.16	25.24
8	-2	-2	0	12.60	13.20	13	3	-3	0	12.31	14.45
0	-2	-2	0	20.40	21.50	22	3	-3	0	34.62	32.60
1	-2	-2	0	30.07	28.38	5	-2	-3	0	7.76	7.86
1	3	-2	0	44.15	42.18	5	-2	-3	0	10.47	10.68
1	3	-2	0	21.58	21.18	7	-2	-3	0	7.47	7.60
3	3	-2	0	28.50	27.39	7	-2	-3	0	3.44	3.35
3	3	-2	0	10.25	12.05	9	-2	-3	0	16.18	15.73
5	3	-2	1	2.40	2.52	9	-2	-3	0	12.10	11.61
5	3	-2	0	11.53	11.37	0	4	-3	0	9.52	8.06
7	3	-2	0	7.62	7.45	0	4	-3	0	9.26	9.06
7	-2	-2	0	5.00	6.00	2	4	-3	0	9.00	10.40
9	-2	-2	0	13.15	12.43	2	4	-3	0	18.23	16.53
9	-2	-2	0	14.55	13.22	4	4	-3	0	25.77	27.16
0	4	-2	0	15.15	-13.30	4	4	-3	0	3.20	-2.15
0	4	-2	0	14.50	-13.30	6	4	-3	0	21.14	19.44
2	4	-2	0	22.01	22.56	6	4	-3	0	15.05	14.57
4	4	-2	0	29.34	31.26	8	4	-3	0	27.10	22.47
4	4	-2	0	40.63	38.57	11	5	-3	0	8.90	8.83
6	4	-2	0	8.40	8.43	3	5	-3	2	2.24	1.90
8	4	-2	0	15.02	16.78	3	5	-3	2	8.66	23.00
8	4	-2	0	16.11	14.40	5	5	-3	2	9.81	10.51
1	5	-2	0	4.55	4.92	5	5	-3	2	7.62	16.11
1	5	-2	0	33.53	22.27	7	5	-3	2	14.90	7.88
3	5	-2	0	19.35	12.60	0	6	-3	1	11.70	11.98
5	5	-2	0	15.70	17.46	2	6	-3	2	11.40	13.88
5	5	-2	0	27.74	14.51	2	6	-3	2	13.21	18.43
7	5	-2	0	20.66	25.16	4	6	-3	2	4.54	10.04
7	5	-2	0	12.00	17.71	4	6	-3	2	3.87	5.96
0	6	-2	0	5.02	11.33	0	4	-4	0	43.32	47.57
0	6	-2	0	4.32	4.63	2	4	-4	0	26.00	26.06
2	6	-2	0	18.78	18.74	2	4	-4	0	3.90	4.00
2	6	-2	0	16.51	17.87	4	4	-4	0	10.40	9.91
4	6	-2	0	14.00	14.81	4	4	-4	0	5.46	-5.52
4	6	-2	0	10.45	11.90	6	4	-4	0	5.28	6.80
6	6	-2	1	2.55	2.06	6	6	-4	0	12.80	12.90
6	6	-2	1	7.06	10.60	8	6	-4	0	22.04	13.00
0	7	-2	0	7.01	5.06	8	6	-4	0	13.01	12.37
2	7	-2	0	19.43	19.50	11	7	-4	0	12.12	12.81
2	7	-2	0	17.48	16.81	11	7	-4	0	22.70	28.23
4	7	-2	0	40.08	51.60	3	7	-4	0	11.32	11.94
4	7	-2	0	10.98	-11.25	5	7	-4	0	10.32	11.08
6	7	-2	0	28.64	21.40	5	7	-4	0	18.85	18.59
6	7	-2	0	22.46	22.90	7	7	-4	0	4.13	4.27
8	7	-2	0	6.55	-6.06	7	7	-4	0	7.10	7.08
8	7	-2	0	24.23	36.90	7	7	-4	0	17.20	17.12
0	8	-2	0	4.02	3.68	0	7	-4	0	12.58	11.80
0	8	-2	0	11.02	10.00	0	7	-4	0	12.01	12.36
1	8	-2	0	10.50	11.04	2	7	-4	1	12.57	12.36
1	8	-2	0	12.60	13.60	2	7	-4	1	2.20	-
3	8	-2	0	22.82	22.34	4	7	-4	1	15.44	13.35
3	8	-2	0	27.85	28.30	4	7	-4	1	2.76	2.70
5	8	-2	0	22.66	20.80	6	7	-4	0	17.00	17.48
5	8	-2	0	11.54	11.46	6	7	-4	0	26.20	26.63
7	8	-2	0	6.57	6.88	6	7	-4	0	28.60	29.23
7	8	-2	0	6.60	13.42	8	7	-4	0	16.25	15.62
9	8	-2	0	11.50	11.75	8	7	-4	1	5.72	6.52
9	8	-2	0	10.00	18.72	11	7	-4	1	2.29	1.70
0	9	-2	0	20.60	27.14	11	7	-4	0	18.97	17.96
0	9	-2	0	24.26	27.14	2	7	-4	0	4.50	4.81
2	9	-2	0	12.52	-14.58	3	7	-4	0	17.20	16.20
2	9	-2	0	52.68	56.56	5	7	-4	0	18.04	19.40
4	9	-2	0	10.21	10.06	5	7	-4	0	11.00	10.57
4	9	-2	0	16.53	15.12	7	7	-4	0	13.27	11.87
6	9	-2	0	11.99	10.80	7	7	-4	0	17.26	16.42
6	9	-2	0	2.20	1.74	0	4	-4	0	24.62	27.10
2	2	0	0	45.47	48.48	2	4	4	0	14.70	15.25

h	k	l	x	F <sub>obs</sub>	F <sub>calc</sub>
2	4	-4	0	3.23	4.45
4	-4	-4	0	8.55	7.22
4	4	-4	0	1.89	1.16
6	-4	-4	0	10.48	11.47
1	5	-4	0	11.69	12.32
1	5	-4	0	14.34	17.84
3	5	-4	0	2.95	4.73
0	0	5	0	18.07	18.03
0	0	5	0	18.07	18.03
2	0	5	0	15.48	16.38
2	0	5	0	17.00	17.38
4	0	5	0	15.02	17.27
1	-1	5	0	18.56	18.31
1	1	-5	0	15.31	15.28
3	1	5	1	2.27	3.50
3	1	-5	0	4.83	5.21
5	1	5	1	7.71	7.50
5	1	-5	0	14.50	13.60
7	1	-5	0	14.20	11.49
0	2	5	0	4.27	4.15
0	2	-5	0	4.13	4.15
2	2	5	0	16.01	16.90
2	2	-5	0	5.07	3.95
4	2	5	0	19.09	15.70
4	2	-5	0	15.52	15.00
6	-2	-5	0	15.55	14.41
1	3	5	0	13.67	13.11
1	3	-5	0	6.89	7.72
3	-3	5	0	7.67	7.96
3	3	-5	1	1.32	.54
5	3	-5	0	12.54	13.48
0	4	-5	0	8.79	10.82
2	4	-5	2	1.36	12.46
2	4	-5	0	10.06	10.50

Table IV - Crystal Data for  $\text{Li}_2\text{SnF}_6 \cdot 2\text{H}_2\text{O}$

System	Monoclinic
Systematic Absences	$h, k, l \quad h+k = 2n$
Space Group	$C2, Cm, C2/m$
Cell Constants	
a	9.818 (3) Å
b	6.101 (2) Å
c	4.7270 (6) Å
$\beta$	90.96 (8)°
Unit Cell Volume	283.09 Å <sup>3</sup>
Reciprocal Cell Constants	
a*	.10187 (3) Å <sup>-1</sup>
b*	.16392 (4) Å <sup>-1</sup>
c*	.21158 (3) Å <sup>-1</sup>
$\beta^*$	89.04 (8)°
Density	
measured	3.40 (9) g/cm <sup>3</sup>
calculated	3.13 (3) g/cm <sup>3</sup>
Number of Formula Units per Unit Cell (Z)	2
X-ray absorption coefficients	
Cu K <sub>α</sub>	72.15 cm <sup>-1</sup>
Mo K <sub>α</sub>	8.69 cm <sup>-1</sup>

hk0, hk1, hk2, hk3, and hk4, using filtered Cu  $K_{\alpha}$  radiation. h0l, h1l, h2l, and 0kl, lkl, 2kl, 3kl, and 4kl photographs were taken with an integrating Buerger precession camera using filtered Mo  $K_{\alpha}$  radiation. There were 759 measurable reflections.

The linear absorption coefficient ( $\mu$ ) for  $\text{Li}_2\text{SnF}_6 \cdot 2\text{H}_2\text{O}$  is  $72.15 \text{ cm}^{-1}$  for Cu  $K_{\alpha}$  radiation and  $8.69 \text{ cm}^{-1}$  for Mo  $K_{\alpha}$  radiation. The corresponding  $\mu R$  for a crystal of average radius 0.06 mm is 0.435 and 0.052 respectively. Absorption corrections were not considered necessary.

The density of the crystals was measured by flotation in a solution of s-tetrabromoethane and methylene iodide. The measured value of  $3.40(9) \text{ g/cm}^3$  agreed well with the calculated value of  $3.31(3) \text{ g/cm}^3$ .

#### B. Determination and Refinement of Structure

The similarity of the space group and cell dimensions of  $\text{Li}_2\text{SnF}_6 \cdot 2\text{H}_2\text{O}$  to  $\text{Li}_2\text{TiF}_6 \cdot 2\text{H}_2\text{O}$  suggested that the structures might be the same. The positional parameters of the latter compound were chosen as an initial model for  $\text{Li}_2\text{SnF}_6 \cdot 2\text{H}_2\text{O}$ , and one cycle of least squares refinement using these values gave  $R_2 = 0.11$ . After anisotropic temperature factors and a suitable weighting scheme were included the final  $R_2$  factor was 0.078.

The final values of the atomic positional and thermal parameters, together with their esd's are listed in Table II and the observed and calculated structure factors are ta-

bulated in Table V.

## ic. Discussion of Structures

### Close-Packing

The compounds  $\text{Li}_2\text{MF}_6 \cdot 2\text{H}_2\text{O}$  ( $\text{M} = \text{Sn}, \text{Ti}$ ) are isostructural. The structure may be described as an approximately close-packed array of fluorine and water with lithium and tin or titanium occupying octahedral interstices. The fluorine and water are arranged within the array so that for every oxygen atom there are twelve approximately equidistant fluorine atoms, with an average oxygen-fluorine distance of  $2.87(1) \text{ \AA}$  for the tin compound and  $2.97(1) \text{ \AA}$  for the titanium compound. If the structure is viewed down the  $c$  axis, then a simple hexagonally close-packed sequence is observed, ABAB....., with M atoms between the A and B layers and lithium atoms between the B and A layers. The ionic radius of the fluorine ion is  $1.33 \text{ \AA}^{(2)}$  and two close-packed layers would require an axis length of  $4.66 \text{ \AA}$ . The  $c$  axis lengths are  $4.77 \text{ \AA}$  for  $\text{M} = \text{Ti}$  and  $4.73 \text{ \AA}$  for  $\text{M} = \text{Sn}$ . The packing is not ideal however as the layers are of composition  $\text{O}(\text{H}_2)\text{F}_3$ . The water molecules are moved out of the plane of the fluorine atoms and a puckering occurs which increases the length of the axis. The difference in the  $z$  coordinates of the oxygen and fluorine atoms indicates the extent of the puckering (See Table II).



Table V. Observed and Calculated Structure Factors for  $\text{Li}_2\text{TiF}_6 \cdot 2\text{H}_2\text{O}$ . Reflections for which  $x = 1$  are unobserved, those for which  $x = 2$  are unreliable and were not included in the refinement.

h	k	l	x	F_obs	F_calc	h	k	l	x	F_obs	F_calc
2	4	6	0	71.00	88.95	2	2	1	0	46.78	49.93
2	4	6	0	26.14	23.66	2	2	-1	0	52.21	51.81
2	4	6	0	55.50	55.48	10	2	-1	0	21.26	19.50
2	4	6	0	45.56	43.07	10	2	-1	0	54.44	55.93
10	2	2	0	42.22	30.87	12	2	-1	0	29.23	30.40
12	2	2	0	56.60	54.97	12	2	-1	0	32.59	34.48
11	2	2	0	74.30	102.36	11	2	-1	0	79.89	82.03
11	2	2	0	79.78	75.07	11	2	-1	0	60.40	58.98
5	5	5	0	68.60	67.53	2	2	-1	0	88.20	73.40
7	7	7	0	54.82	55.74	3	3	-1	0	51.50	49.11
0	0	0	0	44.04	44.44	3	3	-1	0	56.68	58.94
0	0	0	0	40.08	41.45	5	5	-1	0	55.31	58.32
1	1	1	0	21.60	31.07	7	7	-1	0	49.53	48.09
2	2	2	0	72.25	72.65	7	7	-1	0	54.27	52.66
2	2	2	0	43.27	40.42	9	9	-1	0	28.42	23.24
2	2	2	0	62.81	64.55	9	9	-1	0	55.11	58.80
1	1	1	0	113.02	119.49	2	2	-1	0	59.29	65.28
2	2	2	0	46.27	48.90	2	2	-1	0	64.04	64.46
2	2	2	0	20.84	22.93	2	2	-1	0	82.00	84.25
2	2	2	0	32.72	31.96	4	4	-1	0	48.15	45.50
1	1	1	0	55.44	60.20	6	6	-1	0	53.22	49.62
3	3	3	0	66.42	64.06	6	6	-1	0	19.17	15.27
3	3	3	0	72.31	71.96	1	1	-1	0	45.19	49.34
3	3	3	0	61.11	56.50	1	1	-1	0	55.74	58.70
3	3	3	0	42.32	38.68	2	2	-1	0	26.47	25.42
1	1	1	0	34.09	32.44	3	3	-1	0	62.50	59.56
4	4	4	0	110.03	117.55	5	5	-1	0	44.12	41.25
4	4	4	0	55.16	57.32	5	5	-1	0	54.17	50.63
4	4	4	0	34.20	32.89	7	7	-1	0	49.14	47.16
4	4	4	0	45.52	46.89	7	7	-1	0	29.10	24.42
4	4	4	0	27.28	26.92	5	5	-1	0	45.90	44.56
1	1	1	0	22.10	22.61	2	2	-1	0	68.45	62.60
5	5	5	0	61.70	65.73	4	4	-1	0	18.61	21.04
5	5	5	0	49.32	47.99	4	4	-1	0	45.94	42.90
5	5	5	0	40.26	38.52	6	6	-1	0	60.65	46.92
5	5	5	0	25.91	26.00	6	6	-1	0	35.84	24.37
5	5	5	0	36.22	35.99	6	6	-1	0	46.71	40.64
6	6	6	0	46.52	46.85	1	1	-1	0	42.77	42.90
6	6	6	0	36.41	35.47	1	1	-1	0	26.48	24.17
6	6	6	0	29.05	28.85	3	3	-1	0	45.09	43.98
6	6	6	0	66.29	58.63	7	7	-1	0	29.88	29.34
2	2	2	0	22.23	33.67	5	5	-1	0	29.72	37.52
2	2	2	0	32.27	32.70	8	8	-1	0	31.83	33.15
2	2	2	0	37.68	38.39	2	2	-1	0	37.34	37.13
5	5	5	0	43.54	42.47	2	2	-1	0	32.10	31.72
0	0	0	0	41.08	46.04	0	0	-1	0	16.20	-12.02
2	2	2	0	20.08	21.67	2	2	-1	0	65.69	46.98
4	4	4	0	12.67	16.56	2	2	-1	0	88.17	80.12
4	4	4	0	56.05	58.48	4	4	-1	0	105.24	105.76
6	6	6	0	64.23	63.16	4	4	-1	0	109.82	118.46
8	8	8	0	8.04	5.67	5	5	-1	0	59.50	58.76
8	8	8	0	80.00	87.28	6	6	-1	0	52.26	51.59
1	1	1	0	47.54	48.12	8	8	-1	0	62.00	62.90
1	1	1	0	46.16	45.54	8	8	-1	0	59.71	59.20
1	1	1	0	22.29	26.12	2	2	-1	0	40.15	38.62
1	1	1	0	41.22	40.78	2	2	-1	0	37.25	37.24
1	1	1	0	160.42	80.50	2	2	-1	0	12.20	17.17
3	3	3	0	63.51	63.88	2	2	-1	0	11.21	17.71
3	3	3	0	94.03	79.72	1	1	-1	0	81.96	73.05
5	5	5	0	62.98	61.89	1	1	-1	0	60.60	57.59
5	5	5	0	72.04	72.65	3	3	-1	0	74.20	72.58
7	7	7	0	62.02	62.50	3	3	-1	0	76.29	74.41
7	7	7	0	51.71	51.34	5	5	-1	0	52.09	54.05
0	0	0	0	46.22	44.96	5	5	-1	0	65.87	67.49
1	1	1	0	41.59	42.18	5	5	-1	0	55.22	54.54
1	1	1	0	40.25	35.81	7	7	-1	0	49.24	48.66
1	1	1	0	29.00	29.42	7	7	-1	0	43.85	44.20
1	1	1	0	29.22	29.95	9	9	-1	0	43.23	44.67
2	2	2	0	29.22	29.70	1	1	-1	0	20.70	20.26
2	2	2	0	69.11	75.37	1	1	-1	0	24.22	25.71
2	2	2	0	89.72	148.57	1	1	-1	0	22.92	27.64
2	2	2	0	20.20	14.23	1	1	-1	0	22.07	27.46
4	4	4	0	76.84	80.84	2	2	-1	0	67.12	66.79
4	4	4	0	61.08	74.88	2	2	-1	0	109.42	107.68
6	6	6	0	48.28	46.28						
6	6	6	0	62.98	65.65						

h	k	l	x	F_obs	F_calc	h	k	l	x	F_obs	F_calc
-2	-2	2	0	83.60	98.87	0	1	1	0	27.22	28.02
-2	-2	2	0	108.44	107.68	0	1	1	0	43.15	44.75
-2	-2	2	0	61.56	62.87	0	1	1	0	30.24	30.30
-4	-2	2	0	48.92	48.24	1	1	1	0	29.27	31.21
-4	-2	2	0	14.07	13.50	1	1	1	0	23.26	22.92
-6	-2	2	0	15.26	13.61	1	1	1	0	22.60	26.07
-8	-2	2	0	22.72	32.92	2	2	2	0	81.47	78.22
-8	-2	2	0	48.69	48.04	2	2	2	0	18.19	12.72
-10	-2	2	0	55.24	52.37	-2	-2	-2	0	101.94	98.86
-10	-2	2	0	57.67	58.56	-2	-2	-2	0	46.10	43.12
-12	-2	2	0	24.18	27.79	-2	-2	-2	0	57.44	40.20
-12	-2	2	0	32.26	31.40	-2	-2	-2	0	42.91	43.19
-14	-2	2	0	72.17	76.69	-6	-6	-6	0	33.87	34.81
-14	-2	2	0	58.65	63.94	-6	-6	-6	0	40.60	41.28
-16	-2	2	0	58.05	61.61	-6	-6	-6	0	43.65	43.63
-16	-2	2	0	61.76	60.14	-10	-10	-10	0	41.41	43.93
-20	-2	2	0	46.67	47.75	-10	-10	-10	0	18.29	21.66
-20	-2	2	0	42.74	40.92	-12	-12	-12	0	26.98	31.88
-24	-2	2	0	44.82	48.61	-12	-12	-12	0	33.27	32.12
-24	-2	2	0	46.88	41.83	-12	-12	-12	0	41.61	41.97
-28	-2	2	0	44.88	43.01	-12	-12	-12	0	57.26	58.87
-28	-2	2	0	13.10	16.50	-12	-12	-12	0	46.12	48.12
-32	-2	2	0	41.42	41.46	-12	-12	-12	0	66.46	65.51
-32	-2	2	0	57.21	58.53	-15	-15	-15	0	42.18	41.68
-36	-2	2	0	69.40	70.53	-15	-15	-15	0	45.02	43.62
-36	-2	2	0	71.82	77.53	-17	-17	-17	0	37.64	38.60
-40	-2	2	0	46.78	44.07	-17	-17	-17	0	37.28	38.60
-40	-2	2	0	41.11	40.26	-17	-17	-17	0	40.13	37.02
-44	-2	2	0	53.03	47.92	-17	-17	-17	0	38.77	41.17
-44	-2	2	0	49.50	46.33	-17	-17	-17	0	37.89	36.02
-48	-2	2	0	37.93	40.15	-17	-17	-17	0	38.62	40.91
-48	-2	2	0	25.77	35.82	-20	-20	-20	0	43.06	45.97
-52	-2	2	0	46.26	48.31	-20	-20	-20	0	47.27	46.96
-52	-2	2	0	51.21	50.32	-20	-20	-20	0	62.24	64.01
-56	-2	2	0	53.57	45.78	-20	-20	-20	0	21.67	22.69
-56	-2	2	0	55.77	52.64	-24	-24	-24	0	49.70	49.37
-60	-2	2	0	51.24	44.73	-24	-24	-24	0	49.60	48.58
-64	-2	2	0	42.28	40.49	-24	-24	-24	0	18.68	18.33
-64	-2	2	0	37.33	38.31	-24	-24	-24	0	56.09	52.82
-68	-2	2	0	52.45	54.07	-24	-24	-24	0	27.25	42.51
-68	-2	2	0	50.17	51.08	-24	-24	-24	0	22.75	26.27
-72	-2	2	0	46.01	42.47	-24	-24	-24	0	48.55	52.20
-72	-2	2	0	40.91	36.72	-24	-24	-24	0	40.47	38.17
-76	-2	2	0	19.58	22.02	-24	-24	-24	0	41.92	41.53
-76	-2	2	0	41.33	45.05	-24	-24	-24	0	35.56	34.81
-80	-2	2	0	41.07	40.25	-24	-24	-24	0	22.55	26.77
-84	-2	2	0	36.40	35.61	-24	-24	-24	0	37.24	38.10
-84	-2	2	0	32.85	32.27	-24	-24	-24	0	42.82	46.11
-88	-2	2	0	24.76	22.87	-24	-24	-24	0	18.80	22.95
-88	-2	2	0	24.04	28.64	-24	-24	-24	0	51.58	51.71
-92	-2	2	0	24.00	34.22	-24	-24	-24	0	31.09	33.39
-96	-2	2	0	53.08	49.47	-24	-24	-24	0	32.81	32.00
-96	-2	2	0	65.14	61.26	-24	-24	-24	0	26.92	28.97
-100	-2	2	0	60.42	56.11	-24	-24	-24	0	40.67	36.56
-104	-2	2	0	88.87	91.69	-24	-24	-24	0	26.26	28.44
-104	-2	2	0	20.55	15.78	-24	-24	-24	0	40.87	40.26
-108	-2	2	0	62.44	62.68	-24	-24	-24	0	20.27	25.06
-108	-2	2	0	14.16	14.41	-24	-24	-24	0	20.70	30.25
-112	-2	2	0	67.58	70.13	-24	-24	-24	0	24.20	21.35
-112	-2	2	0	25.20	27.80	-24	-24	-24	0	80.80	91.93
-116	-2	2	0	32.28	32.92	-24	-24	-24	0	60.82	61.36
-116	-2	2	0	40.88	29.72	-24	-24	-24	0	36.41	33.53
-120	-2	2	0	22.62	22.66	-24	-24	-24	0	25.80	34.76
-120	-2	2	0	52.55	52.77	-24	-24	-24	0	24.72	25.94
-124	-2	2	0	56.20	57.42	-24	-24	-24	0	25.25	21.24
-124	-2	2	0	70.78	68.87	-24	-24	-24	0	23.27	31.24
-128	-2	2	0	64.00	63.14	-24	-24	-24	0	41.34	43.25
-128	-2	2	0	35.21	32.74	-24	-24	-24	0	28.67	27.02
-132	-2	2	0	25.67	25.06	-24	-24	-24	0	24.44	25.52
-132	-2	2	0	46.82	45.61	-24	-24	-24	0	25.55	24.99
-136	-2	2	0	46.82	47.00	-24	-24	-24	0	32.17	32.24
-140	-2	2	0	46.82	45.61	-24	-24	-24	0	50.48	46.55
-144	-2	2	0	46.82	47.00	-24	-24	-24	0	61.42	61.42
-148	-2	2	0	46.82	45.61	-24	-24	-24	0	41.53	42.36

h	k	l	x	F_obs	F_calc	h	k	l	x	F_obs	F_calc
2	1	-4	0	42.56	43.60	11	1	5	0	22.23	22.02
5	1	-4	0	45.53	47.15	11	1	-5	0	27.87	27.82
5	1	-4	0	24.27	27.27	0	2	-5	0	30.04	28.61
7	1	-4	0	31.07	32.85	2	-2	5	0	40.11	50.12
7	1	-4	0	42.24	44.59	2	2	-5	0	16.01	16.10
9	1	-4	0	29.26	29.11	4	2	-5	0	47.14	45.38
9	1	-4	0	30.45	34.11	4	4	-5	0	43.65	45.02
1	1	-4	0	32.62	31.20	6	2	-5	0	34.62	37.44
1	1	-4	0	26.26	31.20	6	2	5	0	24.65	31.30
1	1	-4	0	24.75	21.42	6	2	5	0	29.00	28.70
1	1	-4	0	26.55	27.31	8	2	-5	0	32.52	31.05
3	2	-4	0	42.52	42.52	10	2	5	0	12.75	14.67
3	2	-4	0	28.99	29.89	10	2	-5	0	34.06	32.93
3	2	-4	0	42.50	40.68	10	2	5	0	25.88	15.72
3	2	-4	0	30.44	31.72	12	2	-5	0	20.27	20.72
4	2	-4	0	52.17	50.31	1	3	5	0	41.52	42.59
4	2	-4	0	57.87	62.16	1	3	-5	0	25.24	34.10
4	2	-4	0	64.48	66.04	1	3	5	0	30.40	34.12
4	2	-4	0	40.24	40.99	2	3	-5	0	29.39	25.55
4	2	-4	0	23.20	27.25	3	4	5	0	34.75	35.68
4	2	-4	0	21.97	22.11	4	4	-5	0	40.32	38.27
4	2	-4	0	18.32	20.06	4	4	5	0	41.36	37.99
4	2	-4	0	21.03	18.82	4	4	-5	0	22.74	18.94
4	2	-4	0	24.04	29.45	4	4	5	0	42.19	39.89
4	2	-4	0	32.43	33.81	4	4	-5	0	42.19	39.89
4	2	-4	0	45.77	46.94	1	5	5	0	32.13	32.98
4	2	-4	0	32.26	37.71	1	5	-5	0	38.02	35.81
4	2	-4	0	46.41	42.72	2	5	5	0	19.13	19.86
4	2	-4	0	44.88	49.47	2	5	-5	0	24.94	30.62
4	2	-4	0	46.72	41.06	2	6	5	0	20.24	32.18
4	2	-4	0	29.28	35.26	2	6	-5	0	14.19	18.61
4	2	-4	0	52.88	43.20	4	6	5	0	34.52	29.72
4	2	-4	0	64.00	64.67	4	6	-5	0	24.45	32.60
4	2	-4	0	47.91	47.37	4	6	5	0	26.63	25.84
4	2	-4	0	30.89	29.38	3	7	-5	0	16.19	17.72
4	2	-4	0	32.89	31.61	4	8	5	0	23.04	23.98
4	2	-4	0	24.41	26.07	4	8	-5	0	20.09	20.61
4	2	-4	0	23.90	29.59	2	9	5	0	20.84	19.75
4	2	-4	0	45.02	37.69	2	9	-5	0	29.88	38.92
4	2	-4	0	40.45	40.23	4	9	5	0	28.18	22.97
4	2	-4	0	46.18	47.08	-4	9	-5	0	42.02	41.57
4	2	-4	0	29.70	34.40	6	9	5	0	18.90	29.54
4	2	-4	0	35.24	32.68	6	9	-5	0	37.44	25.08
4	2	-4	0	20.81	23.78	1	11	5	0	33.92	33.58
4	2	-4	0	22.41	26.60	1	11	-5	0	19.77	24.86
4	2	-4	0	29.72	20.52	3	11	5	0	33.92	33.27
4	2	-4	0	33.55	23.42	3	11	-5	0	31.04	33.44
4	2	-4	0	17.67	21.49	5	11	5	0	20.92	22.82
4	2	-4	0	21.22	28.30	7	11	-5	0	27.92	27.52
4	2	-4	0	22.10	25.58	7	11	5	0	22.88	22.42
4	2	-4	0	29.70	29.98	9	11	-5	0	27.92	23.67
4	2	-4	0	21.45	27.54	9	11	5	0	26.38	24.84
4	2	-4	0	19.85	20.35	0	2	5	0	29.22	30.05
4	2	-4	0	24.26	20.72	2	2	-5	0	29.21	29.17
4	2	-4	0	42.81	42.42	2	2	5	0	24.62	34.80
4	2	-4	0	44.45	44.77	2	2	-5	0	28.14	24.89
4	2	-4	0	49.26	48.71	2	2	5	0	34.57	33.18
4	2	-4	0	15.87	15.88	4	4	-5	0	22.06	22.34
4	2	-4	0	49.07	50.79	6	6	5	0	18.14	16.95
4	2	-4	0	26.08	24.66	6	6	-5	0	18.22	18.19
4	2	-4	0	20.22	29.60	8	8	5	0	14.22	14.07
4	2	-4	0	43.10	37.97	8	8	-5	0	20.57	20.67
4	2	-4	0	12.40	15.80	10	2	5	0	38.31	29.61
4	2	-4	0	45.07	45.42	1	3	-5	0	28.44	25.82
4	2	-4	0	41.62	42.23	1	3	5	0	25.24	26.06
4	2	-4	0	28.55	29.15	3	3	-5	0	20.66	20.71
4	2	-4	0	32.12	33.55	3	3	5	0	24.04	29.48
4	2	-4	0	31.60	23.23	4	4	-5	0	15.13	18.33
4	2	-4	0	27.09	41.65	4	4	5	0	24.26	22.74
4	2	-4	0	25.08	35.39	4	4	-5	0	24.87	27.82
4	2	-4	0	21.24	34.09	4	4	5	0	24.64	24.44
4	2	-4	0	22.08	24.40	4	4	-5	0	24.64	24.44
4	2	-4	0	20.25	22.76	4	4	5	0	24.20	22.02

h	k	l	x	F <sub>obs</sub>	F <sub>calc</sub>
3	5	6	0	19.80	24.77
2	5	-6	0	32.85	27.87
2	6	5	0	21.84	27.14
2	6	-5	0	24.50	24.62
4	6	6	0	30.11	25.76
3	7	-6	0	20.10	19.65

## Octahedra

Alternatively the structure may be described as isolated  $\text{MF}_6$  and  $\text{LiO}_2\text{F}_4$  octahedral groups forming a framework of octahedra all sharing corners. The lithium octahedra share two oxygen atoms with other lithium octahedra and four fluorine atoms with M octahedra. The linked network is illustrated in Figure 4.

The bond lengths and angles for the individual  $\text{TiF}_6$  and  $\text{SnF}_6$  octahedra are given in Table VI. There are two groups of metal-fluorine bond lengths giving a mean value of  $1.94(1) \text{ \AA}$  in the titanium compound and  $1.97(1) \text{ \AA}$  in the tin compound. Examples of other values in  $\text{TiF}_6$  groups are  $1.91 \text{ \AA}$  in  $\text{K}_2\text{TiF}_6$ <sup>(16)</sup> and  $1.86 \text{ \AA}$  in  $\text{CuTiF}_6 \cdot 4\text{H}_2\text{O}$ <sup>(17)</sup>. Tin-fluorine bond lengths in  $\text{Na}_2\text{SnF}_6$  range from  $1.83 \text{ \AA}$  to  $1.96 \text{ \AA}$ <sup>(18)</sup>. The  $\text{MF}_6$  octahedral angles are similar and do not deviate from 90 degrees by more than two degrees.

The titanium and tin atoms are situated at the corners and C-centres of their respective unit cells. Looking at the octahedron down the c axis three fluorine atoms lie above the metal atom and three below. The lithium atoms lie at the positions  $1/4, 1/4, 1/2$  and  $1/4, 3/4, 1/2$  and at the C-centering of these positions. Looking at the octahedron down the c axis two fluorine atoms and an oxygen atom lie above the lithium atom and two fluorine atoms and an oxygen atom lie below.

The bond lengths and angles for the individual  $\text{LiF}_6$

Figure 4 Linkage of Titanium and Lithium Octahedra.

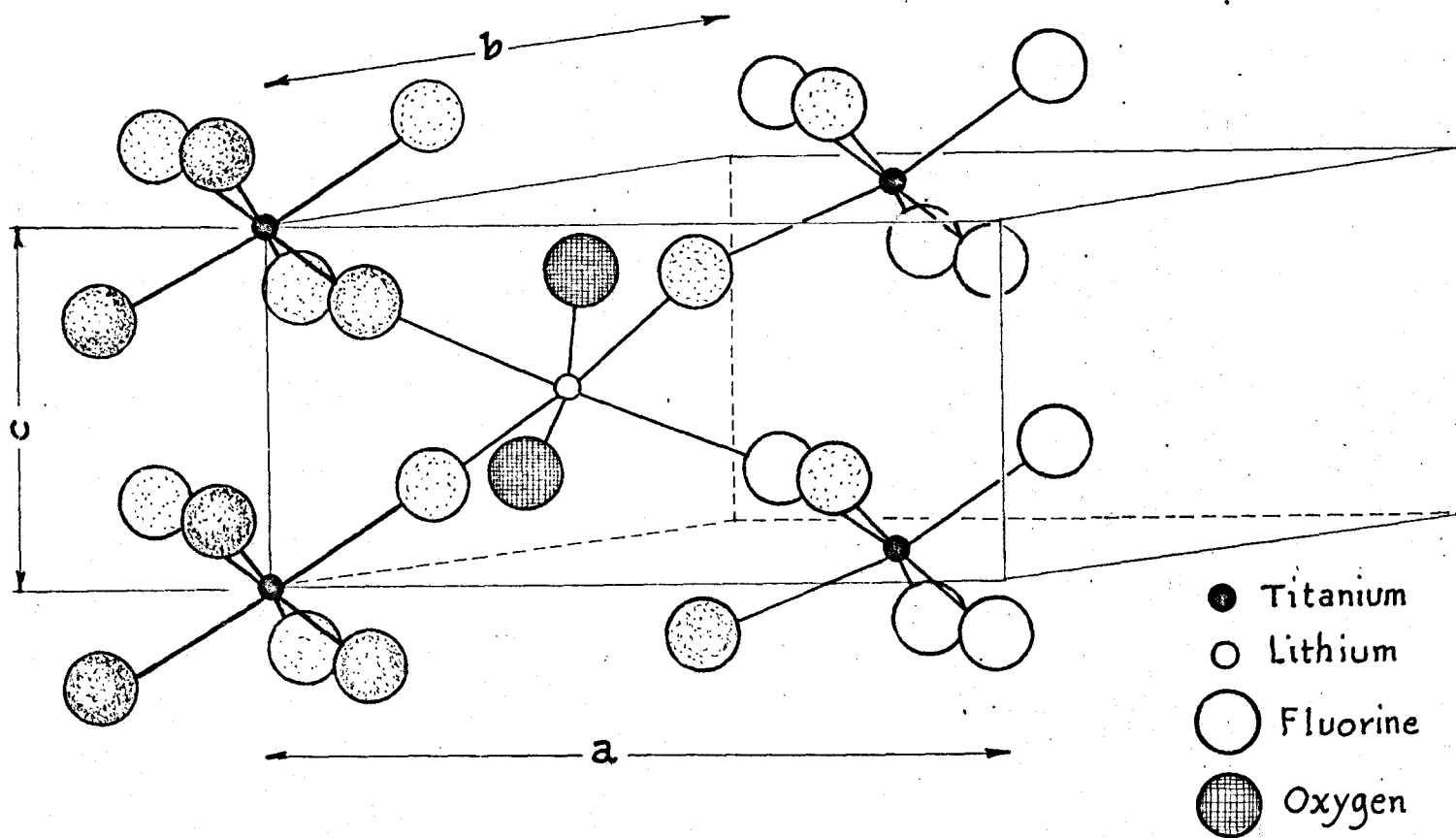


Table VIa. Bond Distances and Angles for  $\text{TiF}_6$  and  $\text{SnF}_6$   
Octahedra

<u>Atom</u>	<u>Neighbours</u>	<u>Distance (Å)</u>	<u>Angles (°)</u>
Ti	4 F <sub>1</sub>	1.90(1)	2 F <sub>1</sub> -Ti-F <sub>1</sub> 93.2(1)
	2 F <sub>3</sub>	1.97(1)	2 F <sub>1</sub> -Ti-F <sub>7</sub> 86.8(1)
		[Mean 1.94(1) ]	4 F <sub>1</sub> -Ti-F <sub>3</sub> 93.5(1)
			4 F <sub>1</sub> -Ti-F <sub>3</sub> 86.5(1)
			[Mean 90.0(1) ]
Sn	4 F <sub>1</sub>	1.96(1)	2 F <sub>1</sub> -Sn-F <sub>1</sub> 88.8(2)
	2 F <sub>3</sub>	1.98(1)	2 F <sub>1</sub> -Sn-F <sub>1</sub> 91.2(2)
		[Mean 1.97(1) ]	4 F <sub>1</sub> -Sn-F <sub>3</sub> 91.5(2)
			4 F <sub>1</sub> -Sn-F <sub>3</sub> 88.5(2)
			[Mean 90.0(1) ]



Table VIb. Bond Distances and Angles for LiF<sub>6</sub> OctahedraTi compound

Li	2 F <sub>1</sub>	2.16(1)	2 F <sub>1</sub> -Li-F <sub>3</sub>	91.9(2)
	2 F <sub>3</sub>	2.19(1)	2 F <sub>1</sub> -Li-F <sub>3</sub>	88.1(2)
		[Mean 2.18(1)]	2 F <sub>1</sub> -Li-O	90.1(2)
	2 O(H <sub>2</sub> )	2.05(1)	2 F <sub>1</sub> -Li-O	89.0(2)
			2 F <sub>3</sub> -Li-O	89.5(2)
			2 F <sub>3</sub> -Li-O	90.1(2)
			[Mean	89.9(2)]

Sn compound

Li	2 F <sub>1</sub>	2.03(1)	2 F <sub>1</sub> -Li-F <sub>3</sub>	90.4(2)
	2 F <sub>3</sub>	2.14(1)	2 F <sub>1</sub> -Li-F <sub>3</sub>	89.6(2)
		[Mean 2.08(1)]	2 F <sub>1</sub> -Li-O	88.9(3)
	2 O(H <sub>2</sub> )	2.06(1)	2 F <sub>1</sub> -Li-O	91.1(3)
			2 F <sub>3</sub> -Li-O	93.4(2)
			2 F <sub>3</sub> -Li-O	86.6(2)
			[Mean	90.0(2)]

octahedra are also given in Table VI. The discrepancy between the lithium-fluorine-1 bond and the lithium-fluorine-3 bond is greater in the tin compound than in the titanium compound, with a mean value of  $2.08(1) \text{ \AA}$  as compared to  $2.18(1) \text{ \AA}$  in the latter. Values for lithium-fluorine distances in other compounds with lithium in octahedral sites are  $2.032(6) \text{ \AA}$  in  $\text{LiSbF}_6$  <sup>(19)</sup> and  $2.01 \text{ \AA}$  in  $\text{Li}_2\text{ZrF}_6$  <sup>(20)</sup>. Thus the titanium result is higher than would be expected. Values for lithium-oxygen distances are  $2.04 \text{ \AA}$  in  $\text{LiNiO}_2$  <sup>(21)</sup> and  $2.01\text{-}2.07 \text{ \AA}$  in  $\text{LiSbO}_3$  <sup>(22)</sup> again for lithium with octahedral coordination.

The shortest fluorine-fluorine distances,  $2.70(1) \text{ \AA}$  belonging to the titanium octahedron and  $2.76(1) \text{ \AA}$  belonging to the tin octahedron, are shorter than those belonging to the lithium octahedra,  $2.99(1) \text{ \AA}$ , but these values are not shorter than the sum of ionic radii for fluorine ( $2.66 \text{ \AA}$ ). Thus there is no real evidence for covalent bonding in these results. (See Table VII).

#### Positions of Hydrogen Atoms

An attempt was made to detect hydrogen atom positions by the calculation of a difference electron density projection down (001). The Fourier coefficients used were the differences between the observed  $hk0$  structure factors and those calculated from parameters refined with three dimensional data. The Li-O-Li bond angle is  $93.0(3)$  degrees in the titanium compound and  $95.4(3)$  degrees in the tin compound which

Table VIIa. Fluorine-fluorine Bond Lengths in  $\text{Li}_2\text{TiF}_6 \cdot 2\text{H}_2\text{O}$ 

<u>Within Ti Octahedron</u>		<u>Within Li Octahedron</u>	
	Å		Å
$F_1 - F_1$	2.68(1)	$F_1 - F_3$	3.07(1)
$F_1 - F_1$	2.70(1)	$F_1 - F_3$	3.00(1)
$F_1 - F_3$	2.76(1)		
$F_1 - F_3$	2.67(1)		
[Mean	2.70(1)]		

Table VIIb. Fluorine-fluorine Bond Lengths in  $\text{Li}_2\text{SnF}_6 \cdot 2\text{H}_2\text{O}$ 

<u>Within Sn Octahedron</u>		<u>Within Li Octahedron</u>	
	Å		Å
$F_1 - F_1$	2.76(1)	$F_1 - F_3$	3.00(1)
$F_1 - F_1$	2.79(1)	$F_1 - F_3$	2.97(1)
$F_1 - F_3$	2.87(1)		
$F_1 - F_3$	2.76(1)		
[Mean	2.75(1)]		

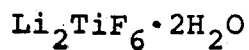
is quite low if a tetrahedral arrangement of  $2\text{Li} + 2\text{H}$  around the oxygen atom is expected<sup>(23)</sup>.

No significant density was found in the region around the oxygen atom assuming oxygen-hydrogen bond lengths of  $1.1 \text{ \AA}$  or less. Also there is no evidence for O-H...F bonds of the type postulated by Wells for  $\text{K}_2\text{TiF}_6 \cdot \text{H}_2\text{O}$ <sup>(24)</sup> since there are no significant differences between the oxygen-fluorine bond lengths. It seems probable that a disordered arrangement occurs and the hydrogen atoms are not directed in any preferential way. Both the tin and titanium compounds gave similar results.

#### Description of the Thermal Motion

The direction cosines of the principal axes of the thermal ellipsoids with respect to the crystal axis were derived for each atom, and are presented in Table VIII together with the root mean square components of thermal motion along the principal axes. The site symmetry of the titanium and tin atoms is  $2/m$ , so one principal axis of the thermal ellipsoid is oriented along the two-fold axis of the crystal (b axis) perpendicular to the mirror plane. Thus the thermal ellipsoid necessarily has an axis of revolution and the direction cosines are zero perpendicular to this axis. The oxygen and the fluorine-3 atoms sit on a mirror plane, with a site symmetry of  $m$ . A mirror plane produces the same effect on the orientation of a thermal ellipsoid as would a two fold axis normal to it, so that the thermal ellipsoids have the same symmetry

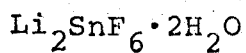
Table VIII Principal Axes Analysis for Anisotropic Temperature Factors



Atom	RMS Displacements (Å <sup>2</sup> )	Direction Cosines wrt		
		a	b	c
Ti	.147(8)	0.6701(11)	0	0.7480(11)
	.130(9)	0	1	0
	.130(9)	0.7422(11)	0	-2.6718(7)
F <sub>1</sub>	.185(11)	0.8824(19)	-0.2445(19)	-0.4038(19)
	.181(12)	-0.2274(13)	0.5262(14)	-0.8189(13)
	.169(11)	0.4118(13)	0.8145(19)	0.4078(14)
F <sub>3</sub>	.194(21)	0.6108(24)	0	0.7904(24)
	.165(19)	0	1	0
	.149(18)	0.7918(25)	0	0.6126(19)
O	.186(25)	0.6616(29)	0	0.7485(26)
	.150(27)	-0.7499(23)	0	0.6632(24)
	.145(28)	0	1	0
Li	.298(90)	-0.7218(89)	-0.5416(84)	0.4337(94)
	.232(88)	-0.6694(95)	0.3866(98)	-0.6330(89)
	.151	0.1759(88)	-0.7472(85)	-0.6413(84)

(continued next page)

Table VIII Principal Axes Analysis for Anisotropic Temperature  
Factors (continued)



Atom	RMS Displacements	(Å <sup>2</sup> )	Direction Cosines wrt.		
			a	b	c
Sn	.108 (3)	0.5614 (5)	0	0.8180 (5)	
	.096 (2)	-0.8275 (5)	0	0.5752 (3)	
	.087 (3)	0	1	0	
F <sub>1</sub>	.169 (16)	0.0433 (27)	-0.8068 (26)	0.5899 (21)	
	.146 (14)	0.9188 (19)	-0.2638 (19)	-0.3090 (17)	
	.098 (13)	0.3923 (25)	0.5287 (19)	0.7460 (21)	
F <sub>3</sub>	.162 (25)	0.5636 (34)	0	0.8165 (38)	
	.158 (19)	0	1	0	
	.100 (26)	0.8260 (30)	0	-0.5774 (26)	
O	.141 (30)	0	1	0	
	.138 (26)	-0.8633 (39)	0	-0.4901 (40)	
	.104 (25)	-0.5046 (32)	0	0.8717 (28)	
Li	.201 (53)	-0.4467 (111)	0.8335 (80)	-0.3176 (134)	
	.160 (61)	-0.8118 (110)	-0.2249 (81)	0.5525 (81)	
	.136 (52)	0.3761 (92)	0.5047 (95)	0.7706 (87)	

as those for the tin and titanium atoms. The lithium atom is located on a centre of symmetry and the thermal ellipsoid has no special symmetry properties. The other fluorine atom is in a general position and the thermal ellipsoid likewise has no special symmetry.

A marked anisotropy is observed in the lithium thermal ellipsoid for both the tin and the titanium compound. This is probably due to the uneven distribution of charge surrounding the lithium atom caused by two neutral water molecules and four negatively charged fluorine ions. The shortest principal axis is directed towards the lithium-oxygen bond. However, the anisotropic temperature factors for the lithium atom had very high esd's and these errors are reflected in the errors on the rms displacements, thus less reliability can be attached to these results than to those for the other atoms.

#### Thermal Corrections on Bond Lengths

Standard errors have been given in Table VI for the bond lengths and angles. A possible systematic error not included in these results is that arising from the thermal motion of the atoms. It is possible to correct the bond distances for temperature effects by making assumptions about their relative motions.<sup>(25)</sup> The values of the thermally correlated bond lengths are given in Table IX assuming that the  $\text{MF}_6$  and the  $\text{LiO}_2\text{F}_4$  groups are undergoing a riding or librational type of motion. The standard errors quoted for corrected distances take into account the standard errors in the uncorrected

Table IX Thermal Corrections for Bond Lengths

	<u>Bond</u>	<u>Riding Model</u>	<u>Uncorrelated</u>
$\text{Li}_2\text{TiF}_6 \cdot 2\text{H}_2\text{O}$			
	Ti-F <sub>1</sub>	1.91(1)	1.94(1)
	Ti-F <sub>3</sub>	1.98(1)	2.01(1)
	Li-O(H <sub>2</sub> )	2.07(1)	2.10(1)
	Li-F <sub>1</sub>	2.18(1)	2.21(1)
	Li-F <sub>3</sub>	2.20(1)	2.24(1)
$\text{Li}_2\text{SnF}_6 \cdot 2\text{H}_2\text{O}$			
	Sn-F <sub>1</sub>	1.97(1)	1.98(1)
	Sn-F <sub>3</sub>	1.99(1)	2.00(1)
	Li-O	2.06(1)	2.08(1)
	Li-F <sub>1</sub>	2.04(1)	2.07(1)
	Li-F <sub>3</sub>	2.15(1)	2.17(1)



values and the standard errors calculated by the least-squares program for the temperature factors.

The groups may not be undergoing a riding motion but instead the relative motions of the atoms might be uncorrelated. The uncorrelated values are also given. The assumption of a riding motion is a better one to make for a covalently bonded group which would undergo a rigid body type motion rather than a random motion of the individual atoms. However, we have no real evidence for a covalently bonded group. Also, with possible uncertainties of  $0.01 \text{ \AA}$  in any of the corrected bondlengths, the difference between the distances is probably not significant. The values for the observed bond lengths as quoted in Table VI should provide the most reliable values for these distances. In addition, the neglect of the hydrogen atoms might be expected to affect the position and the temperature factor of the oxygen atom, hence the thermally corrected lithium-oxygen bond length value could be less reliable than its standard error would indicate.

#### Comparison with other structures

The hk0 photographs of both  $\text{Li}_2\text{TiF}_6 \cdot 2\text{H}_2\text{O}$  and  $\text{Li}_2\text{SnF}_6 \cdot 2\text{H}_2\text{O}$  showed quasi-hexagonal symmetry, and in fact the space group  $C2/m$  is a sub-group of the trigonal space group  $P\bar{3}m1$ , to which a large family of hexafluorides belong. Table X lists these compounds with their cell constants and volumes. The two hydrates are compared with this list by taking the c axis as the trigonal c axis and the b axis as the trigonal a axis. It

Table X  $K_2TiF_6$ -type Crystals Belonging to  $P\bar{3}m1^*$ 

Compound	a (Å)	c (Å)	Vol/molecule (Å <sup>3</sup> )
$K_2MnF_6^{**}$	5.71	4.65	131.3
$K_2VF_6^{**}$	5.67	4.65	129.5
$K_2TiF_6^{**}$	5.715	4.656	131.7
$K_2RuF_6^{**}$	5.76	4.64	133.3
$K_2ReF_6$	5.85	4.60	136.3
$Rb_2TiF_6^{**}$	5.88	4.78	143.1
$Rb_2IrF_6$	5.97	4.79	147.8
$Rb_2ReF_6$	6.01	4.77	149.2
$Rb_2ZrF_6^{**}$	6.16	4.82	158.4
$Ti_2TiF_6^{**}$	5.92	4.84	146.9
$Li_2TiF_6 \cdot 2H_2O$	5.93	4.80	141.7
$(NH_4)_2TiF_6$	5.96	4.82	148.3
$Li_2SnF_6 \cdot 2H_2O$	6.10	4.73	141.5
$(NH_4)_2ReF_6$	6.06	4.77	151.7
$Cs_2TiF_6^{**}$	6.15	4.96	162.5
$Cs_2VF_6$	6.17	4.98	164.2
$Cs_2OsF_6$	6.26	5.00	169.7
$Cs_2ReF_6$	6.30	4.99	171.5
$Cs_2HfF_6$	6.39	5.00	176.8
$Cs_2ZrF_6$	6.41	5.01	178.3

\*For more complete list and references see reference 2.

\*\*These compounds appear in more than one modification.

can be seen that they fit remarkably well into the series. In the following discussion  $K_2TiF_6$ <sup>(16)</sup> will be taken to represent this structure type. Table XI gives the parameters for this compound.

In  $K_2TiF_6$  there are hexagonally close-packed layers of potassium and fluorine atoms perpendicular to the c axis. The position of the potassium ion corresponds very closely to the position of the oxygen ion in the two hydrated fluorides. The twelve fluorine neighbours of the potassium ion are approximately equidistant, falling into three sets. These potassium-fluorine distances are compared in Table XII with the corresponding oxygen-fluorine distances in the tin and titanium compounds. It can be seen that although a singly positive ion has been replaced by a neutral water molecule it seems to have little difference in the over-all close-packed arrangement. This would be expected from the hard sphere model of close-packed structures, so that to a first approximation the structure is determined by the sizes of the constituent ions.

The puckering of the layers is also little influenced by the exchange of potassium for water. The oxygen atom is only slightly further away from the layer of fluorine atoms than the potassium atom. In addition the average fluorine-fluorine distances of  $2.75(1) \overset{\circ}{\text{Å}}$  in the tin octahedron and  $2.70(1) \overset{\circ}{\text{Å}}$  in the titanium octahedron are similar to the values of  $2.75(4) \overset{\circ}{\text{Å}}$  and  $2.68(4) \overset{\circ}{\text{Å}}$  in the titanium octahedron in  $K_2TiF_6$ .

Table XI Crystal Data for  $K_2TiF_6$

System	Trigonal		
Space Group	$P\bar{3}m1$		
Cell Constants			
a	5.715 Å		
c	4.656 Å		
Vol/molecule	131.7 Å <sup>3</sup>		
Number of Formula Units/Unit Cell (Z)	1		
Positional Parameters	x	y	z
Ti	0	0	0
K	2.3	1/3	0.3000
F	0.156	0.314	0.280

Table XII Comparison of Oxygen-Fluorine Distances in

$\text{Li}_2\text{TiF}_6 \cdot 2\text{H}_2\text{O}$  and  $\text{Li}_2\text{SnF}_6 \cdot 2\text{H}_2\text{O}$  with Potassium-Fluorine  
Distances in  $\text{K}_2\text{TiF}_6$  in Å Units

	$\text{K}_2\text{TiF}_6$		$\text{Li}_2\text{TiF}_6 \cdot 2\text{H}_2\text{O}$	$\text{Li}_2\text{SnF}_6 \cdot 2\text{H}_2\text{O}$
	K-F		O-F	O-F
		2	3.07(1)	3.03(1)
6	2.87	2	2.97(1)	2.98(1)
		2	2.90(1)	2.91(1)
3	2.75	1	2.99(1)	2.93(1)
		2	2.98(1)	2.92(1)
3	3.08	1	3.03(1)	3.03(1)
		2	3.08(1)	3.04(1)
Mean	2.90		3.00(1)	2.98(1)

The lithium atom position in the two hydrated fluorides corresponds to an interstitial space in  $K_2TiF_6$ . In this 'empty' octahedron none of the angles deviate from 90 degrees by more than 3 degrees, but if the potassium-fluorine distances are compared with the corresponding oxygen-fluorine distances in the lithium octahedra they are found to be shorter (Table XI). As would be expected the 'empty' octahedron is contracted with respect to the ones containing a lithium atom.

#### Hydrated Fluorides

Although previously unknown, <sup>(26)</sup> it is not surprising to find the lithium compounds  $Li_2TiF_6$  and  $Li_2SnF_6$  hydrated. The lithium ion has a large hydration energy and is often hydrated in its solid salts when the same salts of other alkali metals are non-hydrated, e.g.  $Na_2TiF_6$ ,  $K_2TiF_6$  and  $Na_2SnF_6$  <sup>(27)</sup>.

There are a number of known hydrated fluorides but few crystal structure determinations have been done. Only a few of these have structures in which the oxygen of the water molecule forms part of a close-packed array. In many of them a clathrate of water molecules coordinates about a central ion leading to an open framework structure. This occurs for example in  $CuTiF_6 \cdot 4H_2O$  which is more descriptively written  $(Cu(H_2O)_4)^{++}TiF_6^{--}$ . In this structure there are infinite chains of alternate  $TiF_6^{--}$  units and  $Cu(H_2O)_4^{++}$

units along the 101 axis held together by hydrogen bonding<sup>(17)</sup>.

A certain number of compounds of the general formula  $R_2(MX_5 \cdot H_2O)$  crystallize with the  $K_2PtCl_6$  structure or a slightly deformed variant of it, the water molecule occupying one of the six positions in the octahedral complex ion<sup>(28)</sup>. In this structure there is a cubic sequence of close-packed layers AcBCbABaC where the small letters represent M atoms in interstices. Examples are  $(NH_4)_2(VF_5 \cdot H_2O)$  and the isostructural Rb and Tl salts,  $Tl_2(CrF_5 \cdot H_2O)$  and  $Rb_2(CrF_5 \cdot H_2O)$ . Thus here water molecules and fluorine atoms do combine together to form a close-packed array. These structures however have only been solved from x-ray powder diffraction patterns and a more careful study would be worthwhile to further investigate the environment of the oxygen atom. The crystal  $NaPF_6 \cdot H_2O$  has an orthorhombic cell but with pseudohexagonal symmetry<sup>(29)</sup>. Here the phosphorus atoms are surrounded by a distorted fluorine octahedron and the sodium atoms are surrounded octahedrally by four fluorine atoms and two oxygen atoms. Again the fluorine atoms and water molecules approximate a close-packed array. In this crystal the hydrogen atoms have been located although the  $R_2$  factor obtained was 0.115. The hydrogen atoms are said to form a bridge between two fluorine atoms.

## ii. Crystal Structure Determination of $Na_2TiF_6$

### A. Background

The crystal structure of  $Na_2TiF_6$  was determined by

Cipriani in 1956 from its x-ray powder diffraction pattern<sup>(30)</sup>. According to his investigations,  $\text{Na}_2\text{SiF}_6$ ,  $\text{Na}_2\text{GeF}_6$ , and  $\text{Na}_2\text{TiF}_6$  were isostructural. The symmetry allowed the possibility of three trigonal space groups,  $P321$ ,  $P\bar{3}1m$ , and  $P31m$ . Cipriani chose  $P\bar{3}1m$ , with  $z = 3$ , and showed that the structure consisted essentially of hexagonally close-packed fluorine atoms with octahedral  $\text{TiF}_6$  groups sharing corners and edges. The three different space groups give various possibilities for the sodium positions. In  $P\bar{3}1m$  the alkali metal atoms are all in the same plane, giving a charge distribution that is rather improbable, as pointed out by Wells<sup>(31)</sup>. The same model was proposed for  $\text{Li}_2\text{MnF}_6$  by Hoppe, Liebe and Dähne<sup>(32)</sup> but they questioned the reliability of their  $z$  parameters for the lithium atom. A recent structure analysis of the silicon analog,  $\text{Na}_2\text{SiF}_6$ , by Zalkin, Forrester and Templeton<sup>(33)</sup> showed that the alkali atoms were at different heights ( $z = 0$ , and  $z = 1/2$ ) and that the space group was  $P321$ . The atomic parameters for  $\text{Na}_2\text{SiF}_6$  are given in Table XV. The cell constants are  $a = 8.859(2) \text{ \AA}$ , and  $c = 5.038(2) \text{ \AA}$ .

It was noted by Zalkin et al. that much larger differences between  $F(hk\ell)$  and  $F(kh\ell)$  were being calculated than were found in the measured intensities. They attributed this to twinning by rotation about the  $c$  axis giving

$$xI(hk\ell) + (1-x)I(kh\ell) = J(hk\ell)$$

$$(1-x)I(hk\ell) + xI(kh\ell) = J(kh\ell)$$



where  $x$  is the fraction of the specimen with the correct orientation,  $I(hk\ell)$  is the intensity for an untwinned crystal, and  $J(hk\ell)$  is the intensity for the twinned crystal. They chose  $x = 0.59$  and after applying anisotropic temperature factors they obtained a final  $R_2$  value of 0.085.

The present investigation was carried out to ascertain whether or not  $\text{Na}_2\text{TiF}_6$  was isostructural with the corrected structure of  $\text{Na}_2\text{SiF}_6$ .

#### B. Preliminary Investigations

Crystals of  $\text{Na}_2\text{TiF}_6$  were grown by dissolving commercial grade  $\text{Na}_2\text{TiF}_6$  in 40% HF and slowly cooling. Small hexagonally shaped crystals were obtained. A 'single crystal' measuring  $0.1 \text{ mm} \times 0.1 \text{ mm} \times 0.15 \text{ mm}$ , later shown to be twinned, was selected for x-ray studies.

The symmetry of the crystal was not clear from preliminary photographs but twinning was suspected and the space group was taken to be  $P321$  in analogy with  $\text{Na}_2\text{SiF}_6$ . Accurate cell constants were measured by the technique as outlined in Chapter I, using an  $h0\ell$  precession photograph. The final values are given in Table XIII.

Multiple film x-ray photographs were taken with an equi-inclination integrating Weissenberg camera for layers  $hk0 - hk4$  using filtered  $\text{Cu K}_\alpha$  radiation. The layers  $h0\ell - h4\ell$  were taken with an integrating Buerger precession camera using filtered  $\text{Mo K}_\alpha$  radiation. The intensities of 1579 reflections were measured. The large number of reflections was kept until

Table XIII - Crystal Data for Na<sub>2</sub>TiF<sub>6</sub>

System	Trigonal
Systematic Absences	None
Space Group	P321
Cell Constants	
a	9.316 (3) Å
b	9.316 (3) Å
c	5.142 (5) Å
Unit Cell Volume	386.44 Å <sup>3</sup>
Reciprocal Cell Constants	
a*	.12380 (5) Å <sup>-1</sup>
b*	.12380 (5) Å <sup>-1</sup>
c*	.19447 (2) Å <sup>-1</sup>
Density	
measured	2.71 (9) g/cm <sup>3</sup>
calculated	2.63 (3) g/cm <sup>3</sup>
Number of Formula Units per Unit Cell (Z)	3
X-ray Absorption Coefficients	
Cu K <sub>α</sub>	65.44 cm <sup>-1</sup>
Mo K <sub>α</sub>	6.58 cm <sup>-1</sup>

after all twinning corrections had been made. After correcting and then averaging, 233 reflections were used in the final refinement.

The linear absorption coefficient ( $\mu$ ) for  $\text{Na}_2\text{TiF}_6$  is  $65.44 \text{ cm}^{-1}$  for  $\text{Cu K}_\alpha$  radiation and  $6.58 \text{ cm}^{-1}$  for  $\text{Mo K}_\alpha$  radiation. The corresponding  $\mu R$  for a crystal of average radius 0.1 mm are 0.654 and 0.066 respectively. Absorption corrections were not considered necessary.

The density of the crystals was measured by flotation in a solution of methyl iodide and bromoform. The measured value of  $2.71(9) \text{ g/cm}^3$  agreed well with the calculated value of  $2.63(3) \text{ g/cm}^3$ .

### C. Determination and Refinement of Structure

A model based on the known parameters of  $\text{Na}_2\text{SiF}_6$  was chosen. Refinement of this structure by least squares led to an  $R_2$  factor of 0.18 and no further improvement was obtained. At this point only isotropic temperature factors were applied.

The crystal was considered to be twinned such that  $hkl$  and  $kh\ell$  were interchanged in position. This can be accomplished by rotation about the  $c$  axis or by reflection in  $(100)$ , giving a hexagonal appearance to all layers perpendicular to the  $c$  axis. The untwinned crystal is pseudo-hexagonal, making the twinning difficult to detect, but in the higher layers it was found that  $I(hk\ell)$  and  $I(-h-k\ell)$  were

consistently closer in intensity than  $I(hkl)$  and  $I(-k, h+k, l)$ . Yet, because of the pseudo-hexagonal symmetry the intensities of all six reflections were equivalent to within about 30%. The twinning was taken into account by assuming that each of two parts of the twinned crystal contributed 50% to the total pattern. The structure factor for the twinned crystal then became

$$|F_{hkl}|_T = \sqrt{|F_{hkl}|_1^2 + |F_{hkl}|_2^2}$$

The least squares refinement was continued using  $F_T$  in the place of the normal structure factor. The  $R_2$  factor dropped to 0.095 and when anisotropic temperature factors and a weighting scheme were introduced the final  $R_2$  factor was 0.089. The final values of the atomic positional and thermal parameters, together with their esd's are listed in Table XIV and the observed and calculated structure factors are tabulated in Table XV.

#### D. Discussion of Structure

##### Close-Packing

$\text{Na}_2\text{TiF}_6$  is isostructural with the structure of  $\text{Na}_2\text{SiF}_6$  reported by Zalkin et al. The parameters for both crystals are compared in Table XIV. The close-packed framework of fluorine atoms has been distorted by the presence of the sodium atom, which is too large to fit easily into an interstitial position.

Table XIVa. Final Positional Parameters in  $\text{Na}_2\text{TiF}_6$  and  $\text{Na}_2\text{SiF}_6$ 

Atom	Site Symmetry	x	y	z
$\text{Na}_2\text{TiF}_6$				
1 Ti <sub>1</sub>	32	0	0	0
2 Ti <sub>2</sub>	2	1/3	2/3	0.5034(14)
3 Na <sub>1</sub>	2	0.3784(25)	[0.3784]*	0
3 Na <sub>2</sub>	2	0.7098(24)	[0.7098]	1/2
6 F <sub>1</sub>	1	0.0831(16)	-0.1114(19)	0.7977(28)
6 F <sub>2</sub>	1	0.4477(16)	-0.4083(18)	0.7072(25)
6 F <sub>3</sub>	1	0.2220(19)	-0.2550(16)	0.2969(30)
$\text{Na}_2\text{SiF}_6$ (33)				
1 Ti <sub>1</sub>	32	0	0	0
2 Ti <sub>2</sub>	2	1/3	2/3	0.5062(12)
3 Na <sub>1</sub>	2	0.3790(10)	[0.3790]	0
3 Na <sub>2</sub>	2	0.7143(9)	[0.7143]	1/2
6 F <sub>1</sub>	1	0.0870(18)	-0.0918(17)	0.8099(14)
6 F <sub>2</sub>	1	0.4442(12)	-0.4006(13)	0.7007(14)
6 F <sub>3</sub>	1	0.2299(19)	-0.2599(15)	0.3098(14)

\*Values in brackets indicate parameters which are not independent

Table xIVb. Final Thermal Parameters in  $\text{Na}_2\text{TiF}_6$  and  $\text{Na}_2\text{SiF}_6$

Atom	$U_{11}$	$U_{22}$	$U_{33}$	$U_{12}$	$U_{13}$	$U_{23}$
<u><math>\text{Na}_2\text{TiF}_6</math></u>						
Ti <sub>1</sub>	0.0149 (28)	[0.0149]	0.0147 (32)	[0.0074]	0	0
Ti <sub>2</sub>	0.0189 (20)	[0.0189]	0.0188 (23)	[0.0094]	0	0
Na <sub>1</sub>	0.0193 (67)	[0.0193]	0.0303 (48)	0.0103 (40)	0.0095 (35)	[-0.0095]
Na <sub>2</sub>	0.0374 (69)	[0.0274]	0.0207 (48)	-0.0197 (39)	-0.0095 (34)	[0.0095]
F <sub>1</sub>	0.0323 (79)	0.0303 (69)	0.0442 (52)	0.0188 (59)	0.0068 (82)	0.0069 (87)
F <sub>2</sub>	0.0415 (89)	0.0376 (94)	0.0200 (51)	0.0277 (81)	-0.0030 (63)	0.0022 (65)
F <sub>3</sub>	0.0308 (71)	0.0351 (95)	0.0192 (46)	0.0113 (71)	-0.0071 (61)	0.0002 (73)
<u><math>\text{Na}_2\text{SiF}_6</math></u>						
Si <sub>1</sub>	0.0163 (25)	[0.0163]	0.0238 (50)	[0.0075]	0	0
Si <sub>2</sub>	0.0138 (13)	[0.0138]	0.0163 (25)	[0.0062]	0	0
Na <sub>1</sub>	0.0300 (37)	[0.0230]	0.0163 (19)	0.0056 (19)	0.0006 (13)	[-0.0006]
Na <sub>2</sub>	0.0200 (25)	[0.0200]	0.0312 (50)	0.0044 (19)	-0.0006 (13)	[0.0006]
F <sub>1</sub>	0.0450 (63)	0.0338 (50)	0.0388 (37)	0.0131 (19)	0.0056 (31)	-0.0025 (31)
F <sub>2</sub>	0.0200 (50)	0.0238 (63)	0.0300 (37)	0.0075 (25)	0.0031 (19)	0.0081 (19)
F <sub>3</sub>	0.0238 (50)	0.0312 (50)	0.0300 (37)	0.0081 (19)	-0.0025 (25)	-0.0013 (25)

Table XV. Observed and Calculated Structure Factors for  $\text{Na}_2\text{TiF}_6$ . Reflections with  $x = 1$  were unobserved, those with  $x = 2$  were not used in the refinement.  $F_{\text{calc}_1}$  and  $F_{\text{calc}_2}$  were the contributions to  $F_{\text{calc}_T}$  from the two twins.

h	k	l	x	F <sub>obs</sub>	Phase	F <sub>calc<sub>T</sub></sub>	F <sub>calc<sub>1</sub></sub>	F <sub>calc<sub>2</sub></sub>
2	0	0	1	3.42	-0.00	.93	.66	.66
3	-0	0	0	48.54	-0.00	42.30	29.91	29.91
4	-0	0	2	15.36	0.00	9.49	6.71	6.71
5	-0	0	0	14.65	0.00	14.45	10.22	10.22
5	-0	0	0	34.74	0.00	33.39	23.61	23.61
7	-0	0	1	12.74	0.00	12.25	8.66	8.66
8	-0	0	0	16.18	-0.00	16.13	11.41	11.41
9	-0	0	0	22.93	-0.00	28.58	20.21	20.21
11	-0	0	0	11.79	-0.00	11.00	7.78	7.78
11	-0	0	2	9.19	0.00	5.91	4.18	4.18
13	-2	0	0	80.08	-2.88	74.23	52.49	52.49
3	-2	0	0	36.68	-76.65	32.68	23.11	23.11
4	-2	0	0	47.15	102.98	45.66	32.29	32.29
8	-2	0	0	15.25	-97.74	14.82	10.48	10.48
9	-2	0	0	11.21	128.84	8.25	5.83	5.83
10	-2	0	0	15.16	123.18	17.40	12.30	12.30
11	-2	0	0	26.26	11.89	25.82	18.26	18.26
15	-3	0	0	17.33	114.77	16.70	11.81	11.81
5	-3	0	0	8.45	40.70	7.78	5.50	5.50
6	-3	0	0	133.33	4.91	133.02	94.06	94.06
7	-4	0	0	24.84	-91.68	22.55	15.95	15.95
7	-4	0	0	11.39	-126.84	10.15	7.18	7.18
11	-5	0	0	26.36	1.27	24.49	17.32	17.32
11	-6	0	0	17.15	131.24	15.01	10.61	10.61
11	-7	0	0	6.85	175.89	8.33	5.89	5.89
2	-7	0	0	67.53	5.50	60.17	42.55	42.55
3	-7	0	0	21.65	-58.84	19.83	14.02	14.02
4	-8	0	0	17.20	26.94	17.83	12.61	12.61
4	-8	0	0	80.75	3.85	70.00	49.50	49.50
11	-9	0	1	7.60	-102.78	7.77	5.49	5.49
11	-9	0	0	16.85	115.93	16.34	11.56	11.56
3	-9	0	0	23.00	-20.87	24.00	16.97	16.97
4	-9	0	1	12.36	151.89	11.94	8.44	8.44
4	-10	0	1	7.24	-6.59	7.42	5.25	5.25
4	-10	0	1	11.80	-98.63	8.35	6.26	6.26
5	-10	0	0	17.44	-4.65	16.75	11.85	11.85
11	-11	0	2	22.13	4.03	31.88	22.54	22.54
3	-11	0	0	12.62	-29.74	9.27	6.55	6.55
4	-11	0	0	22.75	17.32	18.67	13.20	13.20
5	-11	0	1	12.69	-81.10	8.06	5.70	5.70
0	0	1	0	50.90	180.00	44.13	31.21	31.21
1	0	1	0	68.72	-0.00	61.89	44.79	42.71
-2	0	1	0	62.51	-0.00	66.73	46.36	48.00
-3	0	1	0	101.92	180.00	115.75	91.95	70.29
-4	0	1	0	2.97	-180.00	2.59	1.48	2.13
-5	0	1	0	47.17	-0.00	53.62	42.57	32.60
-6	0	1	0	38.71	-0.00	37.51	14.09	34.76
-7	0	1	0	3.90	-0.00	3.80	1.80	3.35
-8	0	1	0	27.71	-0.00	28.08	21.46	18.10
-9	0	1	0	11.18	180.00	10.45	6.09	8.50
-10	0	1	2	17.52	-0.00	14.97	10.47	10.70
-11	0	1	0	19.98	-0.00	15.35	11.53	10.14
-11	2	1	0	63.86	113.36	66.18	45.80	46.80
-2	2	1	0	36.03	109.41	37.09	26.22	26.22
-6	2	1	0	34.81	15.14	34.95	25.63	22.64
-7	2	1	0	20.64	50.75	20.44	18.56	8.57
-9	2	1	0	18.31	18.56	18.94	14.00	12.76
-1	3	1	0	40.40	27.99	40.24	28.79	28.11
-4	3	1	0	19.86	0.05	20.72	12.47	16.56
-1	4	1	0	22.80	-72.81	24.04	22.76	7.72
-1	5	1	0	47.50	162.98	51.85	44.86	26.00
-2	5	1	0	62.21	-2.14	62.12	43.54	44.31
-1	6	1	0	39.27	-23.52	38.81	28.12	26.75
-3	6	1	0	20.57	178.39	20.79	14.70	14.70
-1	7	1	0	18.46	-55.14	19.44	10.45	16.39
-2	7	1	0	20.61	175.89	21.09	17.34	12.01
-3	7	1	0	21.89	-33.28	20.72	16.56	12.47
-1	8	1	0	22.59	-179.70	22.71	22.24	4.59
-2	8	1	0	26.56	3.43	38.06	24.25	29.33
-4	8	1	0	22.52	-172.00	23.46	16.59	16.59
-5	8	1	0	42.93	7.30	43.47	30.31	31.16
-1	9	1	0	24.03	-34.05	23.41	17.60	15.43
-3	9	1	0	15.42	-127.80	15.23	2.25	15.16
-4	9	1	0	21.32	9.72	20.56	14.90	14.17
-1	10	1	0	18.42	1.05	17.52	10.09	14.32
-2	10	1	0	15.12	1.63	12.66	5.38	10.94
-3	10	1	0	10.72	-16.43	9.29	7.98	4.76



h	k	l	x	F obs	Phase	F calc <sub>T</sub>	F calc <sub>1</sub>	F calc <sub>2</sub>	
4	-1	0	1	0	14.84	-54.30	13.76	12.86	4.90
5	-1	0	1	1	7.17	-65.00	4.98	3.52	3.52
3	-1	1	1	0	18.55	225.50	18.98	12.87	13.95
4	-1	1	1	0	22.50	152.83	20.11	2.52	19.95
5	-1	1	1	0	22.20	34.11	21.40	15.76	14.48
0	0	0	2	0	13.19	180.00	12.60	8.91	8.91
1	0	0	2	0	6.66	-	6.14	6.08	8.85
2	0	0	2	0	24.52	-	22.83	19.61	11.70
3	0	0	2	0	147.35	-	143.67	89.51	112.38
4	0	0	2	0	28.42	-	25.69	23.00	11.45
5	0	0	2	0	12.68	-	12.70	12.35	2.97
6	0	0	2	0	75.68	-	59.85	45.19	39.25
7	0	0	2	0	19.09	-180.00	17.95	1.13	17.92
8	0	0	2	0	8.87	-	10.74	3.23	10.25
9	0	0	2	0	17.91	-	18.45	12.27	13.78
0	0	0	2	0	17.91	-	18.45	12.27	13.78
1	1	2	2	0	35.39	117.69	34.39	29.96	16.88
-1	1	2	2	0	9.71	-24.80	8.36	5.91	5.91
2	1	2	2	0	66.47	6.38	61.12	43.22	43.22
4	1	2	2	0	12.37	145.32	13.65	7.31	11.52
-1	0	2	2	1	10.19	137.71	10.38	10.03	2.67
3	3	2	2	0	18.09	-16.29	16.87	11.93	11.93
4	3	2	2	0	8.04	-39.63	7.33	4.38	5.88
5	3	2	2	0	15.83	-53.08	17.97	14.50	10.61
1	-4	2	2	0	30.98	-25.66	31.98	18.47	26.11
4	-4	2	2	2	4.46	47.63	10.14	7.17	7.17
6	-4	2	2	2	4.20	4.99	6.84	5.07	4.59
1	-5	2	2	0	45.20	1.85	44.02	26.18	35.39
2	-5	2	2	0	9.56	-60.90	10.66	9.63	4.57
6	-5	2	2	2	2.56	-50.78	5.18	2.38	4.60
1	-6	2	2	0	32.82	120.10	29.26	22.18	19.09
1	-7	2	2	0	26.25	-112.94	27.03	23.15	13.96
2	-7	2	2	0	14.49	-9.02	16.12	13.22	9.23
1	-8	2	2	0	38.75	-	41.22	30.74	27.47
2	-8	2	2	0	8.83	-159.04	8.13	4.79	6.57
3	-8	2	2	0	18.05	-53.08	17.97	14.50	10.61
1	-9	2	2	2	38.24	135.13	7.80	5.92	5.08
3	-9	2	2	0	33.86	-16.62	33.14	23.40	23.46
4	-9	2	2	0	18.46	112.02	18.61	9.46	16.02
2	-10	2	2	0	27.65	1.63	26.67	17.67	19.98
3	-11	2	2	0	8.39	-16.14	10.67	9.62	4.63
5	-11	2	2	0	37.50	-12.09	36.44	25.76	25.76
0	-11	2	2	0	4.03	178.37	6.74	6.00	3.07
4	0	-1	1	2	26.78	11.69	29.69	20.32	21.64
1	0	0	3	0	15.39	-	15.56	11.01	11.01
1	0	0	3	0	12.76	180.00	10.97	6.86	8.57
3	0	0	3	0	54.61	180.00	51.27	49.73	12.44
4	0	0	3	0	22.85	-	24.54	20.66	13.24
5	0	0	3	0	45.93	-	49.17	36.36	33.10
6	0	0	3	0	18.94	-	19.87	19.56	19.86
7	0	0	3	0	13.43	-	14.67	10.53	10.21
8	0	0	3	0	26.84	-	29.15	17.63	23.22
0	0	0	3	0	10.23	-180.00	8.94	6.76	5.85
-1	1	2	2	0	39.21	104.56	37.21	26.31	26.31
-1	2	2	2	0	46.30	-	45.73	31.42	33.22
-1	7	2	2	0	8.06	-177.01	8.53	5.84	6.22
9	2	2	3	0	14.15	-152.45	7.01	6.65	2.22
1	-3	3	3	0	14.87	35.63	14.88	10.88	10.15
3	-3	3	3	2	50.67	-6.75	49.69	37.69	32.37
6	-3	3	3	2	7.99	-178.69	3.46	2.45	2.45
8	-3	3	3	0	9.27	173.29	10.91	9.87	4.63
-1	10	3	3	0	24.70	21.23	23.69	17.47	16.00
1	-4	3	3	0	14.52	-6.99	13.56	8.84	10.28
2	-4	3	3	0	30.77	13.64	29.26	20.59	20.78
1	-5	3	3	0	32.64	122.87	33.89	23.97	23.97
3	-5	3	3	0	27.36	-159.28	29.15	26.27	12.64
1	-6	3	3	0	37.96	14.84	37.08	24.39	27.93
2	-6	3	3	0	28.97	-17.47	33.17	22.88	24.01
2	-7	3	3	0	13.93	68.66	14.67	12.96	6.88
4	-7	3	3	0	14.58	-24.44	17.49	11.55	13.13
1	-8	3	3	0	16.28	-130.57	15.55	12.70	8.98
2	-8	3	3	0	16.07	-152.59	16.81	2.88	16.56
4	-8	3	3	0	26.09	15.94	29.63	21.16	20.74
2	-9	3	3	0	8.44	-169.72	10.15	7.18	7.18
2	-9	3	3	0	17.13	-8.80	19.17	11.04	15.67

h	k	l	x	F <sub>obs</sub>	Phase	F <sub>calc<sub>T</sub></sub>	F <sub>calc<sub>2</sub></sub>	F <sub>calc<sub>2</sub></sub>
4	-	3	0	16.05	-11.13	18.12	13.66	11.90
2	-	3	0	15.87	-27.22	18.53	13.10	13.11
4	-1	3	0	13.29	-4.28	14.85	8.84	11.94
5	-1	3	1	3.11	156.28	2.44	1.72	1.72
0	-1	3	0	111.67	-	105.07	74.29	74.29
1	0	4	0	8.18	180.00	6.38	5.78	2.70
2	0	4	0	12.01	-180.00	13.30	8.10	10.55
3	0	4	0	52.96	-	50.55	46.05	20.86
4	0	4	0	23.12	180.00	24.46	11.85	21.40
5	0	4	2	9.80	-	8.93	3.11	8.37
6	0	4	0	26.82	-	29.11	16.15	24.21
7	0	4	0	13.87	-	14.29	14.24	1.18
8	0	4	0	10.95	-	10.59	10.54	.99
9	0	-4	0	20.14	-	16.47	10.96	12.30
8	1	4	0	7.99	165.26	8.39	4.08	7.33
1	-2	4	0	28.99	1.93	27.89	19.72	19.72
4	-2	4	0	14.80	104.15	16.84	13.20	10.45
-4	-2	4	0	13.73	-8.01	15.29	10.81	10.81
-7	-2	-4	0	9.71	138.02	9.58	2.74	9.18
2	-2	4	0	16.92	-	18.17	14.30	11.21
9	-2	4	2	15.51	-154.43	5.09	3.70	3.50
1	-3	4	0	18.96	-135.91	19.41	16.91	9.53
-6	-3	4	0	49.55	-5.42	47.96	33.91	33.91
-9	-3	4	4	22.14	-14.34	20.35	13.94	14.83
1	-4	4	0	23.82	-135.51	22.33	15.67	15.91
1	-5	4	0	19.68	7.45	22.10	20.24	8.87
2	-5	4	0	15.80	-144.85	15.49	5.32	14.55
1	-6	4	4	9.46	87.88	11.06	6.63	8.86
1	-7	4	0	11.07	16.56	14.01	6.71	12.30
2	-7	4	0	27.74	11.01	28.67	17.78	22.49
3	-7	4	0	7.56	-73.58	6.76	4.40	5.14
2	-8	4	4	9.99	-86.15	8.15	7.59	2.97
2	-8	4	0	3.65	32.23	3.43	3.49	2.63
4	-8	4	4	29.22	5.64	31.57	22.32	22.22
4	-9	4	2	15.08	-136.01	9.63	9.48	1.71
0	-9	5	0	38.04	-180.00	35.07	24.80	24.80
1	-5	5	0	34.96	-	35.03	22.49	26.86
2	-5	5	0	24.79	-	25.53	19.60	16.35
4	-5	5	1	3.41	-180.00	2.85	2.54	1.30
5	-5	5	0	21.71	-	19.79	15.84	11.86
6	-5	5	0	4.69	-180.00	4.80	3.52	3.27
7	-5	5	1	3.11	-	2.91	2.88	.42
2	-5	5	2	17.75	-	11.58	8.65	7.69
1	-5	5	0	20.25	-122.46	22.50	15.91	15.91
3	-5	5	1	7.01	-87.87	7.03	4.89	5.05
4	-5	5	0	10.26	-102.79	10.38	6.25	8.29
5	-5	5	0	16.11	4.20	17.59	12.97	11.88
-6	-5	5	0	14.33	10.21	17.59	11.88	12.97
-7	-5	5	0	7.99	179.98	4.25	4.02	1.38
-1	-5	5	0	8.04	-44.35	10.19	7.23	7.17
-1	-5	5	0	12.40	-25.36	12.95	7.85	10.30
-4	-5	5	0	10.12	-89.49	9.69	6.85	6.85
5	-5	5	1	8.60	156.41	8.58	6.28	5.85
-6	-5	5	0	18.18	28.17	18.47	13.68	12.41
-6	-5	5	0	20.74	-6.97	22.92	17.86	14.36
-7	-5	5	0	8.33	39.77	9.06	6.49	6.33
-1	-5	5	0	11.53	7.66	11.56	8.59	7.73
-3	-5	5	1	6.91	-	3.99	2.39	3.20
3	-5	5	0	15.20	177.42	16.29	11.52	11.52
4	-5	5	0	21.96	-	18.58	14.57	11.54
-5	-5	5	0	27.84	11.54	26.76	19.76	18.04
-8	-5	5	0	27.81	-1.38	23.89	18.02	15.68
0	-5	5	0	47.27	-	40.85	28.89	28.89
1	-5	5	1	3.34	-	1.72	1.08	1.33
2	-5	5	0	8.10	-	8.17	6.38	5.11
3	-5	5	0	36.20	-	30.89	28.31	12.24
4	-5	5	0	9.51	-	9.12	8.67	2.83
5	-6	5	1	5.46	-	5.08	4.91	1.31
5	-6	5	2	25.13	-	18.68	9.95	15.81
1	-6	5	0	13.66	6.21	14.36	10.15	10.15
4	-6	5	0	16.18	6.07	16.85	15.17	7.33
5	-6	5	2	15.12	72.12	6.54	3.44	5.57
1	-6	5	1	8.16	112.68	7.74	5.88	3.55
2	-6	5	0	17.09	-2.39	14.66	10.37	10.37

h	k	l	x	F <sub>obs</sub>	Phase	F <sub>calc<sub>T</sub></sub>	F <sub>calc<sub>1</sub></sub>	F <sub>calc<sub>2</sub></sub>
3	2	6	1	8.22	-74.77	5.64	5.60	.71
4	2	6	1	8.12	92.52	7.30	4.01	6.10
5	2	6	0	17.02	-3.80	15.54	12.56	9.15
1	3	6	0	10.68	-149.80	11.44	8.72	7.41
-6	3	6	0	29.26	-4.55	25.24	17.84	17.84
2	0	-7	0	17.99	-1.00	13.58	10.97	8.00

The ionic radius of  $\text{Na}^+$  is  $0.97\text{\AA}$  whereas the size of the octahedral interstice is appropriate to a sphere of radius  $0.55\text{\AA}$ . Each fluorine atom has twelve approximately equidistant fluorine neighbours with an average fluorine-fluorine distance of  $2.66(2)\text{\AA}$ .

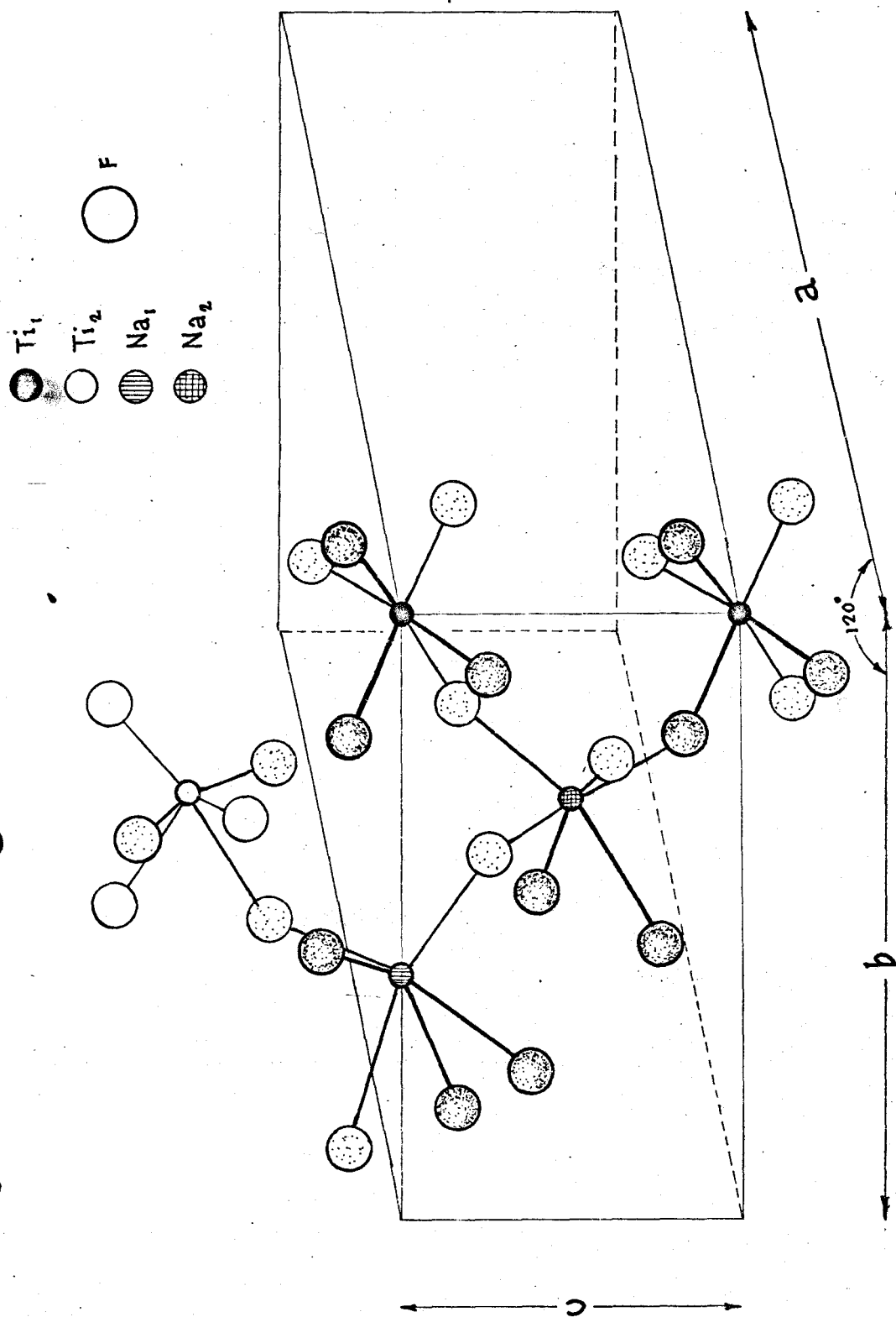
The puckering of the close-packed layers perpendicular to the c axis which was observed in  $\text{Li}_2\text{SnF}_6 \cdot 2\text{H}_2\text{O}$  and  $\text{Li}_2\text{TiF}_6 \cdot 2\text{H}_2\text{O}$  is much more pronounced in  $\text{Na}_2\text{TiF}_6$  with z coordinates for the fluorine atoms being as much as  $0.477\text{\AA}$  apart.

### Octahedra

The  $\text{TiF}_6$  groups share corners and edges with the  $\text{NaF}_6$  groups. This causes a closer approach of the two kinds of cations than occurs in  $\text{K}_2\text{TiF}_6$  where only corners are shared. This presence of shared edges is a feature of instability in other known close-packed structures<sup>(34)</sup>. The linking of the octahedra is shown in Figure 5.

There are two independent kinds of  $\text{TiF}_6$  groups but both are distinguishable as irregular octahedra. The octahedron about titanium-1 is the least distorted having six equal lengths of  $1.89(2)\text{\AA}$ , and F-Ti-F angles ranging from  $81.9(7)$  to  $93.5(7)$  degrees. The titanium-2 octahedron is distorted with titanium-fluorine bond lengths varying from  $1.84(2)\text{\AA}$  to  $1.89(2)\text{\AA}$ , and with angles varying from  $86.6(6)$  to  $92.2(8)$  degrees. Values for titanium-fluorine distances in other crystals are given on page 36. Similar results were obtained for the silicon-fluoride octahedra in

Figure 5 Linkage of Titanium and Sodium Octahedra.



$\text{Na}_2\text{SiF}_6$  (Table XVI). The bond distances and angles for  $\text{Na}_2\text{SiF}_6$  have been calculated using the programs in this laboratory to facilitate comparison (See I-ii-c). Data was taken from Zalkin et al<sup>(33)</sup>.

The arrangement of fluorine atoms about the sodium atom deviates even further from that of a regular octahedron. The bond lengths and angles are given together with those for  $\text{Na}_2\text{SiF}_6$  in Table XVI. Although individual results differ between the two compounds, the mean value for the sodium-fluorine bond distance,  $2.37(2)\overset{\circ}{\text{Å}}$  and the mean values for the octahedral angles,  $99.2(7)\overset{\circ}{\text{Å}}$  are the same. The mean values are also equal in the sodium-2 octahedron within the estimated standard deviations given. Measurements of the sodium-fluorine bond distance in other crystals are  $2.31\overset{\circ}{\text{Å}}$  to  $2.41\overset{\circ}{\text{Å}}$  in  $\text{Na}_2\text{SnF}_6$ <sup>(18)</sup> and  $2.21\overset{\circ}{\text{Å}}$  to  $2.68\overset{\circ}{\text{Å}}$  in  $\text{Na}_3\text{AlF}_6$ <sup>(35)</sup>.

The fluorine-fluorine distances differ in the two compounds however. The smallest fluorine-fluorine distance within the  $\text{SiF}_6$  group in  $\text{Na}_2\text{SiF}_6$  is  $2.34(2)\overset{\circ}{\text{Å}}$  which was considered reasonable evidence that the  $\text{SiF}_6$  group is a complex ion<sup>(36)</sup>. The corresponding distance in  $\text{Na}_2\text{TiF}_6$  is  $2.73(3)\overset{\circ}{\text{Å}}$  and the lowest value is  $2.59(2)\overset{\circ}{\text{Å}}$ . One would require supporting evidence to say with confidence that this implies covalent bonding in  $\text{Na}_2\text{TiF}_6$ . It should be pointed out that isolated  $\text{TiF}_6^{--}$  groups exist in solution but this cannot be used as a criterion of such groups being complex in the crystal too. Comparable or even equal forces from

Table XVIa Bond Distances and Angles for  $\text{TiF}_6$  and  $\text{SiF}_6$ 

<u>Octahedra</u>			
<u><math>\text{TiF}_6</math></u>			
<u>Atom</u>	<u>Neighbours</u>	<u>Distance (Å)</u>	<u>Angles (°)</u>
$\text{Ti}_1$	6 $\text{F}_1$	1.89 (2)	6 $\text{F}_1\text{-Ti-F}_1$ 92.6 (7)
			3 $\text{F}_1\text{-Ti-F}_1$ 81.9 (7)
			93.5 (7)
			[Mean 89.3 (7)]
$\text{Ti}_2$	3 $\text{F}_2$	1.86 (2)	$\text{F}_2\text{-Ti-F}_2$ 90.7 (8)
		1.89 (2)	92.2 (8)
		1.84 (1)	91.2 (8)
	3 $\text{F}_3$	1.87 (2)	$\text{F}_3\text{-Ti-F}_3$ 91.5 (9)
		1.84 (2)	90.1 (8)
		1.89 (2)	91.0 (9)
		[Mean 1.87 (2)]	$\text{F}_2\text{-Ti-F}_3$ 89.1 (6)
			89.0 (5)
			88.6 (7)
			88.6 (6)
		86.8 (6)	
		90.9 (6)	
		[Mean 90.0 (7)]	

Table XVIa(Cont'd). Bond Distances and Angles for  $\text{TiF}_6$  and  $\text{SiF}_6$ 

<u>Octahedra</u>				
<u><math>\text{SiF}_6</math></u>				
<u>Atom</u>	<u>Neighbours</u>	<u>Distances (<math>\text{\AA}</math>)</u>	<u>Angles (<math>^\circ</math>)</u>	
$\text{Si}_1$	6 $\text{F}_1$	1.67(1)	6 $\text{F}_1\text{-Si-F}_1$	90.5(10)
			3 $\text{F}_1\text{-Si-F}_1$	89.5(10)
			3 $\text{F}_1\text{-Si-F}_1$	90.6(10)
			[Mean	90.2(10)]
$\text{Si}_2$	3 $\text{F}_2$	1.69(1)	$\text{F}_2\text{-Si-F}_2$	89.2(10)
		1.72(1)		90.7(10)
		1.67(1)		89.6(10)
	3 $\text{F}_3$	1.69(1)	$\text{F}_3\text{-Si-F}_3$	89.6(10)
		1.66(1)		88.2(10)
		1.70(1)		89.1(10)
	[Mean	1.69(1)]	$\text{F}_2\text{-Si-F}_3$	90.2(10)
				91.5(10)
				90.1(10)
				89.7(10)
			87.8(10)	
			93.5(10)	
			[Mean 89.9(10)]	



Table XVIb. Bond Distances and Angles for NaF<sub>6</sub> OctahedraTi compound

<u>Atom</u>	<u>Neighbours</u>	<u>Distances (Å)</u>	<u>Angles (°)</u>	
Na <sub>1</sub>	2 F <sub>1</sub>	2.44(2)	2 F <sub>1</sub> -Na-F <sub>3</sub> 91.6(9)	
	2 F <sub>2</sub>	2.32(2)	2 F <sub>1</sub> -Na-F <sub>3</sub> 83.7(6)	
	2 F <sub>3</sub>	2.36(2)	1 F <sub>1</sub> -Na-F <sub>1</sub> 61.6(6)	
	[Mean	2.37(2)]	2 F <sub>1</sub> -Na-F <sub>2</sub> 94.3(9)	
			2 F <sub>3</sub> -Na-F <sub>2</sub> 93.0(12)	
			2 F <sub>3</sub> -Na-F <sub>2</sub> 89.3(6)	
			1 F <sub>2</sub> -Na-F <sub>2</sub> 110.6(8)	
			[Mean 99.2(7)]	
	Na <sub>2</sub>	2 F <sub>1</sub>	2.27(2)	1 F <sub>2</sub> -Na-F <sub>2</sub> 83.4(7)
		2 F <sub>2</sub>	2.37(2)	2 F <sub>2</sub> -Na-F <sub>1</sub> 88.1(8)
2 F <sub>3</sub>		2.37(3)	2 F <sub>2</sub> -Na-F <sub>3</sub> 66.4(8)	
[Mean		2.30(2)	2 F <sub>2</sub> -Na-F <sub>3</sub> 93.1(10)	
			2 F <sub>1</sub> -Na-F <sub>3</sub> 101.0(7)	
			2 F <sub>1</sub> -Na-F <sub>3</sub> 95.7(11)	
			1 F <sub>1</sub> -Na-F <sub>1</sub> 103.1(8)	
			[Mean 90.1(8)]	

Table VIb. (cont'd) Bond Distances and Angles for NaF<sub>6</sub> OctahedraSi compound

<u>Atom</u>	<u>Neighbours</u>	<u>Distances (Å)</u>	<u>Angles (°)</u>
Na <sub>1</sub>	2 F <sub>1</sub>	2.45(2)	2 F <sub>1</sub> -Na-F <sub>3</sub> 92.4(10)
	2 F <sub>2</sub>	2.30(1)	2 F <sub>1</sub> -Na-F <sub>3</sub> 86.1(10)
	2 F <sub>3</sub>	2.36(1)	1 F <sub>1</sub> -Na-F <sub>1</sub> 56.8(10)
	[Mean	2.37(2)]	2 F <sub>1</sub> -Na-F <sub>2</sub> 95.0(10)
			2 F <sub>3</sub> -Na-F <sub>2</sub> 93.2(10)
			2 F <sub>3</sub> -Na-F <sub>2</sub> 87.8(10)
			1 F <sub>2</sub> -Na-F <sub>2</sub> 113.3(10)
			[Mean 99.2(10)]
Na <sub>2</sub>	2 F <sub>1</sub>	2.18(1)	1 F <sub>2</sub> -Na-F <sub>2</sub> 85.0(10)
	2 F <sub>2</sub>	2.31(1)	2 F <sub>2</sub> -Na-F <sub>1</sub> 88.8(10)
	2 F <sub>3</sub>	2.31(1)	2 F <sub>2</sub> -Na-F <sub>3</sub> 61.8(10)
	[Mean	2.27(1)]	2 F <sub>2</sub> -Na-F <sub>3</sub> 93.1(10)
			2 F <sub>1</sub> -Na-F <sub>3</sub> 99.1(10)
			2 F <sub>1</sub> -Na-F <sub>3</sub> 101.2(10)
			1 F <sub>1</sub> -Na-F <sub>1</sub> 103.4(10)
			[Mean 90.3(10)]

'outside' a given group are always present in the solid state if linking of octahedra occurs<sup>(37)</sup>. The fluorine-fluorine bond length difference between  $\text{Na}_2\text{TiF}_6$  and  $\text{Na}_2\text{SiF}_6$  may merely be a size effect as the ionic radius for  $\text{Ti}^{+4}$  is  $0.68 \text{ \AA}$  and that for  $\text{Si}^{+4}$  is  $0.41 \text{ \AA}$ .

#### Anisotropic Temperature Factors

The direction cosines of the principal axes of the thermal ellipsoids with respect to the crystal axes were calculated for each atom and are given in Table XVII together with the root mean square components of the thermal motion along the principal axes. The thermal ellipsoids for titanium-1 and titanium-2 are oriented with one principal axis along the three-fold axis of the crystal, while those for sodium-1 and sodium-2 are oriented with one principal axis along the two-fold axes of the crystal. There is greater thermal anisotropy associated with the sodium atoms than with the titanium atoms and this is probably due to the greater distortions involved.

#### Thermal Corrections

Values of thermally corrected titanium-fluorine and sodium-fluorine bond lengths are given in Table XIX, for both a riding motion and an uncorrelated motion. The riding model was used by Zalkin et al. to correct the mean silicon-fluorine bond distance from  $1.68 \text{ \AA}$  to  $1.695(6) \text{ \AA}$ , but it is less certain whether it is a correct model to choose for  $\text{Na}_2\text{TiF}_6$ , due to the uncertainties about covalency.

Table XVII Principal Axis Analysis for Anisotropic Temperature Factors

NaTiF<sub>6</sub>

Atom	RMS Displacement (Å <sup>3</sup> )	Direction Cosines wrt		
		a	b	c
Ti <sub>1</sub>	.141(28)	0	0	1
	.112(32)	0.5000	0.5000	0
	.112(32)	0.5000	0.5000	0
Ti <sub>2</sub>	.137(20)	0	0	1
	.109(23)	0.5000	0.5000	0
	.109(23)	0.5000	0.5000	0
Na <sub>1</sub>	.175(69)	0	0	1
	.140(48)	-0.5000	-0.5000	0
	.137(35)	-0.4873(34)	-0.4873(48)	0
Na <sub>2</sub>	.177(67)	0.5000	0.5000	0
	.142(48)	0	0	1
	.127(39)	-0.3569(34)	-0.3569(35)	0
F <sub>1</sub>	.222(79)	0.1982(59)	0.2824(82)	0.8756(87)
	.172(69)	0.7591(79)	-0.0479(59)	-0.3952(53)
	.154(52)	-0.5494(61)	0.9581(81)	-0.2778(54)
F <sub>2</sub>	.210(89)	-0.6497(81)	-0.3265(63)	0.1104(65)
	.165(94)	0.5516(74)	-0.7663(61)	-0.6124(71)
	.128(51)	-0.5231(66)	0.5534(52)	-0.7828(68)
F <sub>3</sub>	.215(71)	0.7667(95)	-0.8777(46)	-0.2939(72)
	.175(95)	-0.5192(81)	-0.4510(44)	-0.9254(45)
	.125(73)	-0.3778(53)	0.1621(96)	-0.9254(45)

Table XVIII Thermal Corrections for Bond Lengths - Na<sub>2</sub>TiF<sub>6</sub>

<u>Bond</u>	<u>Riding Model</u>	<u>Uncorrelated</u>
Ti <sub>1</sub> - F <sub>1</sub>	1.90 (2)	1.93 (2)
Ti <sub>2</sub> - F <sub>2</sub>	1.87 (2)	1.89 (2)
	1.90 (2)	1.92 (2)
	1.85 (1)	1.87 (1)
Ti <sub>2</sub> - F <sub>3</sub>	1.86 (2)	1.88 (2)
	1.89 (2)	1.91 (2)
	1.90 (2)	1.92 (2)
Na <sub>1</sub> - F <sub>1</sub>	2.44 (2)	2.47 (2)
Na <sub>1</sub> - F <sub>2</sub>	2.32 (2)	2.34 (2)
Na <sub>1</sub> - F <sub>3</sub>	2.36 (2)	2.39 (2)
Na <sub>2</sub> - F <sub>1</sub>	2.27 (2)	2.30 (2)
Na <sub>2</sub> - F <sub>2</sub>	2.38 (2)	2.40 (2)
Na <sub>2</sub> - F <sub>3</sub>	2.38 (3)	2.41 (3)

### Potassium Dithionate

The structures of  $\text{Na}_2\text{TiF}_6$  and  $\text{Na}_2\text{SiF}_6$  are similar to that found in potassium dithionate,  $\text{K}_2\text{S}_2\text{O}_6$  (38,33). The pair of sulphur atoms in each dithionate ion is situated in the titanium position, with potassium corresponding to sodium, and oxygen corresponding to fluorine. The cell constants are  $a = 9.785(1) \text{ \AA}$  and  $c = 6.295(1) \text{ \AA}$ .

### Phase Transitions

A number of compounds of the type  $\text{A}_x\text{BF}_6$  are found to undergo one or more phase transitions (39,40).  $\text{K}_2\text{TiF}_6$ , for example, has the structure already discussed at room temperature, but transforms to two related polymorphs at higher temperatures. The structures differ essentially in the size of their hexagonal  $c$  axis. The ratio of the three  $c$  axes is close to 1:2:3, and the differences of the structures are due to different sequences of essentially the same layers, caused by movement of the interstitial ions into different interstices. The highest temperature polymorph has the  $\text{K}_2\text{PtCl}_6$  type structure (see page 53) with a resultant ideal close-packing of the ions.

A similar rearrangement of interstitial atoms probably occurs in  $\text{Li}_3\text{AlF}_6$ . The structure at room temperature consists of a slightly distorted array of close-packed fluorine atoms with lithium and aluminum atoms in intersti-

ces. (41) The crystal has five polymorphs at higher temperatures but the structures have not been completely characterized. (42, 43, 44, 45)

The structure of cryolite,  $\text{Na}_3\text{AlF}_6$ , is another example in which the size of the sodium atom has caused incompatibility of packing. In this case only 1/3 of the sodium atoms have octahedral coordination. In fact it is more informative to write the formula in the form  $\text{Na}_2(\text{NaAl})\text{F}_6$ . The other 2/3 of the sodium atom form part of the close packed array and are surrounded by twelve fluorine atoms. The structure at room temperature is quite distorted (35), but at higher temperatures cryolite transforms to a cubic structure closely related to the  $\text{K}_2\text{PtCl}_6$  type. (40) Increased thermal movements of the ions (possibly at different amplitudes for the two sets of non-equivalent alkali-metal ions) can presumably compensate for the unfavourable size factors (46).

It was thought that  $\text{Na}_2\text{TiF}_6$  might also show a change in structure upon heating. A single crystal was mounted on a precession camera with a heating element attached, and hk0 photographs were taken at 50°C intervals. At 600°C the crystal had decomposed, and no change in the symmetry was observed in any of the photographs.

## CHAPTER III

### OXIDES

#### i. The Crystal Structure of $\text{LiAl}_5\text{O}_8$

##### A. Background

The mineral spinel,  $\text{MgAl}_2\text{O}_4$ , is the prototype of the spinel structure. This structure is based on a cubic close-packed arrangement of oxygen atoms, in which one half of the octahedral sites and one eighth of the tetrahedral sites are occupied. In a 'normal' spinel,  $\text{XY}_2\text{O}_4$ , trivalent Y ions occupy the octahedral sites, and divalent X ions occupy the tetrahedral sites. There is also the possibility that half of the Y ions are in the tetrahedral sites, the remaining half together with the X ions being distributed over the octahedral sites, the so-called 'inverse' arrangement. Intermediate arrangements are also possible. If the atomic proportion of the divalent ion occurring in the octahedral sites is expressed as  $\delta$ , then  $\delta = 0$  for a normal spinel and  $\delta = 1$  for an inverse spinel. For a completely random distribution of the two kinds of ions between the two kinds of sites,  $\delta = 0.67$ .

The structure of  $\text{LiAl}_5\text{O}_8$  was shown by Kordes<sup>(47)</sup> to be of a spinel type. He assumed that one  $\text{Li}^+$  and one  $\text{Al}^{+3}$  replace two  $\text{Mg}^{++}$  in the structure with the arrangement  $(\text{LiAl})\text{Al}_4\text{O}_8$ . This would place all the  $\text{Li}^+$  ions in tetra-



hedral sites. There is another possibility however, pointed out by Verwey and Heilmann<sup>(48)</sup>, that of  $\text{Al}_2(\text{LiAl}_3)\text{O}_8$  which would place all the  $\text{Li}^+$  ions in octahedral sites. Using Kordes' x-ray powder diffraction results he found that the intensities are in favour of the arrangement  $\text{Al}_2(\text{LiAl}_3)\text{O}_8$ , but that a better arrangement might be obtained by assuming that the actual distribution is an intermediate one perhaps approaching a completely random distribution.

A single crystal study of  $\text{LiAl}_5\text{O}_8$  was undertaken to investigate the distribution of lithium and aluminum in octahedral and tetrahedral sites.

#### B. Preliminary Investigations

$\text{LiAl}_5\text{O}_8$  was prepared according to the method of Kordes<sup>(47)</sup>, and was identified from its x-ray powder diffraction pattern.

A single crystal which measured  $0.045 \text{ mm} \times 0.045 \text{ mm} \times 0.112 \text{ mm}$  was selected for x-ray study. Preliminary x-ray photographs showed that the crystal had cubic symmetry. Systematic absences of  $hk0$ ,  $h+k = 4n$  and  $hkl$ ,  $h+k, k+l = 2n$  were observed. These absences are uniquely consistent with the space group  $\text{Fd}3m$ .

The unit cell constants were accurately determined following the procedure outlined in Chapter I, using an  $h0l$  precession photograph for  $a^*$ . The final value is given in Table XIX.

Table XIX - Crystal Data for LiAl<sub>5</sub>O<sub>8</sub>

System	Cubic
Systematic Absences	hkl h+k = 2n, k+l = 2n hk0 h+k = 4n
Space Group	Fd3m
Cell Constant	
a	7.924(6) Å
Unit Cell Volume	497.75 Å <sup>3</sup>
Reciprocal Cell Constant	
a*	0.12618(6) Å <sup>-1</sup>
Density	
measured	3.61(6) g/cm <sup>3</sup>
calculated	3.62(3) g/cm <sup>3</sup>
Formula Units per Unit Cell (Z)	4
x-ray absorption coefficients	
Cu K	29.81 cm <sup>-1</sup>
Mo K	3.21 cm <sup>-1</sup>

Multiple film x-ray photographs were taken with an equi-inclination integrating Weissenberg camera for layers  $hk0$ ,  $hk1$ ,  $hk2$  using filtered  $CuK\alpha$  radiation. Layers  $hh0$ ,  $hh2$  and  $hh4$  were taken with an integrating Buerger precession camera using filtered  $MoK\alpha$  radiation. A total of 50 unique reflections were used in the final refinement.

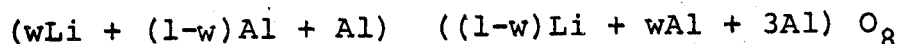
The linear absorption coefficient ( $\mu$ ) for  $LiAl_5O_8$  is  $29.81\text{ cm}^{-1}$  for  $CuK\alpha$  radiation and  $3.21\text{ cm}^{-1}$  for  $MoK\alpha$  radiation. The corresponding  $\mu R$  for a crystal of average radius 0.10 mm is 0.30 and 0.03 respectively. Absorption corrections were not considered necessary.

The density of the crystals was measured by flotation in a solution of *s*-tetra bromoethane and methylene iodide. The measured value of  $3.61(6)\text{ g/cm}^3$  agreed well with the calculated value of  $3.62(3)\text{ g/cm}^3$  assuming four molecules per unit cell.

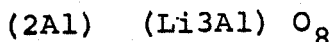
### C. Determination and Refinement of Structure

A spinel model was chosen for the preliminary refinement, assuming the formula  $Al_2(LiAl_3)O_8$ . The aluminum atom was placed in the tetrahedral site  $3/8, 3/8, 3/8$ , and the combined 'atom'  $Alli (LiAl_3)$  was placed in the octahedral site,  $0, 0, 0$ . The scattering factors for this site were weighted appropriately. The oxygen atom was placed in the position  $x, x, x$  with  $x = 0.25$ . An  $R_2$  factor of 0.076 was obtained with isotropic temperature factors. Anisotropic temperature factors

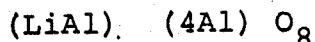
for the oxygen atoms reduced the  $R_2$  factor slightly to 0.072. The occupation of the tetrahedral and octahedral sites in the spinel structure was then considered in terms of a parameter  $w$ :



when  $w = 0$ , we have



when  $w = 1$ , we have



The  $R_2$  factor was then calculated for various values of  $w$ , given in Table XX. By plotting  $w$  vs.  $R_2$  a curve was obtained with a minimum at  $w = 0.09$ . A final least squares run for  $w = 0.09$  gave an  $R_2$  factor of 0.068. The final values of the atomic positional and thermal parameters are given in Table XXI and the observed and calculated structure factors are tabulated in Table XXII.

#### D. Discussion of the structure

The spinel structure for  $\text{LiAl}_5\text{O}_8$  reported by Kordes has been confirmed. The oxygen atoms are close-packed with an average oxygen-oxygen distance of  $2.733(3) \text{ \AA}$ . Ideal close-packing leads to a unit cell length in the packing direction that is a multiple of  $2\sqrt{8/3} R$ , where  $R$  is the radius of the close-packed ion. In the spinel structure the packing direction is along the three fold axis of the cube which would be  $\sqrt{3} a$ .

Table XX  $\text{LiAl}_5\text{O}_8$   $R_2$  for various values  
of w

w	$R_2$
0.00	0.0722
0.01	0.0720
0.02	0.0712
0.05	0.0702
0.10	0.0697
0.13	0.0701
0.15	0.0707
0.20	0.0731

Table XXI Final Parameters in  $\text{LiAl}_5\text{O}_8$

Atom	Site symmetry	$x=y=z$	$U_{\text{iso}}$	$U_{\text{anis}}$
0	$3m$	0.2436(23)		$U_{11}=U_{22}+U_{33}=0.0038(6)$ $U_{12}=U_{13}=U_{23}=0$
Tetrahedral				
Site	$\bar{4}3m$	$3/8$	0.0211	
Octahedral				
Site	$\bar{3}m$	0	0.0169	

Table XXII. Observed and Calculated Structure Factors for  $\text{LiAl}_5\text{O}_8$ . Reflections for which  $x = 1$  were unobserved, those for which  $x = 2$  were unreliable and not included in the refinement. 84

h	k	l	x	F <sub>obs</sub>	F <sub>calc</sub>
4	0	0	0	204.10	191.84
8	0	0	0	148.65	148.60
2	2	0	0	69.74	-70.14
4	4	0	0	227.22	230.35
2	6	0	0	38.83	38.87
6	6	0	0	31.38	-24.70
4	8	0	0	68.75	75.17
1	1	1	2	42.26	-25.72
7	1	1	1	15.30	-3.35
3	3	1	1	11.38	-5.60
5	3	1	0	14.47	12.26
7	3	1	0	41.90	38.11
7	5	1	0	45.25	39.39
7	7	1	1	12.21	-10.05
2	2	2	0	70.42	-60.97
4	2	2	0	48.64	51.65
4	4	2	1	13.86	4.75
6	4	2	0	36.63	-36.63
8	4	2	1	17.50	5.67
6	6	2	1	15.57	-15.69
1	1	3	0	96.82	96.92
3	3	3	0	50.75	-58.27
7	3	3	1	16.52	12.99
5	5	3	0	54.62	59.85
2	2	4	0	40.82	51.65
4	4	4	0	105.15	106.17
8	4	4	0	109.14	107.60
6	6	4	0	24.90	16.69
1	1	5	0	92.42	-95.35
5	1	5	0	21.25	-22.02
3	3	5	0	57.35	62.05
7	3	5	1	17.81	-1.72
5	5	5	0	56.79	-59.63
7	7	5	0	24.56	16.94
2	2	6	0	17.29	-16.66
4	4	6	1	17.30	2.95
8	4	6	1	20.34	4.39
6	6	6	0	22.18	-18.82
7	3	7	1	20.08	-11.49
5	5	7	0	16.57	4.07
2	2	8	0	29.77	-28.32
6	2	8	2	31.84	17.24
8	4	8	0	42.17	49.89
1	1	9	0	17.09	-16.17
3	1	9	0	44.82	41.96
5	1	9	0	46.07	-42.69
3	3	9	1	16.14	7.24
2	2	10	1	14.72	-18.26
1	1	11	0	17.17	14.13

If the radius of the oxygen atoms is taken to be  $1.4 \text{ \AA}$  then ideal close-packing would lead to a cell edge of  $7.953 \text{ \AA}$ . The value found in  $\text{LiAl}_5\text{O}_8$  is  $7.924(6) \text{ \AA}$ , which is closer to the ideal value than most other spinels.

The oxygen is surrounded by a slightly elongated tetrahedron of cations. In the spinel structure, the anion-cation distances become more equal when the anion moves away from the tetrahedral site, and many spinels show this tendency<sup>(49)</sup>. The extent of this distortion can be seen from the deviations of the oxygen parameter  $u$  ( $x + 1/8$ ) from the ideal value of 0.375. In  $\text{LiAl}_5\text{O}_8$ ,  $u$  is equal to 0.369. Some other values for  $u$  in spinel structures are:<sup>(50)</sup>

<u>compound</u>	$u$	$a$ ( $\text{\AA}$ )
$\text{Ag}_2\text{MoO}_4$	0.364	9.26
$\text{Co}_2\text{MgO}_4$	0.375	8.64
$\text{Li}_2\text{NiF}_4$	0.381	8.31
$\text{Al}_2\text{MgO}_4$	0.387	8.08

The four lithium atoms and the twenty aluminum atoms in the unit cell are distributed among the octahedral and tetrahedral interstices. On the average in the tetrahedral sites, there are 7.64 aluminum atoms and 0.36 lithium atoms, and on the average in the octahedral sites there are 12.36 aluminum atoms and 3.64 lithium atoms. These atoms cannot be distinguished within the site so those with tetrahedral



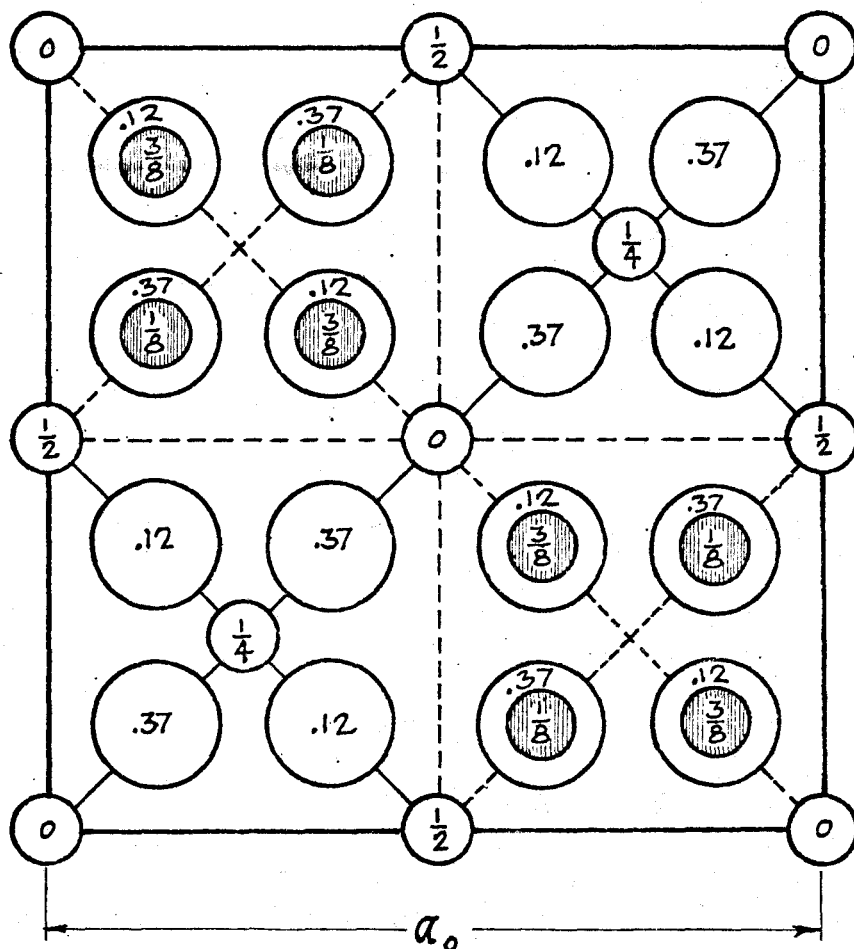
coordination will be called TET, and those with octahedral coordination will be called OCT. Figure 6 shows a projection on a cube face of the atoms in the lower half of the unit cell.

Both the tetrahedron and the octahedron are regular, with a TET-O distance of 1.804(18) Å, and an OCT-O distance of 1.933(18) Å. Average tetrahedral distances for lithium-oxygen and aluminum-oxygen bond lengths are 1.98 Å and 1.76 Å respectively. Using these distances, a distance of 1.804 Å implies a lithium content of about 10% in good agreement with the value of 9% found. The average octahedral distances for lithium-oxygen and aluminum oxygen bonds are 2.04 Å and 1.94 Å respectively. Using the same criterion the OCT-O bond length of 1.934 Å is not consistent with the amount of lithium calculated to be in the octahedral site. The low value may be due to the anion having moved to make the anion-cation distances more equal as suggested earlier. However, see page 105 where the limitations of using 'average' expected values are discussed.

#### Phase transitions in $\text{LiAl}_5\text{O}_8$ and $\text{LiFe}_5\text{O}_8$

$\text{LiAl}_5\text{O}_8$  exists in two stable polymorphic forms. The modification with the spinel structure is a high temperature form which is metastable at room temperature. The low temperature form has primitive cubic symmetry with the space group  $P4_33$ , and transforms to the spinel structure at 1295°C.

· Figure 6 ·



· A projection on a cube face  
of the atoms in the lower half  
of a unit cell of  $\text{LiAl}_5\text{O}_8$  ·



The lowering of symmetry to primitive cubic is thought to be an ordering or rearrangement of the lithium and aluminum atoms in the interstitial sites<sup>(51)</sup>. Datta and Roy have studied the phase transition of  $\text{LiAl}_5\text{O}_8$  using x-ray diffraction patterns and infrared spectroscopy, and have found a series of metastable low temperature forms belonging to the primitive unit cell structure type of the stable low temperature phase. Once formed these phases do not show the  $1295^\circ\text{C}$  phase change to the spinel structure<sup>(52)</sup>. The structure and distribution of cations in these low temperature forms is not known.

$\text{LiFe}_5\text{O}_8$  also has a high temperature spinel structure, and the form  $\text{Fe}_2(\text{LiFe}_3)\text{O}_8$  has been given as the correct distribution of cations. The transition at  $735^\circ\text{C}$  to a primitive cubic low temperature form is then associated with an ordering of the lithium and iron atoms in the octahedral sites<sup>(53)</sup>. Ordered derivatives of the spinel structure are also found in  $\text{CuFe}_5\text{O}_8$  and  $\text{LiGa}_5\text{O}_8$ <sup>(50)</sup>.

## ii. The crystal structure of $\text{LiAlO}_2$

### A. Background

There are two known phases of  $\text{LiAlO}_2$ . The  $\alpha$ -phase is stable at high pressures and temperatures and is metastable at atmospheric pressure and room temperature. When heated to  $900^\circ\text{C}$  it transforms to the  $\gamma$ -phase. The structure<sup>(54)</sup> of the

$\gamma$ -phase is based on an open framework of  $\text{AlO}_4$  tetrahedra and is related to that of  $\alpha$ -cristobolite ( $\text{SiO}_2$ )<sup>(55)</sup>. The lithium atom has tetrahedral coordination. The high pressure  $\alpha$ -phase has a structure based on close-packing of oxygen atoms with aluminum and lithium atoms in octahedral sites<sup>(56)</sup>.

#### B. Preliminary Investigations

$\text{LiAlO}_2$  was prepared previously by a solid state reaction of  $\text{Li}_2\text{CO}_3$  and  $\text{Al}_2\text{O}_3$  at high temperatures<sup>(57)</sup>. A new phase has been prepared by the following method. Forty percent aqueous hydrofluoric acid was slowly added to 0.1 moles of lithium carbonate, and this solution was added to a solution of 0.1 moles of aluminum chloride. A precipitate formed immediately. This was filtered and dried and then heated in a platinum crucible to  $850^\circ\text{C}$ . The crucible was slowly cooled in the oven to room temperature over a period of four days. An x-ray powder diffraction pattern of this precipitate was indexed on the basis of a hexagonal cell, and later x-ray studies showed it to be a new form of  $\text{LiAlO}_2$ , henceforth referred to as  $\beta$ - $\text{LiAlO}_2$ .

A single crystal that measured  $0.024 \text{ mm} \times 0.012 \text{ mm} \times 0.012 \text{ mm}$  was mounted for x-ray studies. Precession  $hk0$  and  $hkl$  and  $h0l$  photographs showed that the crystal was hexagonal with systematic absences,  $00l = 3n$ . The space groups with these absences are  $P6_2$ ,  $P6_4$ ,  $P6_222$  and  $P6_422$ .

The unit cell constants were accurately determined following the procedure outlined in Chapter I, using an  $h0l$  precession photograph for  $a^*$  and  $c^*$ . The values are given in Table XXIII.

Multiple film x-ray photographs were taken with an equi-inclination integrating Weissenberg camera for layers  $h0l$ ,  $h1l$ ,  $h2l$ ,  $h3l$ , and  $h4l$ , using filtered  $\text{CuK}\alpha$  radiation. The photographs  $hk0$ ,  $hkl$ ,  $hk2$ , and  $h2\bar{h}l$  were taken with an integrating Buerger precession camera using filtered  $\text{MoK}$  radiation. A total of 95 unique reflections were used in the final refinement.

The linear absorption coefficient ( $\mu$ ) for  $\text{LiAlO}_2$  is  $25.56 \text{ cm}^{-1}$  for  $\text{CuK}$  radiation and  $2.78 \text{ cm}^{-1}$  for  $\text{MoK}$  radiation. The corresponding  $\mu R$  for a crystal of average radius  $0.016 \text{ mm}$  is  $0.41$  and  $0.04$  respectively. Absorption corrections were not considered necessary.

Assuming three molecules per unit cell, the measured value of the density  $2.45(9) \text{ g/cm}^3$ , agreed well with the calculated value of  $2.47(3) \text{ g/cm}^3$ .

### C. Determination and Refinement of Structure

A comparison of the symmetry and cell dimensions of  $\beta\text{-LiAlO}_2$  with those of  $\beta\text{-quartz}$  ( $\text{SiO}_2$ )<sup>(58)</sup>,  $\beta\text{-spodumene}$  ( $\text{LiAlSi}_2\text{O}_6\text{-III}^*$ )<sup>(59,60)</sup>, and  $\text{Li}_2\text{Al}_2\text{Si}_3\text{O}_{10}$ <sup>(62)</sup>, suggested

---

\*

There are two high temperature modifications of spodumene and they have both been called  $\beta$  at various times. The term spodumene-III for the high quartz structure is used to avoid confusion. Spodumene-II is related to the structure of keatite, another modification of  $\text{SiO}_2$ .<sup>(61)</sup>

Table XXIII Crystal Data for  $\beta$ -LiAlO<sub>2</sub>

System	Hexagonal
Systematic Absences	000 $l$ $l = 3n$
Space Group	P6 <sub>2</sub> 22
Cell Constants	
a	5.255(1) Å
c	5.559(1) Å
Unit Cell Volume	132.95 Å <sup>3</sup>
Reciprocal Cell Constants	
a*	0.21973(1) Å <sup>-1</sup>
c*	0.17988(1) Å <sup>-1</sup>
Density	
measured	2.45(9)
calculated	2.47(3)
Formula Units per unit cell (Z)	3
X-ray absorption coefficients	
Cu K <sub>α</sub>	25.56 cm <sup>-1</sup>
Mo K <sub>α</sub>	2.78 cm <sup>-1</sup>

that the structures might be similar. Both the aluminosilicates are known to have a  $\beta$ -quartz type structure.

<u>compound</u>	a*	c*	symmetry
$\beta$ -LiAlO <sub>2</sub>	5.255(1)	5.559(1)	hexagonal P6 <sub>2</sub> , P6 <sub>4</sub> .P6 <sub>2</sub> 22 P6 <sub>4</sub> 22
SiO <sub>2</sub> ( $\beta$ -quartz)	5.01	5.47	P6 <sub>2</sub> 22
LiAlSi <sub>2</sub> O <sub>6</sub> -III	5.217(1)	5.464(2)	P6 <sub>2</sub> 22
Li <sub>2</sub> Al <sub>2</sub> Si <sub>3</sub> O <sub>10</sub>	5.238(1)	5.472(1)	P6 <sub>2</sub> 22.

The space group and positional parameters of the  $\beta$ -quartz structure were chosen as an initial model for the aluminum and oxygen atoms in LiAlO<sub>2</sub>. The aluminum atom was placed in the position 0,0,1/2 and the oxygen atom in the position x,2x,0 with x = 0.2. Refinement of this structure by least squares led to an R<sub>2</sub> factor of 0.076 with isotropic temperature factors.

The structure of spodume-III is a 'stuffed derivative' of the  $\beta$ -quartz structure. The term 'stuffed derivative' has been defined by Buerger<sup>(63)</sup> in the following manner. A derivative structure is one derived from a simpler basic structure. This can occur by distortion of the simpler structure, or by substitution of its atoms by others of different chemical species. When the substituted atoms have a smaller valence than those for which they substitute, the charge must be balanced by the addition of other atoms. For

the substitution of  $\text{Si}^{+4}$  by  $\text{Al}^{+3}$ , the alkali and alkaline earth ions often perform this function. These extra atoms must then find space accommodation in the structure and are said to be stuffed into these spaces. For example, the lithium ion can be drawn through the interstices of  $\beta$ -quartz at high temperatures with the aid of an electric field but the larger alkali ions,  $\text{Na}^+$  and  $\text{K}^{(64)}$  cannot, indicating that there is only sufficient space to accommodate small ions. Therefore stuffed derivatives of the  $\beta$ -quartz structure containing lithium would be expected to occur. In spodume-III, the oxygen atoms occupy the same positions as those in  $\beta$ -quartz and the aluminum and silicon atoms are randomly distributed on the silicon sites. In the  $\beta$ -quartz structure there are channels parallel to the c axis, and the one lithium ion in the unit cell of  $\text{LiAlSi}_2\text{O}_6$ -III is found with tetrahedral coordination randomly distributed among three equivalent sites situated in these channels. In  $\text{LiAlO}_2$ , three lithium atoms must be accommodated in the same cell volume as  $\text{LiAlSi}_2\text{O}_6$ -III. The use of the lithium site of  $\beta$ -spodumene with the full multiplicity would lead to three lithium atoms with lithium-lithium distances of about  $1.82 \text{ \AA}$ . An acceptable lithium-lithium distance is about  $3.08 \text{ \AA}^{(65)}$  so we would not expect to find more than two lithium atoms randomly distributed among the three equivalent sites. Two lithium atoms were placed in this site and the multiplicity was varied by least



squares. The lowest  $R_2$  factor was 0.06 which gave one and a half atoms in this site.

At this stage a three dimensional difference electron density was calculated to find a position for the other one and a half atoms. The six-fold site  $x,0,0$  was chosen with  $x = 0.33$ . This position also places tetrahedrally coordinated lithium atoms in the channels parallel to the  $c$  axis. Refinement with one and a half atoms in this position reduced the  $R_2$  factor to 0.048, and introduction of anisotropic temperature factors gave a final  $R_2$  factor of 0.044. The final values of the atomic positional and thermal parameters are given in Table XXIV, and the observed and calculated structure factors are tabulated in Table XXV.

#### D. Lithium disorder and superstructure reflections

In the structure thus refined there are one and a half lithium-1 atoms randomly distributed among three equivalent sites in the unit cell. Each site has a probability of  $1/2$  of being occupied. This means that there is a  $1/2$  probability that a lithium atom has a lithium neighbour  $1.85 \text{ \AA}$  away from a site already occupied. This is still an unfavourable situation and can be avoided if instead of being disordered, the lithium atoms are ordered over two unit cells as shown in figure 7. This arrangement would require that the  $c$  axis be doubled. A similar argument applies to the one and a half lithium-2 atoms randomly distributed among six equivalent sites.

Table XXIV Atomic Parameters for  $\beta$ -LiAlO<sub>2</sub>

a. Positional

<u>Atom</u>	<u>Site Symmetry</u>	<u>x</u>	<u>y</u>	<u>z</u>
Al	222	1/2	0	1/2
O	2	0.2015	0.4030(9)	0
Li <sub>1</sub>	222	0	0	1/2
Li <sub>2</sub>	2	0.3695(126)	0	0

b. Thermal

	<u>U<sub>11</sub></u>	<u>U<sub>22</sub></u>	<u>U<sub>33</sub></u>	<u>U<sub>12</sub></u>	<u>U<sub>13</sub></u>
Al	0.0093(8)	0.0082(9)	0.0139(11)	0.0041	0
O	0.0222(16)	0.0191(18)	0.0379(22)	0.0097	0.0097(14)
Li <sub>1</sub>	0.011 (10)	0.019 (14)	0.084 (17)	0.009	0
Li <sub>2</sub>	0.083 (40)	0.161 (11)	0.328 (99)	0.08	0

$U_{23}$  is equal to zero and  $U_{12} = \frac{1}{2} U_{22}$  for all atoms.

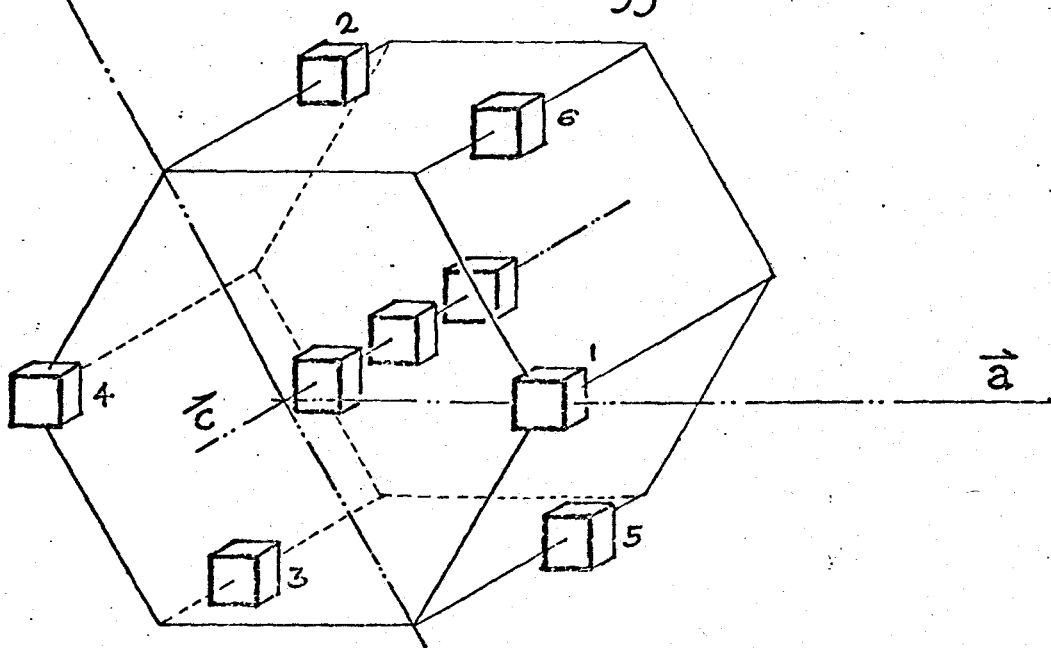
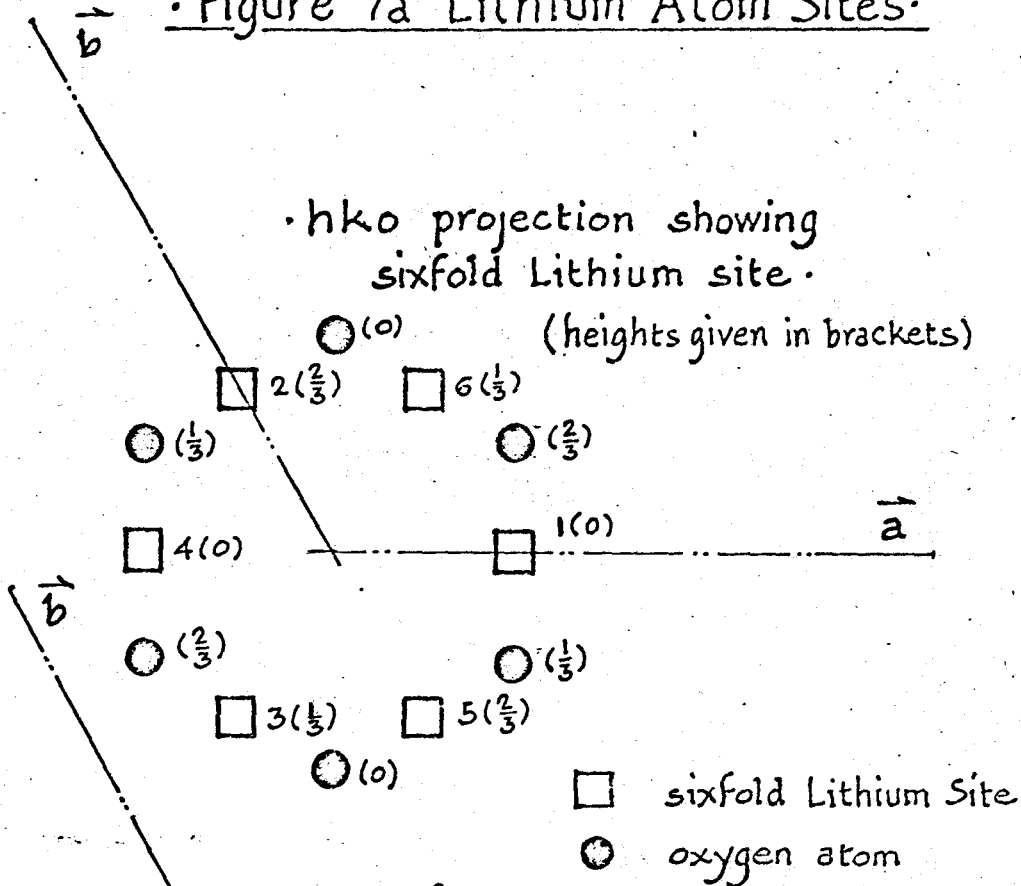
Table XXV. Observed and Calculated Structure Factors for  $\text{LiAlO}_2$ . Reflections with  $x = 1$  were unobserved, those with  $x = 2$  were unreliable and not used in the refinement.

h	k	l	x	F <sub>obs</sub>	σ	F <sub>calc</sub>	A	B
1	0	0	0	11.00	3.21	10.51	-10.61	0.00
2	0	0	0	14.91	3.84	15.89	-15.89	0.00
5	0	0	0	4.73	2.22	4.78	4.78	0.00
11	1	0	0	13.04	3.59	13.80	-13.80	.00
11	2	0	0	6.87	2.49	6.70	6.70	-.00
20	2	3	0	24.61	4.97	27.89	27.89	-.00
11	2	3	3	12.86	3.54	12.63	-12.63	.00
22	3	3	0	8.23	2.71	7.92	-7.92	-.00
22	3	3	3	8.19	2.85	7.95	-7.95	-.00
00	4	0	1	1.82	1.34	.94	.94	-.00
00	4	0	0	16.96	4.10	17.39	17.39	-.00
11	4	4	0	4.07	1.99	3.84	-3.84	-.00
21	4	5	0	10.94	3.41	11.14	11.14	.00
22	5	0	0	3.11	1.79	3.39	-3.39	.00
00	5	6	0	4.18	2.17	4.09	-4.09	-.00
00	6	0	0	9.22	3.11	9.08	9.08	.00
11	7	1	1	30.71	5.59	32.41	16.21	28.07
37	0	0	0	1.99	1.44	1.79	.90	1.55
2	1	1	1	2.41	1.59	2.71	1.35	2.35
11	1	1	1	1.78	1.34	1.63	1.63	-.00
20	2	2	0	11.87	3.54	11.11	11.11	-.00
11	2	2	2	17.35	4.55	17.57	12.00	12.84
20	2	2	3	2.87	1.65	2.90	-1.45	2.51
20	3	1	1	7.89	2.76	7.94	-7.94	.00
11	3	1	1	17.00	4.41	17.48	1.99	-17.36
22	3	1	1	11.49	3.50	11.62	-11.16	3.24
33	3	1	1	6.25	2.52	6.31	3.15	-5.46
50	3	3	0	5.23	2.33	5.22	3.19	-3.88
44	4	1	1	4.22	2.02	4.45	-4.45	-.00
11	4	4	0	8.38	2.95	8.51	6.68	5.28
22	4	4	0	2.90	2.09	4.00	4.00	.08
34	4	5	0	5.06	2.26	4.62	2.52	3.87
00	5	1	1	7.77	2.87	7.95	-7.95	.00
11	5	5	0	5.94	2.56	6.21	4.43	-4.06
11	5	6	1	6.82	2.69	7.04	-6.85	-1.66
11	6	0	0	6.31	2.58	6.47	1.38	6.22
11	6	2	2	6.16	2.44	6.08	-3.04	5.27
11	7	1	1	29.28	5.29	29.97	-14.98	-25.95
11	7	2	2	8.61	2.95	8.98	8.08	.00
22	7	2	2	12.89	3.63	12.73	-3.31	12.30
22	7	3	3	3.15	1.80	3.76	-1.58	-2.74
22	7	3	3	18.23	4.24	18.20	18.20	-.00
22	7	3	3	10.35	3.21	10.98	-9.46	-3.46
33	7	3	3	7.93	2.86	7.67	7.17	-2.72
33	7	4	4	8.37	2.95	8.93	-4.02	-6.96
33	7	4	4	3.07	1.74	2.90	-2.90	.00
44	7	4	4	10.20	3.29	9.80	-2.80	9.39
33	7	5	5	3.52	1.99	3.65	3.64	.23
33	7	5	5	7.42	2.72	6.77	-3.80	5.61
00	7	5	5	7.64	2.82	7.67	7.67	-.00
11	7	5	5	7.90	2.89	7.96	-2.32	-7.61
22	7	5	5	6.51	2.57	4.65	4.47	1.27
22	7	7	7	6.25	2.53	5.28	5.28	.00
50	8	2	2	3.76	1.95	3.89	-.76	3.82
00	8	3	3	2.34	1.59	2.33	-2.33	.00
00	8	3	3	4.00	2.20	4.49	4.49	.00
22	8	3	3	27.37	5.42	27.61	-27.61	.00
22	8	3	3	1.64	1.26	.32	-.32	.00
44	8	3	3	15.54	3.95	14.32	-14.32	.00
00	8	3	3	7.15	2.60	8.40	8.40	-.00
11	8	3	3	2.31	1.36	2.26	2.26	-.00
22	8	3	3	12.16	3.33	11.88	11.84	.92
22	8	3	3	2.42	1.54	2.12	2.09	.37
34	8	3	3	3.22	1.72	3.06	2.96	-.77
22	8	3	3	11.76	3.26	11.71	-11.21	.00
22	8	3	3	2.04	1.41	.77	.21	.18
3	8	3	3	5.15	2.24	5.95	5.95	-.00

h	k	l	x	F <sub>obs</sub>	$\sigma$	F <sub>calc</sub>	A	B
1	0	4	0	8.44	2.85	7.93	-3.96	-6.87
2	0	4	0	4.83	2.15	4.53	-2.27	-3.92
3	0	4	0	12.15	3.40	11.65	-5.83	-10.09
4	0	4	0	3.09	1.79	3.02	-1.51	-2.61
1	1	4	0	17.84	4.16	18.30	-9.15	15.84
2	1	4	0	9.25	2.98	8.75	8.59	-1.68
3	1	4	0	7.26	2.70	7.21	-.09	7.01
4	1	4	0	7.27	2.68	7.70	7.48	-1.83
2	2	4	1	2.07	1.45	1.21	-.60	1.05
3	2	4	0	6.92	2.60	6.96	-5.21	-4.60
-3	6	4	0	7.35	2.57	6.82	-3.41	-5.90
1	6	5	0	13.07	3.64	13.01	-6.50	-11.26
2	0	5	0	2.49	1.45	2.34	-1.17	2.03
3	0	5	0	4.71	2.07	5.08	2.54	-4.40
1	1	5	0	5.15	2.13	4.89	2.44	4.23
3	1	5	0	7.97	2.82	8.61	6.55	5.59
2	2	5	0	1.83	1.33	1.75	-.88	-1.52
-1	3	5	0	8.42	2.94	8.36	5.30	-6.47
0	4	5	0	8.98	0.00	8.98	-.98	-.00
0	5	5	0	18.07	3.82	16.96	16.96	-1.00
1	0	6	0	3.47	1.75	3.90	-3.90	-1.00
-2	0	6	0	7.36	2.67	8.34	8.34	-1.00
2	1	6	1	1.26	1.10	.92	-.69	.61
-2	1	6	0	4.01	1.88	4.28	-4.28	.00
0	3	6	2	2.56	1.59	4.53	-4.53	.00
-2	4	6	0	11.13	3.28	10.10	10.10	-1.00
-1	2	7	0	3.44	1.80	3.31	1.65	2.86

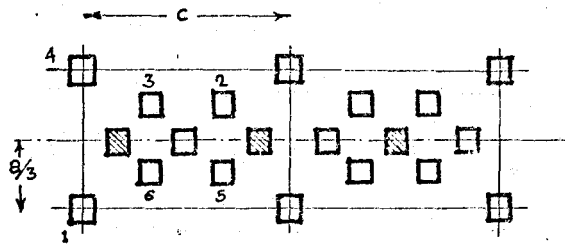
• Figure 7a Lithium Atom Sites •

• hko projection showing sixfold Lithium site •

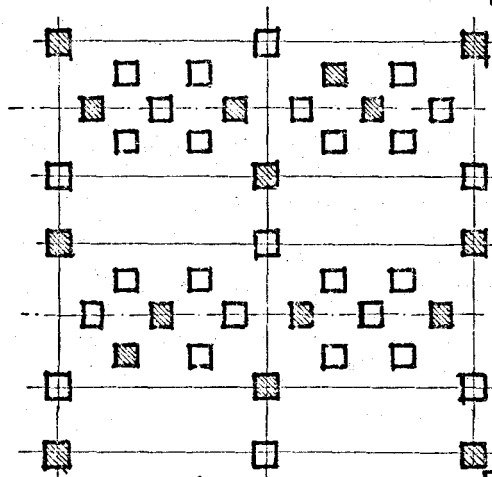
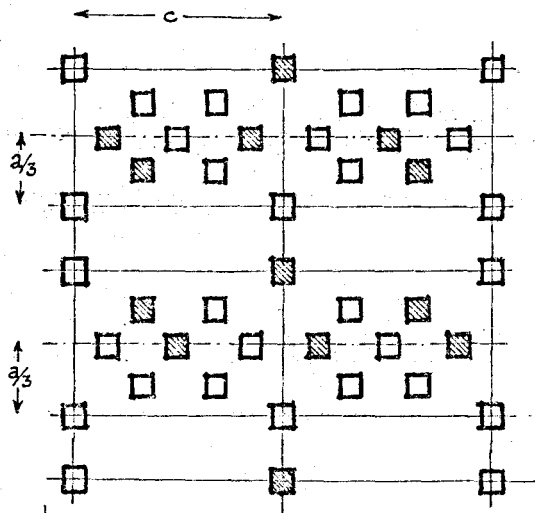


• Projection showing all Lithium sites •

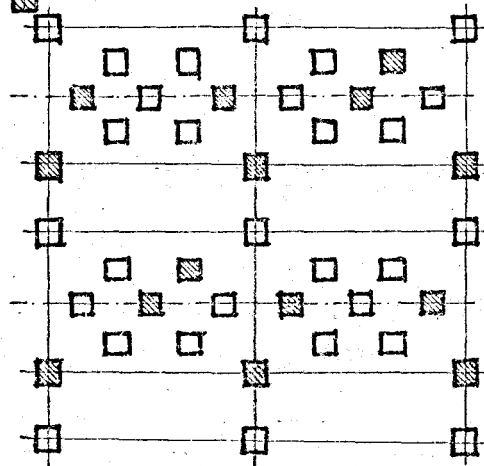
• Figure 7b Possible Occupation of Lithium Sites •



• c-axis doubled  
ordering of Lithium 1.



• Three examples of  
a-axis doubled.



Several ordered arrangements are possible if the a axis is doubled as well as the c axis. Some of these are shown in figure 7. If this type of doubling occurs then there should be photographic evidence for it, although the extra reflections would be expected to be weak due to the low x-ray scattering power of the lithium atom.

A four day exposure of an h0l Weissenberg photograph of  $\beta$ -LiAlO<sub>2</sub> was taken. Very faint reflections were observed in positions which indicated doubling of the c and the a axes. No further investigations were carried out, but the assumption of some kind of ordering of the lithium atoms was shown to be justified. Thus the structure of  $\beta$ -LiAlO<sub>2</sub> has been refined in a subcell of the true cell, and the atoms may occupy only approximately the positions found by the refinement. This should be borne in mind in the next section when the structure is discussed in detail.

The occurrence of ordering of the 'stuffed' atoms in a  $\beta$ -quartz type structure has been observed in other crystals. Single crystal photographs of  $\beta$ -eucryptite, LiAlSiO<sub>4</sub>, show weak superstructure reflections in addition to the main reflections of a  $\beta$ -quartz-like subcell<sup>(66,67)</sup>, indicating a doubling of the c and the a axis. The intensity and sharpness of the superstructure reflections depend on the crystallization conditions and further thermal treatment. These weak reflections are attributed to the ordering of the silicon and aluminum



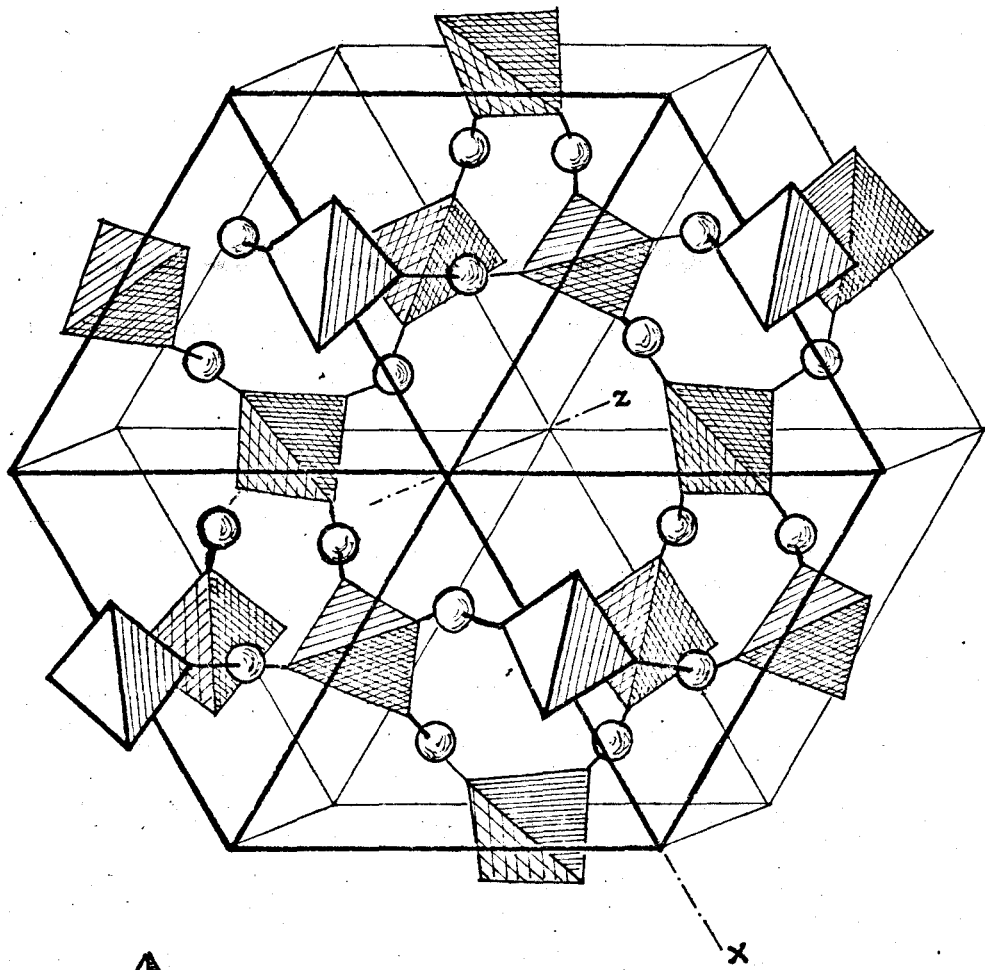
atoms as well as ordering of the lithium atom. Saalfeld reports a doubled a and c axis in spodumene-III although this was not confirmed or commented on by Chi-Tang Li<sup>(68,59)</sup>.

The system  $\text{MgO} \cdot \text{Al}_2\text{O}_3 \cdot x\text{SiO}_2$  also produces crystals which have the stuffed high quartz structure<sup>(69)</sup>. The  $\text{Mg}^{++}$  ion (0.65 Å) has a radius which is almost identical to that of the  $\text{Li}^+$  ion (0.68 Å), and therefore can also fit into the channels parallel to the c axis. The crystals  $x = 3$  and  $x = 4$  have been studied by Schulz et al.<sup>(70)</sup>. Both these crystals have the  $\beta$ -quartz-like subcell,  $x = 3$ :  $a = 5.18$  Å,  $c = 5.36$  Å;  $x = 4$ :  $a = 5.16$  Å,  $c = 5.39$  Å. Weak extra reflections were observed which indicated doubling of the c and the a axes. There is also some evidence that  $\beta$ -quartz-like structures are formed in the system  $\text{FeO} \cdot \text{Al}_2\text{O}_3 \cdot x\text{SiO}_2$  system although not enough is known yet to say whether superstructure reflections appear<sup>(69)</sup>.

#### E. Discussion of structure

The basic oxygen and aluminum framework is built up of  $\text{AlO}_4$  tetrahedra linked together so that every oxygen atom is common to two tetrahedra. Besides two aluminum neighbours each oxygen atom has six adjacent oxygen atoms at an average distance of 2.607(3) Å. The tetrahedra form interconnecting helices (see Figure 8) and at the center of these helices there are channels parallel to the c axis which are occupied

Figure 8



Aluminum and Oxygen  
bonding in  $\beta\text{-LiAlO}_2$

by the lithium atoms at tetrahedral sites. The aluminum and lithium tetrahedra share corners and edges.

Bond distances and angles for  $\beta$ -LiAlO<sub>2</sub> are given in Table XXVI together with those for Li<sub>2</sub>Al<sub>2</sub>Si<sub>3</sub>O<sub>10</sub>, LiAlSi<sub>2</sub>O<sub>6</sub>-III and  $\beta$ -quartz. Although the differences are small, a systematic trend in distances and angles can be seen as increasing amounts of aluminum and lithium are added to the  $\beta$ -quartz structure. The M-O bond distance increases as would be expected. Four of the angles in the M tetrahedra increase, and two decrease. In The Li<sub>1</sub>-tetrahedra the Li-O distance decreases. This contraction of the lithium tetrahedron is accompanied by an increase in the distance between the two types of cations.

The AlO<sub>4</sub> tetrahedron is slightly distorted with angles varying from 102.89(12)° to 112.47(2)° and an aluminum-oxygen bond length of 1.666(4) Å. This bond length is much shorter than the value of 1.75 Å given by Smith and Bailey as the average expected in alumino-silicates for tetrahedrally coordinated aluminum<sup>(71)</sup>. There are a number of possible explanations for a shortening of the aluminum-oxygen bond. First and foremost it must be remembered that the refinement leading to these calculated bond lengths was carried out in a subcell of the true cell and it may be that the atom positions are approximate. Keeping this in mind, it is still likely that such a large effect is real, and that some shortening of the bond occurs. The AlO<sub>4</sub> tetrahedra share edges with the LiO<sub>4</sub>

Table XXVI Interatomic Distances and Angles in  $\beta$ -LiAlO<sub>2</sub>,  
 $\text{LiAlSi}_2\text{O}_6$ -III,  $\text{Li}_2\text{Al}_2\text{Si}_3\text{O}_{10}$  and  $\beta$ -quartz (A)

	<u><math>\beta</math>-LiAlO<sub>2</sub></u> (M = Al)	<u><math>\text{Li}_2\text{Al}_2\text{Si}_3\text{O}_{10}</math></u>	<u><math>\text{LiAlSi}_2\text{O}_6</math>-III</u> (M = Al, Si)	<u><math>\beta</math>-quartz</u> (M = Si)
<u>M tetrahedra</u>				
4 M-O	1.666(4)	1.649(1)	1.641(1)	1.594
2 O-M-O	112.47(02)	111.7(2)	111.1(3)	110.2
2 O-M-O	113.25(17)	112.8(1)	112.6(1)	111.5
2 O-M-O	102.89(12)	104.0(3)	104.9(4)	106.7
<u>Li<sub>1</sub> tetrahedra</u>				
4 Li-O	2.054(4)	2.064(4)	2.068(5)	
2 O-Li-O	126.4(1)	126.7(2)	126.65(04)	
2 O-Li-O	127.0(2)	127.6(1)	127.7(1)	
2 O-Li-O	78.7(1)	78.0(1)	77.9(1)	
<u>Li<sub>2</sub> tetrahedra</u>				
2 Li-O	2.097(12)			
2 Li-O	2.671(49)			
1 O-Li-O	134.0(6)			
1 O-Li-O	126.2(17)			
1 O-Li-O	103.3(4)			
1 O-Li-O	102.7(29)			
1 O-Li-O	98.2(23)			
1 O-Li-O	70.2(8)			
<u>Other</u>				
M-Li <sub>1</sub>	2.627(1)	3.619(1)	2.609(1)	
M-Li <sub>2</sub>	2.553(93)			
M-O-M	149.3(3)	150.8	151.6(4)	152.8(5)

tetrahedra and this edge sharing may contribute to the effect. The (SiAl)-O bond lengths in spodumene-III and in  $\text{Li}_2\text{Al}_2\text{Si}_3\text{O}_{10}$  are also shorter than the distances expected for the ratio Si:Al of 2:1 and 3:2 respectively. Chi-Tang Li attributes these discrepancies to edge sharing between the (SiAl) tetrahedra and the Li tetrahedra. However, in  $\gamma\text{-LiAlO}_2$  edge sharing also occurs between lithium and aluminum tetrahedra and the aluminum-oxygen bond length in this compound is  $1.76 \text{ \AA}$ . The average (AlSi)-O bond distance in leucite,  $(\text{K},\text{Na})\text{AlSi}_2\text{O}_6$  was found to be about  $0.04 \text{ \AA}$  less than the value expected for this composition of silicon and aluminum, whereas the author was expecting a higher value than that predicted because the structure determination was carried out at high temperatures<sup>(72)</sup>.

It is probable that it is not meaningful to compare aluminum-oxygen and silicon-oxygen bond lengths with average values in aluminosilicates, especially as these averages have been computed over all types of structures. A comprehensive study by Smith and Bailey of aluminum and silicon in tetrahedral coordination<sup>(71)</sup> has revealed several trends in aluminum-oxygen and silicon-oxygen bond lengths. For example, they have shown that the linkage of tetrahedra has a significant effect on tetrahedral distances. The silicon-oxygen bond length seems to increase from  $1.54 \text{ \AA}$  in a framework silicate to  $1.70 \text{ \AA}$  in a structure with isolated tetrahedra. Evaluation of the effect of tetrahedral linkage on the aluminum-oxygen

distances was difficult because of scarcity of data, but they noted a similar decrease in bond length from isolated tetrahedra to framework structure. The decrease in the aluminum case was greater in magnitude than in that of the silicon. This observation would be consistent with a low value in the framework structure of  $\beta$ -LiAlO<sub>2</sub> and the other  $\beta$ -quartz structures. It has also been found that in many cases a large range of silicon-oxygen and aluminum-oxygen distances is found within one structure. In anorthite, BaAl<sub>2</sub>Si<sub>2</sub>O<sub>8</sub>, for example, the aluminum-oxygen tetrahedral bond distance varies from 1.695(4) Å to 1.820(4) Å, and in Li<sub>2</sub>Si<sub>2</sub>O<sub>5</sub> the silicon-oxygen bond distance varies from 1.57 Å to 1.67 Å, and in CaTiOSiO<sub>4</sub> from 1.54 Å to 1.74 Å (50).

These variations depend on a very complex system of interacting forces and there is currently no chemical theory which can adequately explain them. Smith and Bailey emphasize the fact that an empirical approach is the only reliable one at present and in a continuing investigation they are looking for correlations between bond lengths and such effects as external cations and shared polyhedral edges. In connection with the latter it is interesting to note that a very low value of 1.60 Å for the aluminum-oxygen bond length was reported for KAlO<sub>2</sub><sup>(73)</sup>. This structure is a 'stuffed derivative' of cristobalite, in which the potassium ions have a coordination of twelve and the polyhedra around potassium

share faces with the tetrahedra around aluminum. It has already been noted that the sharing of tetrahedral edges can shorten the aluminum-oxygen bond length, and it would be expected that the sharing of faces would shorten it even more. Theoretically, if the distance between A atoms (i.e. A - X - A) is unity for tetrahedra AX<sub>4</sub> sharing corners, then for shared edges this distance is reduced to 0.58 and for shared faces it is reduced to 0.33<sup>(74)</sup>.

Bond lengths in both AlO<sub>4</sub> and SiO<sub>4</sub> tetrahedra have also been surveyed by Brown and Gibbs<sup>(75,76)</sup>. They have noted that the M-O distance is correlated with the M-O-M bond angle, the types of M cations in M-O-M linkages, e.g. Si-O-Si, Si-O-Al, or Al-O-Al, and with the number and types of cations which are coordinating with the oxygen atom. In addition, they have made estimates of the d-p  $\pi$ -overlap integral for the MO<sub>4</sub> tetrahedral ion, and these together with data from x-ray emission studies have led them to suggest that d-p  $\pi$ -bonding also plays an important role in the variation of M-O bond lengths, although the exact nature of the role is not yet known. In any case it would seem that since the M-O distances in  $\beta$ -quartz, spodumene-III, Li<sub>2</sub>Al<sub>2</sub>Si<sub>3</sub>O<sub>10</sub>, and  $\beta$ -LiAlO<sub>2</sub> are all below the 'average' value expected, there must be a correlation between this type of framework structure and the low bond length.

Both the LiO<sub>4</sub> tetrahedra in  $\beta$ -LiAlO<sub>2</sub> are distorted. The lithium<sub>1</sub>-oxygen bond distance is 2.055(4)<sup>o</sup>Å and the O-Li<sub>1</sub>-O

tetrahedral angles range from  $78.75(10)^\circ$  to  $126.99(15)^\circ$ , with an average of  $110.71(12)^\circ$ . The lithium<sub>2</sub>-oxygen bond distance is greater, with an average of  $2.38(3) \text{ \AA}$  and the angles are more distorted with an average of  $106.77^\circ$ . Some lithium oxygen bond lengths found in other crystals for tetrahedrally coordinated lithium are:  $2.003 \text{ \AA}$  in  $\gamma\text{LiAlO}_2$ ,  $2.068 \text{ \AA}$  in  $\text{LiBO}_2$ ,  $1.947 \text{ \AA}$  in  $\text{Li}_2\text{SO}_4 \cdot \text{H}_2\text{O}$ , and  $1.985 \text{ \AA}$  in  $\text{LiGaO}_2$ <sup>(59)</sup>. The first two examples are also cases where lithium polyhedra share edges with other cation polyhedra.

Both lithium tetrahedra share edges with aluminum tetrahedra and the oxygen-oxygen bond length is shorter for these shared edges viz.  $2.607(4) \text{ \AA}$ , compared to an average distance of  $2.718(4) \text{ \AA}$  for the aluminum tetrahedra and  $3.204(9)$  for the lithium tetrahedra. Shared edges are also found in  $\gamma\text{-LiAlO}_2$  where the oxygen-oxygen bond length for the shared edge is  $2.737 \text{ \AA}$ , compared to an average distance of  $2.896(4) \text{ \AA}$  for the aluminum tetrahedra and  $3.342(3) \text{ \AA}$  for the lithium tetrahedra.

The system  $\text{Li}_2\text{O} \cdot \text{Al}_2\text{O}_3 \cdot x\text{SiO}_2$ <sup>(77)</sup>

$\beta\text{-LiAlO}_2$  can be considered as the first member ( $x=0$ ) of a series of  $\beta$ -quartz-like compounds belonging to the system,  $\text{Li}_2\text{O} \cdot \text{Al}_2\text{O}_3 \cdot x\text{SiO}_2$ . Table XXVII gives the first few members of the series and their cell constants. For the first four members of the series, there is an increase in the length of the a axis with increasing amounts of aluminum and lithium,



Table XXVII  $\beta$ -quartz structures in the  $\text{Li}_2\text{O}\cdot\text{Al}_2\text{O}_3\cdot x\text{SiO}_2$  system

Name	formula	x	a (Å)	c (Å)	ref.
	$\beta\text{-LiAlO}_2$	0	5.255(1)	5.559(1)	
$\beta$ -eucryptite	$\text{LiAlSiO}_4$	2	5.246(1)×2	5.587(1)×2	61,62
	$\text{Li}_2\text{Al}_2\text{Si}_3\text{O}_{16}$	3	5.238(1)	5.472(1)	75
$\beta$ -spodumene	$\text{LiAlSi}_2\text{O}_6$	4	5.217(1)	5.464(2)	55,56
lithium orthoclase	$\text{LiAlSi}_3\text{O}_8$	6	5.27	5.28 ×2	63
$\alpha$ -petalite	$\text{LiAlSi}_4\text{O}_{10}$	8	5.14	5.88 ×2	76
$\beta$ -quartz	$\text{SiO}_2$	$\infty$	5.01	5.47	58

whereas the c axis increases to  $x = 2$  then decreases.

Accurate parameters are not available for the members  $x = 6$  and  $x = 8$  and it is possible that these would follow the same trend. The last but one compound listed,  $\alpha$ -petalite, has monoclinic symmetry, but the structure is still closely related to that of the  $\beta$ -quartz structure<sup>(78)</sup>. In the  $\text{MgO-Al}_2\text{O}_3-x\text{SiO}_2$  system (page 92), a similar expansion of the a axis is observed with increasing amounts of aluminum and magnesium, but the c axis contracts.

Hummel<sup>(79)</sup>, Henglein<sup>(80)</sup>, and Roy<sup>(81,82)</sup> have found a series of solid solutions with the high-quartz structure existing between  $\text{SiO}_2$  and  $\text{Li}_2\text{O}\cdot\text{Al}_2\text{O}_3$ , although not all members of the series are stable as shown by Skinner and Evans<sup>(83)</sup>. Roy reports that the quartz which crystallized from the system  $\text{Li}_2\text{O-Al}_2\text{O}_3\text{-SiO}_2$  had cell dimensions at room temperature considerably larger than those of low quartz and similar to those of high quartz at  $600^\circ\text{C}$ . Compounds of formula  $\text{Li}_2\text{O}\cdot\text{Al}_2\text{O}_3\cdot 8-10 \text{SiO}_2$  were heated between  $750$  and  $900^\circ\text{C}$  and the resultant products were examined by x-ray powder diffraction. It is possible that the 'quartz' he obtained was  $\beta\text{-LiAlO}_2$ , although not enough detail was given for a positive identification<sup>(81)</sup>.

#### The structure of $\gamma\text{-LiAlO}_2$

The structure of  $\gamma\text{-LiAlO}_2$  has been solved by single crystal methods by Marezio<sup>(54)</sup> and is closely related to that of  $\alpha$ -cristobalite ( $\text{SiO}_2$ )<sup>(55)</sup>. The crystal data for the two

structures are compared below.

	<u><math>\gamma</math>-LiAlO<sub>2</sub></u>	<u><math>\alpha</math>-cristabolite</u>
a	5.1587 Å	4.978 Å
c	6.2679 Å	6.948 Å
Z	4	4
Volume	170 Å <sup>3</sup>	166 Å <sup>3</sup>
Space Group	P4 <sub>1</sub> 2 <sub>1</sub> 2	P4 <sub>1</sub> 2 <sub>1</sub> 2

The aluminum and oxygen atoms are in the same positions as the silicon and oxygen atoms in  $\alpha$ -cristobalite.

Al(4a)	xx0	x = 0.3241*	0.3
O (8b)	xyz	x = 0.2094	0.2398
		y = 0.1631	0.1032
		z = 0.2277	0.1784
Li(4a)		x = 0.6874	

The structure of  $\gamma$ -LiAlO<sub>2</sub> can be considered a 'stuffed derivative' of  $\alpha$ -cristobalite. The AlO<sub>4</sub> tetrahedra are linked together by sharing corners to form an infinite three dimensional framework. With the addition of the Li<sup>+</sup> atoms in tetrahedral sites, each of the lithium and aluminum tetrahedra

---

\*The following transformation has been made to the LiAlO<sub>2</sub> coordinates reported by Marezio to facilitate comparison.

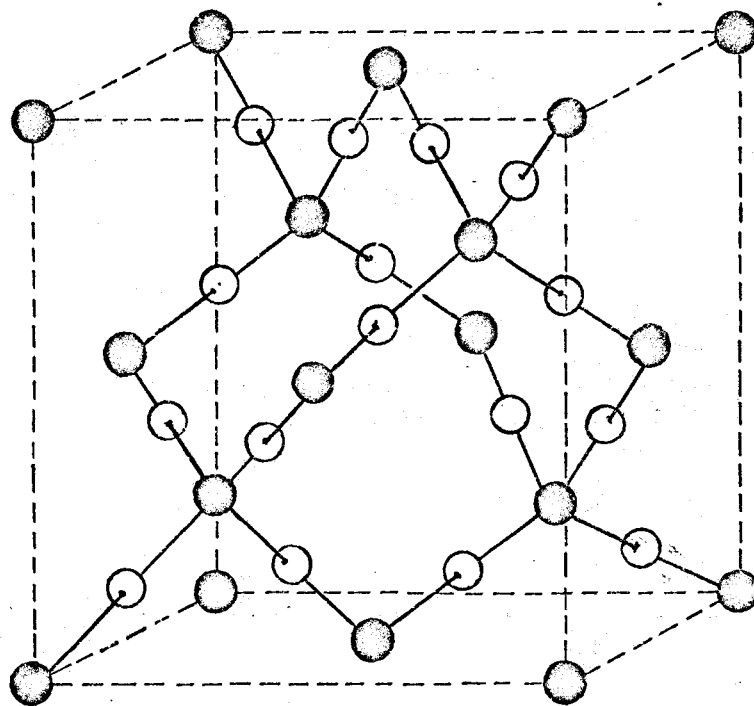
$$x = 1/2 - y, y = 1/2 - x, z = -z$$

shares one of its edges with another tetrahedron of a different kind. Thus each oxygen atom is shared among four tetrahedra, two aluminum centred and two lithium centred. The linking of the tetrahedra is different from that in the  $\beta$ -quartz as can be seen from figures 8 and 9. The high temperature  $\beta$ -form of cristobalite is an idealized symmetrical form of  $\alpha$ -cristobalite, which results in slightly larger holes. Several crystals are known which can be considered 'stuffed derivatives' of the  $\beta$ -form. The slightly larger spaces can accommodate the larger cations such as  $\text{Na}^+$  and  $\text{K}^+$  so that compounds such as  $\text{Na}(\text{AlSi})\text{O}_8$ ,  $\text{Na}_2\text{CaSiO}_8$ ,  $\text{KAlO}_2$  and  $\text{NaAlO}_2$  are found with this structure.

#### Phase transitions and the structure of $\alpha$ - $\text{LiAlO}_2$

The conditions for the phase transition between  $\beta$  and  $\gamma$ - $\text{LiAlO}_2$  are not known but this transformation would involve the breaking of Al-O-Al bonds and the linking together of the tetrahedra in a different way. A reconstructive transition of this sort would be first order and would be expected to be quite 'sluggish' in analogy with the transition between quartz and cristobalite.

$\alpha$ - $\text{LiAlO}_2$  has been shown to be a stable high pressure and high temperature phase, metastable at room temperature and atmospheric pressure<sup>(56)</sup>. Above 600°C and atmospheric pressure  $\alpha$ - $\text{LiAlO}_2$  is irreversibly converted to the  $\gamma$ -phase, with a decrease in density of 0.786 g/cm<sup>3</sup>. The structure of



$\beta$ -cristobalite (cubic)

· Figure 9 ·

the  $\alpha$ -phase, solved from an x-ray powder diffraction pattern, is based on a close-packing of oxygen atoms with lithium and aluminum atoms in octahedral interstitial sites. This change from an open framework structure to a close-packed structure explains the large change in density. The crystal has the space group symmetry  $R\bar{3}m$  and can be described as a distorted superlattice of a sodium chloride structure elongated along a three-fold axis.

## CHAPTER IV

### CONCLUSION

In this study of some ternary oxides,  $A_x B_y O_n$ , and fluorides,  $A_x B_y F_n$ , it has been shown that a large number of them occur as close-packed structures, either with the anions packing together with the cations in interstitial sites, or with anions and cations packing together. It is seen that the type of structure is strongly dependent on the relative sizes of the ions and their radius ratios, the simple ionic theory holding true because of the strong electronegative character of the oxygen and fluorine atoms. However, in all five of the structures studied, there were cations whose coordination was not uniquely predictable by the values of their radius ratios and these ions occur in different structures with different coordination numbers. These are examples of ions whose radius ratio is close to the critical value for transition from one coordination number to another.

#### Coordination of aluminum and silicon

The value of the Al:O radius ratio is 0.357. From the table in Appendix I it can be seen that the critical value for transition from six to four coordination is 0.414.

The Al:O ratio is so close to this value that the aluminum atom occurs in crystal structures with both types of coordination. As shown already, this can occur even in the same compound, either in the same phase as in  $\text{LiAl}_5\text{O}_8$ , or in a different modification as occurs in  $\text{LiAlO}_2$ .

This versatility of the aluminum atom is especially evident in the alumino-silicates. In these compounds, aluminum substitutes for silicon in a tetrahedral site and/or behaves as an interstitial with six-fold coordination, in both close-packed and open framework structures. For example, in sillimanite  $\text{Al}(\text{AlSi})\text{O}_5$ , the aluminum has both four and six coordination, whereas in another modification, cyanite,  $\text{Al}_2\text{SiO}_5$ , the oxygen atoms are cubic close-packed with aluminum in octahedral sites and silicon in tetrahedral sites.\*

The radius ratio for Si:O, 0.293, is further away from the critical value, and six-fold coordination in silicon compounds is rare. The high pressure form of  $\text{SiO}_2$ , coesite, formed at 40.4 kbar and  $750^\circ\text{C}$  still has silicon in four-fold coordination<sup>(84,85)</sup>, whereas only 35 kbar and  $850^\circ\text{C}$  were required to form  $\alpha\text{-LiAlO}_2$ . Orthoclase,  $\text{KAlSi}_3\text{O}_8$ , transforms at 100 kbar and  $1000^\circ\text{C}$  to a hollandite-type structure in which all the silicon and aluminum atoms are in octahedral

\*When references are not specifically given they can be found in the comprehensive bibliographies in references 2 and 23.



coordination<sup>(86)</sup>. Other examples of silicon in six-fold coordination are  $\text{SiP}_2\text{O}_7$ ,  $\text{K}_2\text{SiF}_6$ ,  $\text{Na}_2\text{SiF}_6$ ,  $(\text{SiAc}_3)\text{AuCl}_4$  (Ac = acetylacetonate), and  $\text{SiTe}_2$ . In the latter compound the bonds are metallic in character.

Tetrahedral coordination of silicon by oxygen is considered a fundamental characteristic of all silicate structures. The difference in electronegativity between silicon and oxygen is 1.7 and this value corresponds to a bond which is 40% ionic. Thus a considerable degree of covalent character is attributed to the silicon-oxygen bond<sup>(87)</sup>. The difference in electronegativity between aluminum and oxygen is 2.0 corresponding to a bond which is 46% ionic. This slightly greater degree of ionicity in the aluminum-oxygen bond seems insufficient to explain the greater tendency of aluminum to form octahedral as well as tetrahedral coordination, and the criterion of the radius ratio would appear to be adequate to explain the difference.

Wells has pointed out that it is dangerous to draw conclusions about the ionic-covalent character of M-O bonds in a particular oxy compound of M from the value assigned to the electronegativity coefficients, since the character of the M-O bond will depend on the environment of the oxygen atom. There is, for example, a difference in the type of bonding between octahedral and tetrahedral coordination for aluminum. In sillimanite where aluminum has both four and six coordination,

the bonds in the tetrahedra possess more covalent character than in the octahedra<sup>(87)</sup>. A difference in bond strength has been shown by Kolesova in the case of  $\text{LiAlO}_2$ <sup>(88)</sup> using infrared spectroscopy. The octahedrally coordinated aluminum in  $\alpha\text{-LiAlO}_2$  has an aluminum oxygen stretching frequency of  $760\text{ cm}^{-1}$  and the tetrahedrally coordinated aluminum in  $\gamma\text{-LiAlO}_2$  has an aluminum-oxygen stretching frequency of  $817\text{ cm}^{-1}$ . A higher frequency implies greater bond strength which can in turn imply higher bond order. The greater bond strength leads to the shorter aluminum-oxygen bond length for the tetrahedrally coordinated aluminum.

The Al:F radius ratio of 0.368 is closer to the critical value than that of Al:O, and there are many examples of aluminum in octahedral sites in close-packed ternary fluoride structures.  $\text{Li}_3\text{AlF}_6$  and  $\text{Na}_3\text{AlF}_6$  have already been mentioned and other examples are  $(\text{NH}_4)_3\text{AlF}_6$ ,  $\text{Na}_3\text{Li}_3\text{Al}_3\text{F}_{12}$  (cryolithionite)  $\text{Tl}_2\text{AlF}_5$ ,  $\text{TlAlF}_4$ , and  $\text{Na}_5\text{Al}_3\text{F}_{14}$  (chiolite). The bonding in these compounds is ionic, and the structures only differ in the linking of  $\text{AlF}_6$  octahedra. Ternary fluorides with aluminum in tetrahedral coordination do not seem to be known.

#### Coordination of lithium

The Li:F radius ratio is 0.441 and accordingly the lithium ion in ternary fluorides is nearly always found in octahedral coordination,  $\text{Li}_2\text{ZrF}_6$  and  $\text{Li}_3\text{AlF}_6$  being typical

examples. An exception is found however in the inverse spinel structure of  $\text{Li}_2\text{NiF}_4$  where 1/2 of the lithium ions are in tetrahedral sites and 1/2 in octahedral sites. Tetrahedral coordination for lithium also occurs in  $\text{Li}_2\text{BeF}_4$  which has a phenacite-type structure.

The Li:O radius ratio of 0.428 is closer to the critical value of 0.414 for change of coordination from four to six and there are many examples of both types of coordination in ternary oxides. It has already been seen in  $\text{LiAl}_5\text{O}_8$  that the lithium atom occupies both tetrahedral and octahedral sites in the spinel structure, and in  $\text{LiAlO}_2$  that there is a change from four to six coordination at higher pressures. Four coordination has been found in all the lithium 'stuffed' quartz derivatives. In  $\text{Li}_2\text{SO}_4$  the low temperature form has tetrahedral coordination of lithium whereas a high temperature modification has a mixture of tetrahedral and octahedral coordination. In  $\text{Li}_2\text{TiF}_6 \cdot 2\text{H}_2\text{O}$  and  $\text{Li}_2\text{SnF}_6 \cdot 2\text{H}_2\text{O}$  the lithium atom is surrounded by four fluorine atoms and two oxygen atoms in a distorted octahedral site. Other examples of octahedral coordination in close-packed structures are found in  $\text{LiSbO}_3$ ,  $\text{LiFeO}_2$ , and  $\text{LiNbO}_3$ . The spinel structures,  $\text{Li}_2\text{WO}_4$  and  $\text{Li}_2\text{MoO}_4$  have four fold coordination for lithium as do  $\text{Li}_2\text{Si}_2\text{O}_5$ ,  $\text{Li}_2\text{Ge}_2\text{O}_5$  and  $\text{Li}_3\text{XO}_4$  ( $X = \text{P, As, V}$ ).

### Coordination of sodium

In  $\text{Na}_2\text{TiF}_6$ ,  $\text{Na}_2\text{SiF}_6$  and  $\text{Na}_3\text{AlF}_6$  the size of the sodium atom causes distortions in the close-packing of the fluorine atoms. In the first two examples sodium has a distorted octahedral environment and in cryolite, 1/3 of the sodium atoms have octahedral coordination and the other 2/3 form part of the close-packed array with a coordination number of twelve. In this structure the distortion can be seen as rotations of  $\text{AlF}_6$  octahedra whereby the fluoride ions move away from the edges of the unit cell to enlarge the space available for the octahedrally coordinated sodium ion. The sodium ions with twelve coordination have six fluoride ions which are closer than the other six, giving them an irregular coordination of six. The sodium ion in the perovskite-type structures,  $\text{NaMeF}_3$  (Me = Mg, Ni, Zn, Cu, Co, Fe, Cr, Mn) also has an irregular coordination of six within a coordination sphere of twelve.

The Na:F radius ratio is 0.70 which is close to the critical value for transition from six to eight coordination, 0.732 (see Appendix I). A strict coordination of eight for sodium in ternary fluorides is not often found however, it being more usual to have a distorted six coordination, often with the octahedra sharing corners and edges as in  $\text{Na}_2\text{TiF}_6$  and  $\text{Na}_2\text{SnF}_6$ . The compound  $\text{NaAlF}_4$  has a compressed cubic coordination of eight fluoride ions from eight different  $\text{AlF}_6$

octahedra about each sodium ion. The  $\text{Na}_2\text{UF}_6$  structure is a slightly deformed fluoride structure in which both types of positive ion are eight coordinated. This crystal is another example of coordination change from one modification to another. In the  $\beta$  form of  $\text{Na}_2\text{UF}_6$  the sodium has six coordination and the uranium has nine. In  $\text{Na}_3\text{UF}_7$  and  $\text{Na}_2\text{CuF}_4$  sodium has a coordination of seven.

The Na:O radius ratio of 0.75 is also close to the critical value and a similar variation in coordination for sodium is found in the ternary oxides. Octahedral coordination is the most common, and there are less distortions in the close-packing of the oxygen atoms as the larger radius of the oxygen allows more space in the octahedral site for the sodium atom. Examples are  $\text{NaSbO}_3$ ,  $\text{NaBiO}_3$ , and  $\text{NaFeO}_2$ . Octahedral coordination for sodium is also well represented in the silicates although eight is sometimes found. In  $\text{NaAlFASO}_4$ , sodium is coordinated to six oxygen atoms with sodium-oxygen distances ranging from 2.40 Å to 2.47 Å, and to one fluorine atom, with a sodium-fluorine distance of 2.35 Å. In the low temperature form of  $\text{Na}_2\text{SO}_4$ , sodium has six coordination but changes to ten in the high temperature modification. Exceptions to the radius ratio rule are found in  $\text{Na}_2\text{O}$  where sodium has four coordination in an antiferite arrangement and in  $\text{NaOH}$ , where sodium has five nearest  $\text{OH}^-$  neighbours at five of the apices of an octahedron.

The crystals that have been discussed are those in which the geometrical conditions are equally favourable for more than one structural arrangement. It is not surprising then that many of them show one or more transitions from one form to another, brought about by changes in temperature and pressure. In some cases, atoms with more than one type of coordination are found in the same structure, and redistribution of coordination type can also lead to structural transitions.

Appendix - Radius Ratio and the Simple Ionic Theory

The simple ionic theory makes four basic assumptions:

1. Ions are charged, incompressible, nonpolarizable spheres.
2. An arrangement of ions of one charge about an ion of the opposite charge is stable only if the central ion is in contact with each of its neighbours. This places a lower limit to the ratio of the radius of the central ion to that of the surrounding ions for each type of coordination polyhedron (see table below). Since positive ions are almost always smaller than the negative ions which accompany them in crystals this restriction means effectively that the coordination number of small metal ions is often limited by the radius ratio rules, while the coordination numbers of anions are rarely limited in this way.
3. The coordination number is as large as possible, subject to condition (2).
4. The arrangement of the coordinated groups minimizes the electrostatic repulsion energy between them.

This simple model still forms a satisfactory background to a great part of the theory of the stereochemistry of ionic solids.

Limiting Radius Ratios for Various Coordination Polyhedra

Polyhedron	Coordination number	Minimum Radius Ratio
Equilateral Triangle	3	0.155

Polyhedron	Coordination number	Minimum Radius Ratio
Tetrahedron	4	0.225
Octahedron	6	0.414
Cube	8	0.732



Bibliography

1. A systematic survey of cubic crystal structures. A. L. Loeb, J. Solid State Chem. 1, 237 (1970). Dr. Loeb offers an alternative model to systematically correlate ionic structures. This model includes bcc structures which are not covered in the close-packed model.
2. Structural Chemistry of Octahedral Fluoro complexes of the transition elements. p. 61. D. Babel, Structure and Bonding 3, 3 (1967).
3. Crystal-structure analysis. M. J. Buerger. John Wiley and Sons Inc., New York, 1960.
4. Vector Space. M. J. Buerger. John Wiley and Sons Inc., New York, 1959.
5. X-ray Crystallography. M. J. Buerger. John Wiley and Sons Inc., New York, 1942.
6. International Tables for X-ray Crystallography. Kynock Press, Birmingham, Vol. I, 1952, Vol. II, 1959, Vol. III. 1962.
7. The Optical Principles of the Diffraction of X-rays. R. W. James, G. Bell and Sons Ltd., London, 1962.
8. The Determination of Crystal Structures. H. Lipson and W. Cochran. G. Bell and Sons Ltd. London, 1962.
9. X-ray Structure Determination. G. H. Stout and L. H. Jensen. Collier-Macmillan Ltd., London, 1968.
10. The Calculation of Atomic Structures. D. R. Hartree, John Wiley, London, 1957.
11. A Direct Method for the determination of the components of interatomic distances in crystals. A.L. Patterson, Z. Krist. 90, 517 (1935).
12. W. L. Bragg, Proc. Roy. Soc. A 123, 537 (1929).
13. Some properties of the  $(F_o - F_c)$  synthesis. W. Cochran. Acta Cryst. 4, 408 (1951).
14. Computing methods and the phase problem in x-ray crystal analysis. D.W.J. Cruickshank, D.E. Pilling, A. Bujosa, F.M. Lovell, M. R. Truter, New York (1961).

15. The structures of anatase and rutile. D.T. Cromer and K.D. Herrington, J. Amer. Chem. Soc. 77, 4708 (1955).
16. The crystal structure of  $K_2TiF_6$ . S. Siegel, Acta Cryst. 5, 683 (1952).
17. Crystal structure of  $CuTiF_6 \cdot 4H_2O$ . J. Fischer, G. Keib, R. Weiss. Acta Cryst. 22, 338 (1967).
18. Zur Kristallstruktur von  $Na_2SnF_6$ . Ch. Hebecker, H.G. v Schnering, and R. Hoppe. Naturwissenschaften 53 154 (1966).
19. The crystal structure of  $LiSbF_6$ . J. H. Burns. Acta Cryst. 15, 1098 (1962).
20. Zur Kristallstruktur von  $Li_2ZrF_6$ . R. Hoppe and W. Dähne. Naturwissenschaften 47 397 (1960).
21. The crystal structure of  $LiNiO_2$ . L. D. Dyer, B.S. Bone Jr., and G. P. Smith, JACS 76 1499 (1954).
22. The crystal structure of  $LiSbO_3$ . M. Edstrand and N. Ingui. Acta Chem. Scand. 8 1021 (1954).
23. Structural inorganic chemistry, 3rd ed. page 594. A.F. Wells. Oxford University Press, London, 1962.
24. Reference 23, page 588.
25. Temperature corrections on bond lengths. W. R. Busing and H. A. Levy. Acta Cryst. 17, 142 (1964).
26. C. Marignac. Ann. Mines 5 15 (1859).
27. Advanced inorganic chemistry, page 165. F. Cotton, G. Wilkinson. Interscience (1962).
28. Gazz. Chim. Ital. 62, 380.
29. Die Kristallstruktur des wasserhaltigen natriumhexafluorophosphats. H. Bode and G. Teufer. Acta Cryst. 9 825 (1955).
30. Recherche strutturistische e cristallografiche sul fluorotitanato di sodio. C. Cipriani. Periodico Mineral. 24 361 (1956).
31. Reference 23, page 366.
32. Über fluoromanganate der alkali metalle. R. Hoppe, W. Liebe and W. Dähne. Z. anorg. allgem. chem. 307, 276 (1961).

33. The crystal structure of sodium fluosilicate. A. Zalkin, J.D. Forrester and D.H. Templeton. Acta Cryst. 17, 1408 (1964).
34. Close-packed structures of  $M_nBX_4$  stoichiometry containing tetrahedral  $BX_4$  groups. C. Calvo. unpublished.
35. Structure of cryolite. St. V. Naray-Szabo and K. Sasvari, Z. Krist. 99 27 (1938).
36. Reference 2, page 14.
37. Reference 2, page 64.
38. The structure of potassium dithionate. E. Stanley. Acta Cryst. 9, 897 (1956).
39. Reference 2, page 16.
40. Transitions in crystal structures of cryolite and related fluorides. E. G. Steward and H. P. Rooksby. Acta Cryst. 6 49 (1953).
41. The crystal structure of  $Li_3AlF_6$ . J. H. Burns, A. C. Tennissen and G. D. Brunton. Acta Cryst. B 24, 225 (1968).
42. Polymorphism in  $Li_3AlF_6$ . G. Garton, B. M. Wanklyn, J. Inorg. Nucl. Chem. 27 2466 (1965).
43. Phase transitions and structure of lithium cryolite. J.L. Holm. Acta Chem. Scand. 20 1167 (1966).
44. Heat of formation and transition temperatures of solid lithium hexafluoroaluminate. P.D. Greene, P. Gross and C. Hayman. Trans. Farad. Soc. 64 (3) 633 (1967).
45. A note on the polymorphy and structure of  $Li_3AlF_6$ . J. L. Holm and B. Jansson. Acta Chem. Scand. 23 1055 (1969).
46. Reference 23, page 370.
47. Crystal and Chemical Investigations of Aluminum Compounds with Spinel Lattice and of  $\alpha$ - $Fe_2O_3$ . E. Kordes, Z. Krist. 91, 193 (1935).
48. Physical Properties and Cation Arrangement of Oxides with Spinel Structures. E.J.W. Verwey and E.L. Heilmann, J. Chem. Phys. 15, 174 (1947).

49. Classification, Representation and Prediction of Crystal Structures of Ionic Compounds. E. W. Gorter, J. Solid State Chem. 1, 279 (1970).
50. Crystal Structures. Volume 3. R. G. Wyckoff. Wiley and Sons, New York, 1960.
51. Superstructure in Spinel. P. B. Braun. Nature 170, 1123 (1952).
52. Phase Transitions in  $\text{LiAl}_5\text{O}_8$ . R. K. Datta and R. Roy. J. Amer. Cer. Soc. 46, 388 (1963).
53. The Electrostatic Contribution to the Lattice Energy of Some ordered Spinel. F. de Boer. J. H. van Danten, and E.J.W. Verwey. J. Chem. Phys. 18, 1032 (1950).
54. The crystal structure and anomalous dispersion of  $\gamma$ - $\text{LiAlO}_2$ . M. Marezio. Acta Cryst. 19, 396 (1965).
55. The structure of  $\alpha$ -cristobalite. W. Nieuwenkamp. Z. Krist. 92, 82 (1935).
56. High pressure synthesis and crystal structure of  $\text{LiAlO}_2$ . M. Marezio and J. P. Remeika. Phys. Rev. 3143 (1966). <sup>2</sup>
57. Uber eine neue modification des  $\text{LiAlO}_2$ . H. Lehmann and H. Hesselbarth. Z. fur anorg. allgem. chem. 313 117 (1961).
58. Mechanism of the phase transition in quartz. R. A. Young. AROSR-2569 (1962).
59. The crystal structure of  $\text{LiAlSi}_2\text{O}_6$ -III. Chi-Tang Li. Z. Krist. 127, 327 (1968).
60. The crystal structure of spodumene-III. P. T. Clarke and J. M. Spink. Z. Krist. 130, 420 (1970).
61. The crystal structure of  $\text{LiAlSi}_2\text{O}_6$ -II. Chi-Tang Li and D. R. Peacor. Z. Krist. 126, 46 (1968).
62. Crystal structure of  $\text{Li}_2\text{Al}_2\text{Si}_3\text{O}_{10}$ . Chi-Tang Li. Z. Krist. 132, 118 (1970).
63. Stuffed derivatives of silica. M. J. Buerger. Am. Min. 39, 600 (1954).
64. Diffusion of lithium ions through quartz in an electric field. P.H. Harris and C. E. Waring. J. Phys. Chem. 41, 1077 (1937).

65. C. S. Barrett. Acta Cryst. 9, 671 (1956).
66. Structure and superstructure of  $\beta$ -eucryptite. T. Tscherry and Y. Schulz. Naturwiss. 57, 194 (1970).
67. Synthese und Kristallstruktur des eukryptits. V. Helmut and G. G. Winkler. Acta Cryst. 1, 27 (1948).
68. Zum thermischen umwandlung und kristallographie von petalit und spodumen. H. Saalfeld. Z. Krist. 115, 420 (1961).
69. Metastable solid solutions with quartz-type structures on the join  $\text{SiO}_2\text{-MgAl}_2\text{O}_4$ . W. Schreyer and J. F. Schairer. Z. Krist. 116, 60 (1961).
70. Structural characteristics of a Mg-Al silicate of the high quartz type. H. Schulz, W. Hoffmann, and G. M. Muchow. Naturwiss. 5, 242 (1970).
71. Second review of Al-O and Si-O tetrahedral distances. J.V. Smith and S.W. Bailey. Acta Cryst. 16, 801 (1963).
72. A high-temperature single crystal diffractometer study of leucite  $(\text{K,Na})\text{AlSi}_2\text{O}_6$ . D. R. Peacor. Z. Krist. 127, 213 (1968).
73. Crystal structure of  $\text{KAlO}_2$ . T.F.W. Barth. J. Chem. Phys. 3, 323 (1935).
74. Reference 23, page 85.
75. The nature and the variation in length of the Si-O and Al-O bonds in framework silicates. G. E. Brown, G. V. Gibbs and P.H. Ribbe. Am. Min. 54, 1044 (1969).
76. Stereochemistry and ordering in the tetrahedral portion of silicates. G.E. Brown and G.V. Gibbs. Am. Min. 55, 1587 (1970).
77. Silicate Science. Vol. I. Silicate Structures. W. Eitel. Academic Press, New York, 1964.
78. Zur Kristallstruktur von Petalit,  $\text{LiAlSi}_4\text{O}_{10}$ . Acta Cryst. 14, 339 (1961).
79. Thermal expansion properties of some synthetic lithia minerals. F. A. Hummel. J. Am. Cer. Soc. 34, 235 (1951).
80. Zur kenntnis der hoch temperature modificationen von lithium-aluminum-silikaten. E. Henglein. Fortschr. Min. 34, 40 (1956).

81. Silica O, a new common form of silica. R. Roy. Z. Krist. 111, 185 (1959).
82. The system lithium-metasilicate-spodumene-silica. R. Roy and E. F. Osborn. J. Am. Chem. Soc. 71, 2086 (1949).
83. Crystal chemistry of  $\beta$ -spodume solid solutions on the join  $\text{Li}_2\text{O}\cdot\text{Al}_2\text{O}_3\cdot\text{SiO}_2$ . B.J. Skinner and H.T. Evans. Am. J. Sci. 312 (1960).
84. The crystal structure of coesite, the dense high-pressure form of silica. T. Zoltai, M. J. Buerger. Z. Krist. 111, 129 (1959).
85. Quartz-coesite stability relationships at high temperatures and pressures. G.J.F. MacDonald. Am. J. Sci. 254, 749 (1956).
86. Phase transformations and the constitution of the mantle. A.E. Ringwood. Phys. Earth Planet Interiors. 3, 109 (1970).
87. Structure of molecules and the chemical bond. Y.K. Syrkin and M.E. Dyatkina. Dover Publications Inc., New York, 1964.
88. Aluminum coordination by spectroscopy. V. A. Kolesova. CA 58:6345. Izv. Akad. Nauk. SSSR, Otd. Khim. Nauk 2082 (1962).